Behavior of Gadolinium-based Diagnostics in Water Treatment

Dissertation

zur Erlangung des akademischen Grades eines
Doktors der Naturwissenschaften
– Dr. rer. nat. –

vorgelegt von

Maike Cyris

geboren in Salzkotten

Institut für Instrumentelle Analytische Chemie
der
Universität Duisburg-Essen

2013

Die vorliegende Arbeit wurde im Zeitraum von November 2009 bis Februar 2013 im Arbeitskreis von Prof. Dr. T.C. Schmidt am Institut für Instrumentelle Analytische Chemie der Universität Duisburg-Essen durchgeführt, sowie am IWW – Zentrum Wasser, einem An-Institut der Universität Duisburg-Essen, durchgeführt.

Tag der Disputation: 25.04.2013

Gutachter:	Prof. Dr. T.C. Schmidt
	Prof. Dr. U. Karst
Vorsitzender:	Prof. Dr. S. Rumann

Summary

Wastewater treatment plants throughout Europe are retrofitted for a sufficient removal of micropollutants. Most target compounds are eliminated efficiently at reasonable costs by oxidation. Sorption processes, on the other hand, are favored as no transformation products are formed. For oxidation, ozone is preferred presently. Its action is divided in two main reaction pathways: Via ozone and via hydroxyl radicals formed by ozone-matrix reactions. Oxidation efficiency strongly depends on reaction rate constants. Sorption processes are usually characterized, including sorption strength, by determination of isotherms. Also, for description of filtration processes isotherm data are necessary.

So far, gadolinium chelates, used as contrast agents in magnetic resonance imaging, have not been investigated in both advanced wastewater treatment processes. The stable chelates are excreted without metabolization. Conventional wastewater treatment does not remove them substantially. They remain intact and no free Gd(III) is released. This may be changed due to oxidative treatment which potentially destroys the chelates, and Gd(III) ions which are toxic, contrary to the chelated form, may be liberated.

Monitoring campaigns in wastewater and drinking water have been performed to demonstrate the relevance of gadolinium in such treatment steps. In a European monitoring campaign an average concentration of 118 ng L^{-1} gadolinium has been determined for 75 wastewater treatment plants effluents, corresponding to a non-geogenic gadolinium concentration of 116 ng L^{-1}. In drinking water in the Ruhr area, a densely populated region in Germany, gadolinium and the anomaly were measurable by a factor of five lower than the average in the investigated wastewater samples. The determined concentrations in drinking water are lower than acute toxic effect concentration. The speciation of gadolinium in the investigated samples is unknown, as only total element concentration has been determined, however, it is strongly assumed that the anthropogenic gadolinium fraction is present as chelate.

Adsorption characteristics were evaluated by bottle point isotherm experiments on different activated carbon types and activated polymer based sorbents. The Freundlich coefficients vary between 0.013 and 2.83 $(\mu mol\ kg^{-1})(L\ \mu mol^{-1})^{1/n}$ for Gd-BT-DO3A, on Chemviron RD 90® and on the best synthetic adsorbent,

respectively. Lab scale experiments with small adsorber columns in a drinking water matrix gave insight in the behavior during fixed-bed adsorption processes. The breakthrough was described successfully by the Linear Driving Force model. Modeling has shown that a description of experimental results is only possible by including dissolved organic carbon isotherm results from drinking water in the model, to describe an additional competitive adsorption effect within the fixed-bed adsorber, different from direct competition. First investigations in a wastewater treatment plant proved a poor adsorption of gadolinium similar to iodinated X-ray contrast media such as iopamidole. Therefore, gadolinium will hardly be removed from wastewater by implementation of a further adsorptive treatment step. However, gadolinium may be utilized as indicator substance for breakthrough.

Rate constants of the chelates with ozone and hydroxyl radicals have been determined under pseudo-first-order conditions. Rate constants for the ozone reaction were determined to be $< 50\ M^{-1}\,s^{-1}$ for all tested chelates. Hence, the chelates may be considered ozone refractory. For determination of hydroxyl radical rate constants different methods were applied. Radicals were generated either by pulse radiolysis, in this case rate constant were determined directly and by competition with thiocyanate, or by the peroxone process, where only competition kinetics were applied (*para*-chlorobenzoic acid and *tert*-butanol as competitors). From pulse radiolysis determinations (rate constants $> 10^9\ M^{-1}\,s^{-1}$) it is concluded that a reaction in wastewater via hydroxyl radicals is possible. No toxic transformation products were detected in the applied cytotoxicity, genotoxicity and estrogenity tests. Concerning the speciation of gadolinium after oxidation, it is suggested that gadolinium ions form new chelates with ligands formed during oxidation. These new chelates may be less stable than the original chelates which benefits transmetalation. This process is also of interest for other chelates present in a water matrix.

In this study it could be demonstrated, that gadolinium is not removed efficiently by the investigated treatment steps. Research on effects of oxidative treatment on metal-organic species is recommended, especially in cases, where the metal ion is toxic.

Kurzfassung

Zurzeit werden in ganz Europa Kläranlagen mit zusätzlichen Aufbereitungsstufen ausgerüstet, um Spurenstoffe besser zu entfernen. Die meisten Spurenstoffe werden durch Oxidation kostengünstig entfernt. Sorptionsprozesse werden hingegen bevorzugt, da keine Transformationsprodukte entstehen. Der Reaktionsweg des für die Oxidation präferierten Ozons wird in Pfade über Ozon und über Hydroylradikale, die durch Ozon-Matrix Reaktionen entstehen, geteilt. Die Oxidationseffizienz hängt stark von den Reaktionsgeschwindigkeiten der Stoffe ab. Sorptionsprozesse werden üblicherweise durch Sorptionsisothermen beschrieben, einschließlich der Sorptionsstärke. Zur Beschreibung von Filtrationsprozessen sind ebenfalls Isothermendaten notwendig.

Bisher wurde das Verhalten von Gadolinium Chelaten, die als Kontrastmittel in der Magnetresonanztomographie verwendet werden, nicht in den genannten Aufbereitungsstufen untersucht. Die stabilen Chelate werden unmetabolisiert ausgeschieden und nur unzureichend in konventionellen Kläranlagen entfernt. Sie bleiben intakt und Gd(III) wird nicht freigesetzt. Dies könnte durch oxidative Verfahren geändert werden, da diese potentiell in der Lage sind Chelate zu zerstören und Gd(III), das im Gegensatz zu der Chelatform toxisch ist, freizusetzen.

Untersuchungen in Trink- und Abwasser wurden durchgeführt, um die Relevanz von Gadolinium in den Aufbereitungsstufen zu zeigen. In einer europaweiten Studie wurde in 75 Kläranlagen eine durchschnittliche Konzentration von 118 ng L^{-1} Gadolinium ermittelt, was einer nicht-geogenen Konzentration von 116 ng L^{-1} entspricht. Im Trinkwasser aus dem Ruhrgebiet wurde eine fünfmal geringere Gadolinium Konzentration und Anomalie ermittelt als in den untersuchten Abwasserproben. Die im Trinkwasser bestimmten Konzentrationen sind geringer als akute Toxizitätskonzentrationen. Die Speziation des Gadoliniums in den untersuchten Proben wurde nicht bestimmt, jedoch wird angenommen, dass die anthropogene Gadoliniumfraktion als Chelat vorliegt.

Adsorptionseigenschaften wurden für unterschiedliche Aktivkohletypen und aktivierte Polymer-basierte Sorbentien ermittelt. Der Freundlich Koeffizient ist für Gd-BT-DO3A zwischen 0.013 und 2.83 (µmol kg^{-1})(L µmol^{-1})$^{1/n}$ bezogen auf Chemviron RD 90® und das am stärksten aktivierte synthetische Adsorbent. Laborversuche mit Kleinfiltersäulen, die mit Trinkwasser betrieben wurden, geben Einblick in das

Adsorptionsverhalten während der Festbett-Filtration. Das Durchbruchverhalten wurde anhand des Linear Driving Force Modells beschrieben. Um die experimentellen Daten zu beschreiben, wurden Isothermen des gelösten organischen Kohlenstoffs in das Modell integriert. Dadurch wurde ein Filtrations-Kompetitionseffekt nachgewiesen, der sich von dem direkten Kompetitionseffekt unterscheidet. Erste Untersuchungen in einer Kläranlage verifizierten die schlechte Adsorbierbarkeit des Gadoliniums, die ähnlich der des Röntgen-Kontrastmittels Iopamidol ist. Daher wird Gadolinium aus Abwasser durch Adsorptionsstufen kaum entfernt werden. Jedoch kann Gadolinium als Indikatorsubstanz für die Ermittlung von Filterdurchbrüchen verwendet werden.

Die Geschwindigkeitskonstanten der Reaktion der Chelate mit Ozon und Hydroxylradikalen wurden unter Bedingungen pseudo-erster Ordnung bestimmt. Die Konstante für die Reaktion mit Ozon ist für alle Chelate < 50 M^{-1} s^{-1}. Daher können die Chelate als Ozon-refraktär bezeichnet werden. Zur Bestimmung von Geschwindigkeitskonstanten mit Hydroxylradikalen wurden verschiedene Methoden angewandt. Wurden die Radikale durch Pulsradiolyse erzeugt, erfolgte die Bestimmung der Geschwindigkeitskonstanten entweder direkt oder anhand einer Kompetition mit Thiocyanat. Bei einer Generierung der Radikale durch den Peroxon-Prozess, erfolgte die Bestimmung nur durch Kompetitionskinetiken (mit *para*-Chlorbenzoesäure und *tert*-Butanol). Die Ergebnisse der Pulsradiolyse Bestimmungen (Geschwindigkeitskonstanten > 10^9 M^{-1} s^{-1}) zeigen, dass eine Reaktion mit Hydroxylradikalen im Abwasser möglich ist. Die Reaktionsprodukte der Oxidationen zeigten keinen Effekt in den angewandten Zell- und Gentoxizitätstests, sowie dem Östrogenitätstest. Hinsichtlich der Speziation des Gadoliniums wird angenommen, dass neue Chelate gebildet werden, die jedoch weniger stabil sein können, was eine Transmetallierung begünstigt. Dies ist auch für andere Chelate in der Wasseraufbereitung von Interesse.

In dieser Studie konnte erstmalig gezeigt werden, dass Gadolinium kaum durch die untersuchten Aufbereitungsstufen entfernt wird. Der Effekt der oxidativen Aufbereitung auf metall-organische Spezies, bedarf jedoch weiterer Untersuchung, insbesondere in Fällen in denen das freie Metallion als toxisch gilt.

Table of Content

Summary ..... **I**

Kurzfassung ..... **III**

1 General Introduction **1**

1.1 Preface *1*

1.2 Gadolinium in medical diagnostics *3*
1.2.1 Gadolinium chelates in magnetic resonance imaging 3
1.2.2 Magnetic resonance imaging and contrast enhancement 5

1.3 Characteristics of Gadolinium-Diagnostics *7*

1.4 Water treatment processes *12*
1.4.1 Overview on water treatment processes 12
1.4.2 Ozonation of water 15
1.4.3 Adsorption processes in water treatment 22

1.5 Scope *24*

1.6 Supplement *26*

1.7 References *27*

2 Important aspects in the determination of gadolinium in aquatic samples **35**

2.1 Introduction *35*

2.2 Methods *39*
2.2.1 Chemicals and Materials 39
2.2.2 ICP-MS 40
2.2.3 Spectral data 41
2.2.4 Interactions with glass 41
2.2.5 HILIC-ICP-MS 42
2.2.6 Sample preconcentration 43

2.3 Results and discussion *46*
2.3.1 Spectral data 46
2.3.2 Interactions with glass 46
2.3.3 Determination of complexes with HILIC-ICP-MS 48
2.3.4 Sample preconcentration 52

2.4 Conclusions *55*

2.5 Supplement *57*

2.6 Literature *58*

3 Occurrence of gadolinium in the water cycle **63**

3.1 Introduction *63*

3.2 Experimental *69*
3.2.1 Sampling 69
3.2.2 Instrumentation 70
3.2.3 Calculation of the anomaly 70

3.3 Results *72*

3.4 Conclusion *82*

3.5 Supplement *84*
3.5.1 Detailed results of the pan-European study 84
3.5.2 Detailed results of the gadolinium anomaly in the Ruhr area 88
3.6 References *89*

4 Adsorption of gadolinium-based diagnostics in water treatment 95
4.1 Introduction *95*
4.2 Experimental *98*
4.2.1 Chemicals and Materials 98
4.2.2 Adsorption experiments 99
4.2.3 Measurements 102
4.2.4 Modeling of fixed-bed filters 102
4.3 Results and discussion *104*
4.4 Conclusion *111*
4.5 Supplement *112*
4.5.1 Description of the wastewater treatment plant 112
4.5.2 Modeling input parameters 113
4.5.3 Use of the gadolinium anomaly in filter experiments in a wastewater treatment plant 114
4.6 References *117*

5 Reaction of Gadolinium Chelates with Ozone and Hydroxyl Radicals 121
5.1 Introduction *121*
5.2 Experimental *123*
5.2.1 Reagents 123
5.2.2 Rate constants 124
5.2.3 Toxicity tests 127
5.3 Results and discussion: *129*
5.4 Conclusion *140*
5.5 Supplement *141*
5.5.1 Details for determination of rate constants 141
5.5.2 Estrogenity tests 146
5.6 Literature *148*

6 Concluding Remarks and Future Perspectives 153
6.1 References *157*

7 Appendix 159
7.1 Abbreviations *159*
7.2 List of publications *165*
7.3 Curriculum Vitae *167*
7.4 Erklärung *169*
7.5 Acknowledgment *171*

1 General Introduction

1.1 Preface

Gadolinium is a rare earth element (REE) which is widely used in applications such as radar technologies, compact discs, microwaves and many more. However, since the 1980`s there is another very important application of gadolinium. It is used as contrast agent in medical diagnostics because of its paramagnetic properties. The application of gadolinium diagnostics has been very successful. Only considering the time between 1998 and 2008 its applications worldwide increased almost tenfold (1998: 20 million applications worldwide [1]); 2008: 150-180 million applications worldwide [2]).

There are no numbers available on the production volume for gadolinium. However, estimations of Angerer et al. [3] point out an annual production volume of 4500 t gadolinium in the year 2006. Based on the assumption that 1.2 g Gd are used for each application in diagnostics [4], this specific consumption amounts to ca. 5% (180-220 t Gd / y^{-1}) of the total gadolinium produced. Yet, one has to consider that the gadolinium diagnostics are excreted mainly unmetabolized from the body [5] and reach the sewage system. In conventional wastewater treatment plants (WWTPs) gadolinium diagnostics are not effectively removed [4, 6] and enter the environment and potentially drinking water. In 1999, 1,100 kg Gd were emitted to the environment in Germany [7], which is ca. 5% of the total amount of gadolinium used for diagnostics worldwide. By extrapolation of all these numbers (7.5 fold increase in 10 y in applications related to 1998 (→ 225 million applications y^{-1} worldwide in 2013), 4.6% of all applications in Germany, use of 1.2 g Gd per application) in Germany in 2013, ca. 12 t Gd / y^{-1} are used for this purpose and consequently released via the sewage system to the environment. An Impact on the aquatic environment from other gadolinium applications is rather unlikely. Other applications of gadolinium (see above) usually incorporate gadolinium into a material, which is not disposed via the sewage system. Only illegal dumps and a subsequent leaching may contribute to a further anthropogenic impact on the aquatic environment.

The gadolinium diagnostics are not toxic. However, water treatment processes might change the speciation of gadolinium and a toxicological relevant species can potentially be formed. Its increasing use in diagnostics and the potential of species transformation aroused concern on its prevalence in the water cycle. This study gives insight in the behavior of gadolinium diagnostics in advanced water treatment technologies.

For a comprehensive overview of the motivation of this work, background information on water treatment and gadolinium chelates will be given in the following introductive chapters. First the function of gadolinium diagnostics will be explained, to understand their necessity in medical diagnostics (cf. chapter 1.2). Furthermore, chemical and physical properties as well as basic toxicological data of the diagnostics will be presented (cf. chapter 1.3). These data are necessary to predict and understand environmental behavior and consequently environmental effects. Subsequently, details on water treatment will be presented (cf. chapter 1.4). The overall scope of this study is to give information on the behavior of gadolinium diagnostics during advanced water treatment processes, in detail oxidation and adsorption. For the evaluation of oxidation reactions in water treatment it is necessary to have knowledge on the kinetics of such reactions. In chapter 1.4.2, an explanation of the kinetic concept which is used in this study is given. For characterization of sorption processes isotherms are used. Different isotherms are used to describe sorption processes. A short introduction on sorption isotherms and their relevance for evaluation in water treatment is presented in chapter 1.4.3.

1.2 Gadolinium in medical diagnostics

1.2.1 Gadolinium chelates in magnetic resonance imaging

Gadolinium chelates are applied in medical diagnostics for contrast enhancement in magnetic resonance imaging (MRI). However, contrast enhancing elements, such as gadolinium, are toxic in concentrations needed for clinical imaging [8]. The general mechanism of metal toxicity is coordination of the metal to donating groups in bio-macromolecules, e.g. proteins, and subsequently a modified molecular structure [8]. By such a coordination, membrane function or enzyme activity can be disturbed [8]. In case of Gd(III), voltage-gated calcium channels are blocked in the range of a few ng kg^{-1} to a few µg kg^{-1}, as Gd(III) has a similar ion radius as Ca(II) (107.8 pm and 114 pm, respectively) [1]. Hence, physiological processes, dependent on Ca(II) fluxes, are inhibited, e.g. contraction of smooth, skeletal and cardiac muscle, transmission of nervous influx or blood coagulation [1].

Due to these effects gadolinium is applied in a chelated form. Magnevist® (Gd-DTPA) was first introduced to the market, followed by other linear chelates (Gd-DTPA-BMA and Gd-BOPTA) and later by the macrocyclic chelates Gd-BT-DO3A and Gd-DOTA [5]. Up to date, in Germany nine chemically different gadolinium diagnostics are licensed (cf. Figure 1.1).

By complexation of Gd(III) its toxicity is reduced remarkably. The lethal dosage for 50% of a population (LD_{50}), in this case for rats, is increasing from 0.1 mmol kg^{-1} (for $GdCl_3$) to 14 mmol kg^{-1}, when gadolinium is complexed with DTPA-BMA [8]. Factors influencing the toxicity of the element species are among others solubility, selectivity and osmolality. Data on these parameters are given for all gadolinium chelates in the following chapter (cf.chapter 1.3).

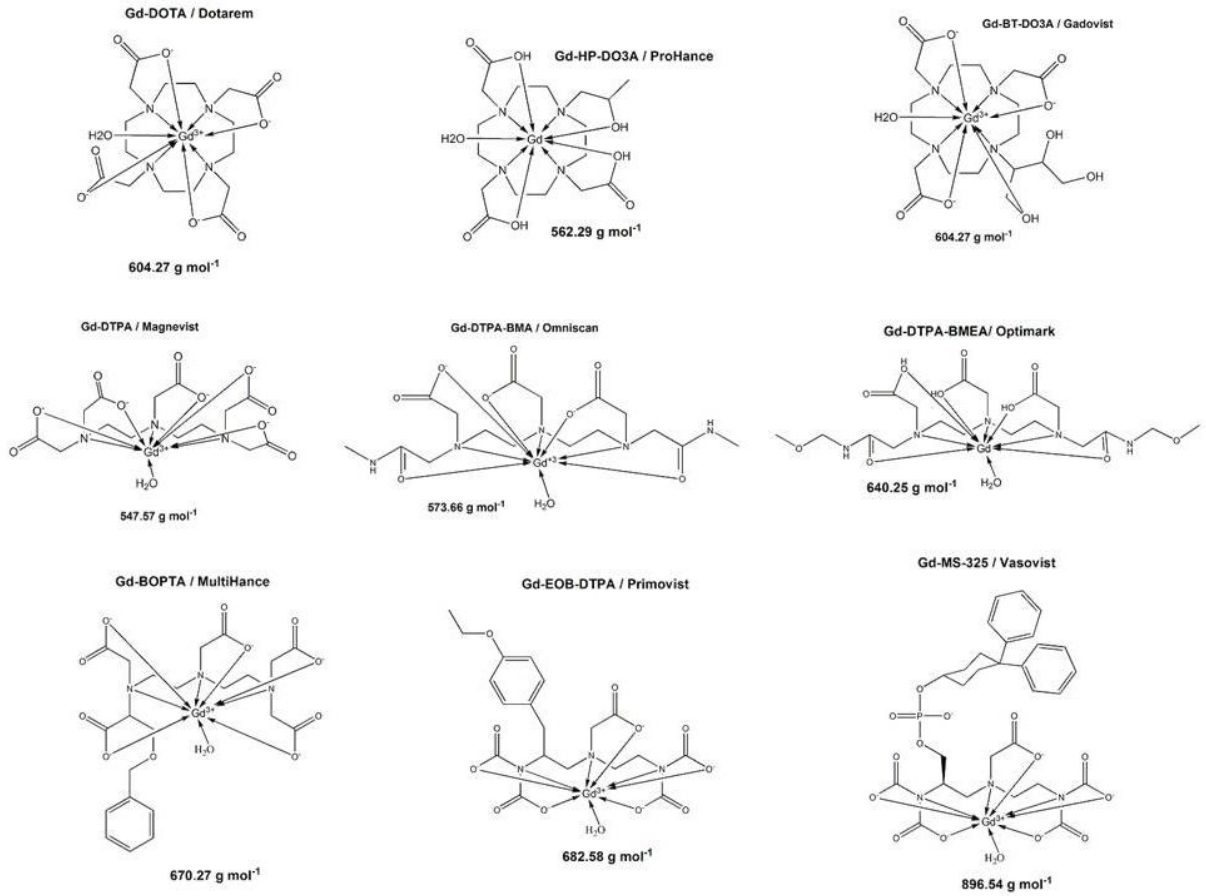

Figure 1.1: Gadolinium diagnostics licensed in Germany; below each molecule the molecular weight is given; first row: macrocyclic extracellular fluid agents (ionic and non-ionic); second row: linear extracellular fluid agents (ionic and non-ionic); third row: organ specific contrast agents (Gd-BOPTA and Gd-EOP-DTPA) and albumin-binding blood pool agent (Gd-MS-325); first row ligands are DOTA or DOTA-like; second and third row ligands are DTPA or DTPA-like

Complexation as precautionary measure seems to be insufficient in certain cases. In 1996 the disease nephrogenic systemic fibrosis (NSF) was reported for the first time and soon afterwards linked to the application of gadolinium based contrast agents [9, 10]. Up to date, there are more than 190 biopsy-proven cases published in peer-reviewed journals [9]. All NSF patients suffered, prior to application of the diagnostics, from severe or even end-stage renal failure [10]. Most of these cases are linked to Gd-DTPA-BMA (82%) [9, 11]. Symptoms, which may vary in severity, are a formation of excess skin tissue (skin fibrosis) and fibrosing of other organs [12-14]. The mechanism responsible for NSF is assumed to be triggered by transmetalation of the gadolinium chelates, resulting in a release of free Gd(III) and consequently interactions of Gd(III) with biomolecules [9, 11, 15].

1.2.2 Magnetic resonance imaging and contrast enhancement

MRI is widely used for imaging anatomical structures. Three-dimensional (3D) images of living organisms can be obtained by this method without using ionizing radiation, as in X-ray methods (e.g. computer tomography (CT), computed axial tomography (CAT), or positron emission tomography (PET). The obtained images are used for the identification of malfunctional tissue.

MRI has to be understood, to understand the way the diagnostics work. It is generally speaking the medical application of nuclear magnetic resonance (NMR), which is used in analytical chemistry most commonly for the determination of molecular structures. NMR (including MRI) is based on the spin of atoms. The magnetic field of the nuclei is dependent on direction and speed of the rotation. The spin of the nuclei can be determined by measuring the magnetic moment of the nuclei, yielding a discrete value. The Pauli-Principle states that spins are usually present as couples with opposite direction. Atoms with an odd number of protons have an overall spin which is not equal to zero. These are of special interest for NMR spectroscopy. For MRI, especially hydrogen atoms are relevant, as their magnetic moment is rather high and they are the most frequent atoms in living organisms [16].

The average magnetic moment of the protons is aligned to magnetic field direction by application of an external magnetic field. An additional radio frequency yields a varying electromagnetic field. The resulting resonance frequency energy can be absorbed and changes the proton spin in the magnetic field. Without this electromagnetic field, the spins return to the thermodynamic equilibrium and overall magnetization becomes aligned with the static magnetic field. This relaxation generates a radio frequency signal which can be measured. [17]

Different paramagnetic substances, which are characterized by unpaired electrons, e.g. Mn(II), Mn(III), Fe(III), Cu(II), and Gd(III), are applied in MRI to increase the signal strength and consequently the contrast [16]. Gadolinium with its high number of unpaired electrons (7 unpaired electrons) and its ability to efficiently influence nearby nuclei as well, is the most important element for MRI diagnostics [16].

The electrons of the contrast agent are also influenced by the magnetic field applied in MRI. The magnetic moment of the electrons is aligned to the magnetic field. However, the magnetic moment of the electrons is ~680 fold larger than the one of protons [18]. Hence, protons in vicinity are influenced by the electrons. In case of

Gd(III), the unpaired electrons are inducing the relaxation of water molecules in MRI. By this, it decreases the spin-lattice relaxation time (T_1) and spin-spin relaxation time (T_2) [8]. The longitudinal and transverse relaxation rates ($1/T_1$ and $1/T_2$, respectively) are both influencing the observed solvent relaxation rate (T_{obs}), as this is the sum of the diamagnetic (subscript dia) and paramagnetic spin (subscript para) [19]:

$$\left(\frac{1}{T_i}\right)_{obs} = \left(\frac{1}{T_i}\right)_{dia} + \left(\frac{1}{T_i}\right)_{para} \qquad i = 1,2 \qquad \text{(1.1) [19]}$$

Gadolinium diagnostics are best suitable for T_1 weighted imaging, as the percentage change in $1/T_1$ in tissue is greater than that in $1/T_2$ [5]. T_1 weighted imaging is most prominent in MRI applications, as advances in MRI development have favored this method [5]. The paramagnetic fraction is dependent on the concentration of the paramagnetic species [19]:

$$\left(\frac{1}{T_i}\right)_{obs} = \left(\frac{1}{T_i}\right)_{dia} + r_i[Gd] \qquad \begin{matrix} i = 1,2 \\ r_i = \text{relaxivity} \end{matrix} \qquad \text{(1.2) [19]}$$

Furthermore, paramagnetic relaxation enhancement is divided into two components, the inner-sphere and the outer-sphere relaxation [19]:

$$\left(\frac{1}{T_i}\right)_{para} = \left(\frac{1}{T_i}\right)_{inner-sphere} + \left(\frac{1}{T_i}\right)_{outer-sphere} \qquad i = 1,2 \qquad \text{(1.3) [19]}$$

For inner-sphere relaxation the water molecule has to be bound directly to the metal or via hydrogen bonds. Outer-sphere relaxation refers to molecules which pass the chelate (translational diffusion) [19]. The distance of the closest approach of outer-sphere water molecules and the diffusional correlation time of outer-sphere water molecules contribute, among others, to relaxivity, especially if the chelate contains no inner-sphere water molecules [16]. However, these contributions are usually very small when inner-sphere water molecules are present and are hence negligible for Gadolinium contrast agents [20]. Inner-sphere relaxation is influenced by factors such as the number of inner-sphere water molecules, residence life time of inner-sphere water molecules, and rotational tumbling time [16]. All of these factors are considered, when a ligand for chelating the Gd(III) is designed [20], to yield a final product which is sufficiently increasing relaxation rates and consequently enhancing contrast between healthy and ailing tissue.

1.3 Characteristics of Gadolinium-Diagnostics

Information on the general properties on the gadolinium chelates was compiled. Other metal-ligand systems were investigated to enable a comparison between the different systems in order to deduct certain properties for the gadolinium chelates. In detail, stability of the chelates, which is of great importance for estimation of the toxicity and reactivity of the chelates, rate constants for the reaction of different metal-ligand systems with hydroxyl radicals and ozone have been compiled for comparison. This information is used to estimate behavior during the water treatment processes which are investigated. Hence, these data are required for the experimental design. These data are presented in Table 1.1. It is notable, that there is a difference between the thermodynamic stability constant and the conditional stability constant at a physiological pH (pH = 7.4) [5, 10]. The stability constants differ by pH dependency. The thermodynamic stability constant is defined as follows [21]:

$$M + L \rightarrow ML \qquad K_{ML} = \frac{[ML]}{[M][L]} \tag{1.4}$$

The conditional stability constant may be calculated, by using the dissociation constants (K_1, K_2, K_3, ... , K_n) as follows [5]:

$$K_{cond,ML} = \frac{K_{ML}}{\left(1 + K_1[H^+] + K_1K_2[H^+]^2 + ... + K_1K_2...K_n[H^+]^n\right)} \tag{1.5}$$

The conditional stability constant (at pH 7.4) is lower than the thermodynamic stability constant for the gadolinium chelates [5]. (For a comparison of thermodynamic and conditional stability constants cf. 1.6)

Furthermore, data presented in Table 1.2 is of interest for characterization of the behavior of gadolinium diagnostics in medicine as well as in environment and water treatment. Data on osmolarity is of great importance for estimation of physiological complications which may appear due to administration of the chelates, e.g. intracellular dehydration, crenation of erythrocytes, and coma [8]. Relaxivity is the most important factor for description of the suitability as contrast agent (cf. chapter 1.2). In general, the contrast enhancing effect is increasing with increasing relaxivity. The octanol / water partitioning coefficient (P_{OW}) is important indicator for the description of environmental behavior. As this data was not available for the gadolinium chelates and estimations by calculations (based on SMILES

notations) are unreliable, especially for molecules containing amine groups, another partitioning coefficient is shown. The butanol / water partitioning coefficient ($P_{Butanol/Water}$) differs from the P_{OW} by the higher water solubility of butanol. Water solubility might be estimated by using the $P_{Butanol/Water}$. Furthermore it gives indices on molecules sorption affinity on various matters.

Toxicity of gadolinium and its chelates is dependent on its speciation. In general, the toxicity of Gd(III) is decreasing by chelation. Also, the toxicity of the ligand is decreasing (e.g. LD_{50} for HP-DO3A is 0.1 mmol kg^{-1} and 12 mmol kg^{-1} for Gd-HP-DO3A [8]). In Table 1.3 toxicity data on gadolinium and its chelates is presented. Additional to the LD_{50} also the half maximal Effective Concentration (EC_{50}) for growth inhibition of fresh water algae and the No Observed Effect Concentration (NOEC) on the same algae are given. Both toxicological endpoints are recommended by the Organisation for Economic Co-operation and Development (OECD) for ecotoxicological assessment of chemicals [38].

Table 1.1: Complex stability constants (thermodynamic or physiologic (pH 7.4; italic)) and reaction rate constants (in M^{-1} s^{-1}) for different coordinated ligands with hydroxyl radicals and ozone, log $K_{thermodynamic}$ for the other gadolinium diagnostics are: 16.6 for Gd-DTPA-BMEA, 23.5 for Gd-EOB-DTPA, 22.1 for Gd-MS325 and 23.8 for Gd-HP-DO3A [10]

Central ion	Constant	Ligand								
		NTA	EDTA	DTPA	Oxalic acid	Acetic acid	DOTA	BT-DO3A	DTPA-BMA	BOPTA
Fe(II)	Log K	8.8 [22]	14.3 [22]	16.6 [22]	2.3 [23]	1.82 [24]	20.2 [25]			
	$k_{\bullet OH}$									
	k_{O3}									
Fe(III)	Log K	15.9 [22]	25.0 [22]	28.0 [22]	7.56 [23]	3.38 [24]	29.4 [26]			*23.4* [10]
	$k_{\bullet OH}$	1.6×10^8 [27]	5×10^8 [27]	1.5×10^9 [28]						
	k_{O3}		3.3×10^2 [29]	<10 [28]						
Mg(II)	Log K	5.5 [22]	8.7 [22]	9.3 [22]	2.61 [24]	1.25 [24]	11.15 [26]			
	$k_{\bullet OH}$									
	k_{O3}									
Ca(II)	Log K	6.4 [22]	10.5 [22]	10.7 [22]	2.30 [23]	1.24 [24]	16.37 [26]		7.17 [30]	
	$k_{\bullet OH}$		3.5×10^9 [27]							
	k_{O3}		$\sim 10^5$ [29]	6200 [28]						
Gd(III)	Log K	11.5 [22]	17.4 [22]	22.5 [22]	7.01 [24]	1.82 [24]	24.0 [26]	21.8 [31]	16.9 [32]	22.6 [32]
	$k_{\bullet OH}$									
	k_{O3}									
La(III)	Log K	10.3 [22]	15.5 [22]	19.5 [22]	4.47 [23]	2.02 [24]				
	$k_{\bullet OH}$									
	k_{O3}									
Al(III)	Log K	11.1 [33]	16.5 [34]	18.7 [35]	6.06 [23]		17.0 [36]			
	$k_{\bullet OH}$									
	k_{O3}									
Zn (II)	Log K	10.6 [22]	16.5 [22]	18.3 [22]	4.85 [24]	1.04 [23]	21.05 [10]		12.0 [30]	*13.9* [10]
	$k_{\bullet OH}$			2.4×10^9 [28]			18.7 [25]			
	k_{O3}			3500 [28]						
Cu(II)	Log K	13.6 [21]	18.9 [30]	21.4 [30]	4.49 [23]	1.89 [24]	22.6 [5]		13.0 [30]	*17.3* [10]
	$k_{\bullet OH}$									
	k_{O3}									
Free ligand	$k_{\bullet OH}$	2.5×10^9 [27]	4×10^8 [27]	3.9×10^9 [37]						
	k_{O3}	9.8×10^5 [1]	3.2×10^6 [1]							

In case of a lack of data on molecular properties, as well as on environmental behavior, different computational models are available to estimate such data. It has been considered to apply such models as the data on properties of the gadolinium chelates is incomplete. Popular tools for the estimation of substance properties and their behavior in the environment are Quantitative Structure-Activity Relationships (QSARs). Estimations made by these models include not only on physico-chemical properties, but also biological activity, biodegradation and –accumulation. The data provided are considered as reliable and have thus found their way into legal regulatory processes (e.g. EU Regulation concerning the Registration, Evaluation, Authorisation and Restriction of Chemicals (REACH) recommends QSAR modeling for risk management). However, the essential input parameter for QSAR based models is the simplified molecular-input line-entry system (Smiles). This system enables to note any structure in a linear way, e.g. Diclofenac (cf. Figure 1.2). Yet, there is no rule for the notation of chelates which is accepted by common modeling programs such as EPIsuite (US EPA) or SPARC (ARChem). A notation of the ligand and the specific metal always results either in a covalent bond instead of a coordinated bond or the correct description is not accepted by the specific program. The suggested SMILES notation results in a wrongly displayed structure (cf. Figure 1.2). Hence, further estimations on toxicity and environmental processes by QSAR were not possible.

Table 1.2: Physico-chemical data of gadolinium diagnostics; pK_a is given for the ligands; *data are given for the medical solution which is different from the pure gadolinium chelate (excess ligand in formulation, e.g. (Omniscan: DTPA-BMA 12 g L^{-1} excess, Optimark: DTPA-BMEA 28.4 g L^{-1} excess, Magnevist (dimeglumine-Gd-DTPA): DTPA 0.4 g L^{-1} excess, Multihance: BOPTA 0.4 g L^{-1} excess [39]), [a]data given for a temperature of 37°C

	Osmolarity (mmol kg^{-1} water)	Relaxivity (T_1 at 40°C and 20 MHz in $mM^{-1}s^{-1}$)	Log $P_{Butanol/Water}$	pK_a (only for ligands)
$GdCl_3$		11.3 [8]		
Gd-NTA				9.8, 2.6, 1.6 [40]
Gd-EDTA		6.9 [41]	-2.8 [42]	10.2, 6.1, 2.7, 2.6 [40]
Gd-DTPA-BMA	789 [8]*	3.9 [8]	-2.1 [8]*	9.4, 4.4, 3.3, 1.4 [43]
Gd-HP-DO3A	630 [8]*	3.7 [8]	-2.0 [5]	12, 9.4, 4.3, 3.3 [43]
Gd-DOTA	1170 [8]*	3.5 [8]*	-3.1 [8]*	11.4, 9.7, 4.5, 4.4 [43]
Gd-DTPA	1940 [8]*	3.8 [8]*	-3.2 [5]*	10.2, 8.6, 4.2, 2.9, 1.8 [43]
Gd-DTPA-BMEA	1110 [1]*	4.7 [5]		9.3, 4.5, 3.3 [43]
Gd-BOPTA	1970 [1]*	4.4 [44]	-2.2 [5]	10.7, 8.3, 4.4, 2.8, 2.1 [44]
Gd-BT-DO3A	1603 [1]*	3.7 [1]	-2 [5]	
Gd-EOB-DTPA	688 [1]*	5.3 [1]	-2.1 [5]	
Gd-MS325	825 [10]*	6.6 [5][a]	-2.1 [5]	
Gd-DO3A		4.8 [5]	-2.2 [42]	11.6, 9.2, 4.4, 3.5 [43]

Table 1.3: Toxicological data on different gadolinium chelates; *data are given for the medical solution which is different from the pure gadolinium chelate (excess ligand in formulation, e.g. (Omniscan: DTPA-BMA 12 g L^{-1} excess, Optimark: DTPA-BMEA 28.4 g L^{-1} excess, Magnevist (dimeglumine-Gd-DTPA): DTPA 0.4 g L^{-1} excess, Multihance: BOPTA 0.4 g L^{-1} excess [39]), [a] Data given for meglumine-Gd-EDTA; meglumine is an additive for some of the gadolinium diagnostics as well, e.g. Dotarem and Multihance

Substance	LD_{50} mmol kg^{-1}; mice	EC_{50} mg L^{-1} (mmol L^{-1}); Algae test with Desmodesmus subspicatus	NOEC mg L^{-1} (mmol L^{-1}); Algae test with Desmodesmus subspicatus
$GdCl_3$	0.1 [8]		4.9 [18]
DTPA	0.1 [8]		
DTPA-BMA	0.1 [8]		
DOTA	0.1 [8]		
HP-DO3A	0.1 [8]		
Gd-DTPA	5.6 (0.2) [30]*	> 100 (0.18) [45]*	100 (0.18) [45]*
Gd-DTPA-BMA	14.8 (0.7) [30]		20 (0.03) [18]*
Gd-DOTA	15 [8]		
Gd-HP-DO3A	12 [8]		> 100 (0.18) [18]
Gd-EDTA	0.3 (0.1) [30][a]		
Gd-DO3A	7-9 [5]		
Gd-BT-DO3A		> 937 (1.55) [45]*	937 (1.55) [45]*
Gd-EOB-DTPA		> 500 (0.73) [45]*	120 (0.18) [45]*
Gd-MS325		> 80 (0.08)[45]*	80 (0.08) [45]*

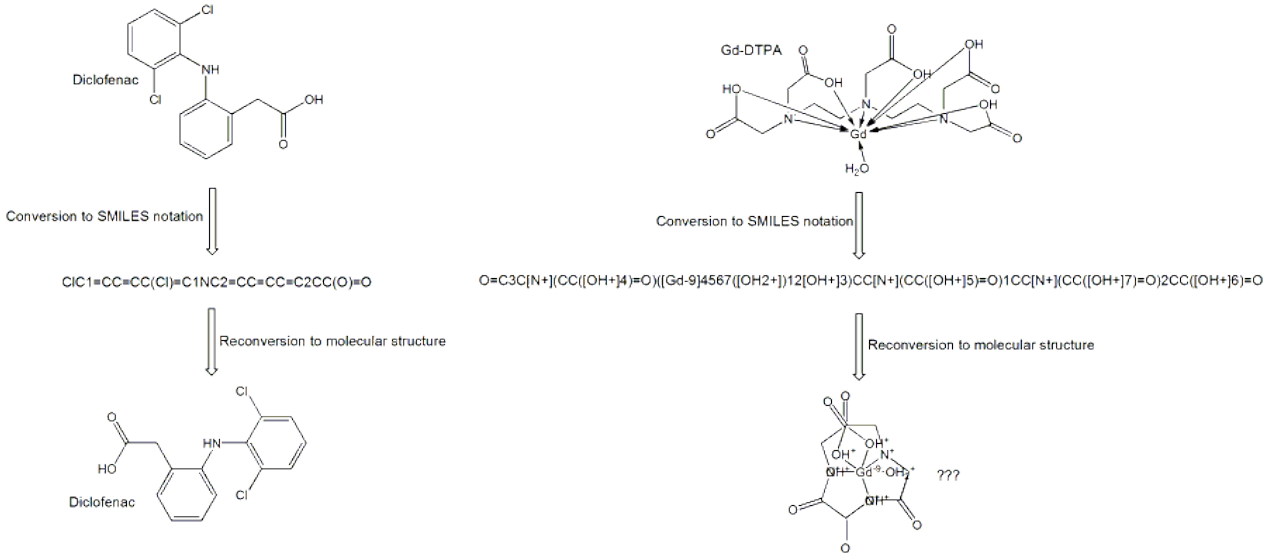

Figure 1.2: Conversion of a metal chelate, in this case Gd-DTPA which is the active agent in Magnevist, into the SMILES notation and reconversion of the SMILES notation to the molecular structure by the same software (ChemDraw, Cambrige Software)

1.4 Water treatment processes

1.4.1 Overview on water treatment processes

Water treatment is generally divided into two major areas, drinking water treatment and wastewater treatment. Drinking water treatment processes are applied for raw waters of different quality. The matrix composition of the raw water mainly differs by the source of the raw water. In general, the use of ground water for drinking water production is preferred as surface waters are often more polluted. Important processes used for drinking water production are shown in Table 1.4.

Table 1.4: Important processes in drinking water treatment

Process	Treatment objective
Screening (Screen filters)	Removal of solids
Coagulation and flocculation	Removal of colloids
Filtration (Sand filtration or activated carbon filter, membrane filtration)	Removal of suspended solids (inorganic and organic substances, including microorganisms, in case of activated carbon filtration also adsorption processes)
Adsorption (activated carbon filtration)	Adsorption of dissolved organic carbon (DOC), removal of color, odor, taste, micropollutants
Oxidation (ozonation, chlorine treatment)	Reduction of DOC, color, odor, taste, micropollutants and disinfection

As an origin for surface water pollution the point source WWTP is of great importance. The treated wastewater is discharged into the receiving waters and all substances which are not retained by the wastewater treatment process enter the water cycle via this route. Important treatment steps which are applied in WWTPs are shown in Figure 1.3. In the last decades, detections of trace substances in surface and ground waters led to discussions on the efficiency of the wastewater treatment processes and subsequently additional treatment was proposed [46-48].

Pharmaceuticals are of special concern as they have a biological effect. However, personal care products and industrial chemicals may also affect organisms. Endocrine disruptors are an example for such substances. The natural hormone 17β-estradiol (E2) is one of the main female sex hormones. Its synthetic derivate 17α-Ethinylestradiol (EE2) is used for contraception. EE2 has been found in the aquatic environment and concern about feminization of aquatic organisms arose [49, 50]. However, not only EE2 was found to disrupt the endocrine systems of such organisms, but also other chemicals, such as nonylphenols, bisphenols, and polychlorinated biphenyls. These substances do not have an estrogenic effect as strong as the natural hormone which they mimic, but some are persistent and potentially accumulate in the environment [51, 52].

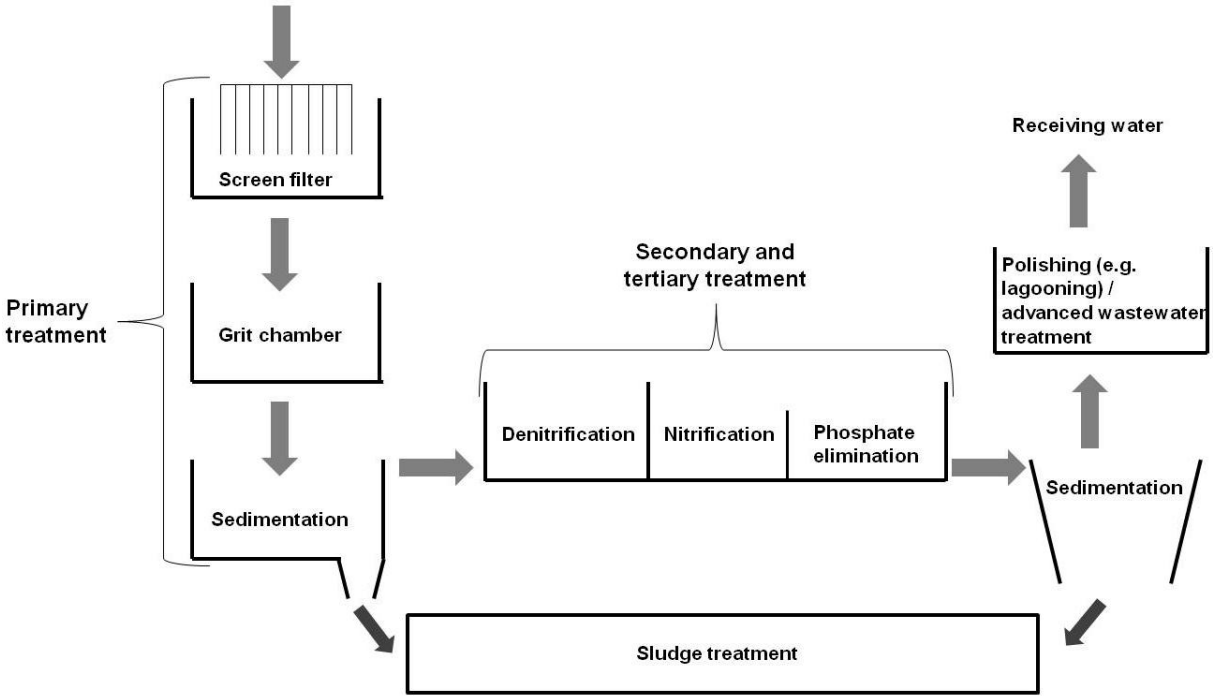

Figure 1.3: Flow chart of a typical wastewater treatment plant

It is discussed to retrofit wastewater treatment plants with advanced treatment steps to reduce concentrations of those substances with biological effects and / or persistent substances in surface waters [46-48]. Oxidative treatment steps, activated carbon treatment and membrane processes are discussed most widely [46, 48]. The application of these processes in drinking water production is common practice, especially ozonation and adsorption on activated carbon. The general mechanisms of these processes for the abatement of pollutants are the same for wastewater

treatment and raw water treatment for drinking water production. Yet matrix effects are far more relevant in wastewater treatment than in drinking water production, which has to be considered when such processes are designed. The application of ozone and generation of OH-Radicals via UV/Hydrogen peroxide are proposed for oxidative treatment. In some model WWTPs they are already in use, e.g.:

- Application of ozone:
  In Duisburg-Vierlinden (Germany) with subsequent biological treatment in a turbulent fluidized bed; in Bad Sassendorf (Germany) with subsequent polishing pond
- UV-treatment:
  Monschau-Kalterherberg (Germany); Einruhr (Germany)

Dosage of powdered activated carbon (PAC) or filtration with granulated activated carbon (GAC) are proposed for treatment with activated carbon. In some model WWTPs both are already in use, e.g.:

- PAC:
  Buchenhofen (Wuppertal, Germany) with removal via sand filtration; Lage (Germany) with no further treatment
- GAC:
  Düren-Merken (Germany); WWTP Obere Lutter (Gütersloh, Germany)

In some cases even a combination of both above presented treatment processes is applied, e.g.:

- WWTP Schwerte (Germany): ozonation with a subsequent PAC dosage, recirculation to biological treatment step

Also, the application of membrane bioreactors (MBR) is already established in some plants, e.g.:

- WWTP Aachen-Soers (Germany)
- WWTP Eitorf (Germany)

In this study the behavior of gadolinium diagnostics in adsorptive water treatment steps has been studied, as well as the oxidation of the diagnostics by ozonation. Details for the evaluation of both processes are given in the following subsections.

1.4.2 Ozonation of water

The treatment of drinking water by ozone is primarily used for disinfection purposes. Another important aspect is the oxidation of organic substances. In wastewater treatment, oxidation of micropollutants is usually the main aspect when applying ozone. Yet, in some cases the focus may also be on disinfection purposes. Application of ozone is characterized as advanced oxidation process (AOP) in such a matrix, as hydroxyl radicals are formed in situ [53]. Hence, it is necessary to investigate both reaction pathways for the evaluation of micropollutant oxidation in wastewater: the direct ozone reaction and the hydroxyl radical reaction pathway.

One of the most important aspects for evaluation of oxidative treatment is the determination of reaction rate constants in order to be able to discriminate between feasible reactions in water treatment and such which are unlikely in the given time span for treatment. Calculations using the rate constant of the specific reactions may be performed to evaluate the process and estimate potential transformation of the probe compound.

An oxidation reaction can be described by equation 1.6. The rate law presented in equation 1.7 can be derived from equation 1.6. If the reaction is first order, i.e., the reaction is only dependent on the concentration of one of the reactants, k_{Ox} may be derived by neglecting one of the reactants.

$$P + \eta Ox \xrightarrow{k_{Ox}} products \tag{1.6}$$

$$\frac{d[P]}{dt} = k_{Ox} \times [P] \times \eta[Ox] \tag{1.7}$$

k_{Ox} = Second order reaction rate constant of the oxidation reaction

[P] = Concentration of the probe compound

[Ox] = Concentration of the oxidant

η = Stoichiometric number

Small rate constants (< 1000 M^{-1} s^{-1}) can be determined under (pseudo-)first order conditions for direct reactions with ozone [54]. This condition is achieved by applying an excess of probe compound to oxidant [54]. Hence, the probe compound concentration is constant during the process and the decay of oxidant can be monitored. Integrating equation 1.7 then yields:

$$\ln \frac{[Ox]}{[Ox]_0} = -k_{Ox}[P] \times t = -k_{obs} \times t \qquad (1.8)$$

k_{obs} = Observed pseudo-first order reaction rate constant of the oxidation reaction

t = Time

A plot of $\ln([Ox]/[Ox]_0)$ versus time yields $-k_{obs}$. Subsequently, k_{Ox} can be calculated from a rearranged equation 1.8. A prerequisite of this approach is that only one oxidant is present. However, hydroxyl radicals may be formed in ozone reactions which may react further with the probe compound and by this interfere with the rate constant determination [54]. To avoid such reactions, a radical scavenger is added to the reaction solutions. This radical scavenger is characterized by a low reaction rate constant with ozone and a high rate constant with hydroxyl radicals. Typically, aliphatic alcohols are used as radical scavengers [55]. In this work, this concept was applied for the determination of rate constants for the reactions with ozone.

Different concepts have been applied for the determination of rate constants with hydroxyl radicals. Hydroxyl radicals may be generated by different methods, some of which are summarized in Table 1.5. Due to the disadvantages of the Fenton-(like)-processes and the UV light based processes (cf. Table 1.5) only the peroxone and the pulse radiolysis method have been used for the generation of hydroxyl radicals.

Table 1.5: Methods for the generation of hydroxyl radicals and their (dis)advantages concerning the applicability for determination of gadolinium chelate reaction rate constants

Processes	General mechanism	Advantages	Disadvantages
Pulse radiolysis	Hydroxyl radicals and hydrogen radicals are formed by applying ionizing radiation [56]	• Considered as most reliable method [56] • Constant radical exposition	• Availability of pulse generator
UV-based processes (e.g. UV / H_2O_2)	Generation of radicals via photolysis [57]	• An economic method for laboratory experiments, as additionally direct photolysis reactions may be investigated	• Glass ware to avoid light absorption → Gadolinium chelates and other chelates interact with glass [4, 58, 59]
Fenton or Fenton-like-processes	Oxidation of a (transition-) metal by hydrogen peroxide, yielding hydroxyl radicals [60, 61].	• An economic method for laboratory experiments	• Transmetalation may occur • The Fenton process is not fully understood by now [60]
Peroxone	Reaction of hydrogen peroxide with ozone yields hydroxyl radicals [62]	• An economic method for laboratory experiments • No transmetalation by reactants • Interactions with glass may be avoided	• Availability of ozone generator

The mechanism for radical generation via pulse radiolysis is presented in the following:

H_2O + ionising radiation → $H_2O^{\bullet+}$ + e^- (1.9)

H_2O + ionising radiation → H_2O^* (1.10)

$H_2O^{\bullet+} \rightarrow {}^{\bullet}OH + H^+$ (1.11)

$H_2O^* \rightarrow {}^{\bullet}OH + H^{\bullet}$ (1.12)

$e^- + nH_2O \rightarrow e_{aq}^-$ (1.13)

$e_{aq}^- + N_2O + H_2O \rightarrow {}^{\bullet}OH + N_2 + OH^-$ (1.14)

By the radiation, a water radical cation is formed (cf. eq. 1.9) which deprotonates to a hydroxyl radical (cf. eq. 1.11). Furthermore, the excited water molecule formed by radiation (cf. eq. 1.10) decomposes into a hydrogen and hydroxyl radical (cf. eq. 1.12). The electron which is formed in reaction 1.9 is solvated by water (cf. eq. 1.13) and forms in presence of dinitrogen oxide a further hydroxyl radical (cf. eq. 1.14). [54]

The influence of hydrogen radicals, which are also formed by pulse radiolysis, is neglected due to the following reasons. First, the hydroxyl radical yield is considerably higher compared to the one of hydrogen radicals (9/1 ratio for ${}^{\bullet}OH$ / ${}^{\bullet}H$) [54, 63]; secondly, hydroxyl radical reaction rate constants are by orders of magnitude higher than those of hydrogen radicals [54].

As the peroxone process has been applied for the generation of hydroxyl radicals as well, this method is also described in more detail. In the peroxone process, it has to be differentiated between a mechanism which is commonly stated in literature (cf. eq. 1.15-1.19) and a more recently suggested one (cf. eq. 1.20-1.24) [54]. The new mechanism is an attempt to explain the experimentally observed yield of hydroxyl radicals which is only half of the one expected from the hitherto accepted mechanism (ratio ozone / hydroxyl radical 0.5 instead of 1) [54, 64].

$$HO_2^- + O_3 \rightarrow HO_2^\bullet + O_3^{\bullet-} \quad (1.15)$$

$$HO_2^\bullet \rightleftharpoons O_2^{\bullet-} + H^+ \quad (1.16)$$

$$O_2^{\bullet-} + O_3 \rightarrow O_2 + O_3^{\bullet-} \quad (1.17)$$

$$O_3^{\bullet-} + H^+ \rightleftharpoons HO_3^\bullet \quad (1.18)$$

$$HO_3^\bullet \rightarrow {}^\bullet OH + O_2 \quad (1.19)$$

The reaction sequence above (old mechanism), is started by an electron transfer reaction, yielding a hydroperoxyl radical and an ozonide radical anion (cf. eq. 1.15) [65]. The formed hydroperoxyl radical is in equilibrium with a hyperoxide anion and a proton (cf. eq. 1.16). The hyperoxide anion yields dioxygen and another ozonide radical anion by an electron transfer to ozone (cf. eq. 1.17). Protonation of the ozonide radical anion forms a hydrogen trioxide radical (cf. eq. 1.18). This decomposes into a hydroxyl radical and dioxygen (cf. eq. 1.19). Hence, the overall ratio ozone to hydroxyl radical is one (i.e., from two ozone molecules two ozonide radical anions are formed, yielding two hydroxyl radicals). [54]

In contrast to the mechanism presented above, an ozone / hydroxyl radical ratio of 0.5 is monitored in experiments which made a revision of the process necessary [54]. For such a revision, the following reactions are proposed [54, 64, 66]:

$$HO_2^- + O_3 \rightarrow HO_5^- \quad (1.20)$$

$$HO_5^- \rightarrow HO_2^\bullet + O_3^{\bullet-} \quad (1.21)$$

$$HO_5^- \rightarrow 2\ {}^3O_2 + OH^- \quad (1.22)$$

$$O_3^{\bullet-} \rightleftharpoons O^{\bullet-} + O_2 \quad (1.23)$$

$$O^{\bullet-} + H^+ \rightleftharpoons {}^\bullet OH \quad (1.24)$$

This reaction sequence is induced by formation of an ozone adduct (cf. eq. 1.20) which is slightly more exergonic than the electron transfer reaction (cf. eq. 1.15) [54].The formed adduct is transformed to a hydroperoxyl radical and an ozonide radical anion (cf. eq. 1.21) or into two triplet dioxygens and a hydroxide anion (cf. eq. 1.22). Both reactions occur equally. The ozonide radical anion is in equilibrium with the $O^{\bullet -}$ and dioxygen (cf. eq. 1.23). Furthermore, the radical anion and hydrogen are in equilibrium with a hydroxyl radical (cf. eq. 1.24). Rather than the previously assumed reactions (cf. eq. 1.18 and 1.19), these equilibrium reactions take place. Overall two moles of ozone yield one mole of hydroxyl radicals. [54, 64]

The differences in the mechanisms are important, as the radical yield is essential for a correct experimental set up. This is in particular the case in determinations of rate constants by competition kinetics, since the oxidant concentration has to be significantly lower than the one of probe compound and competitor (details given below). When applying the peroxone process, it is necessary to take the pK_a of hydrogen peroxide ($pK_a = 11.8$) into account. The dissociation rate of hydrogen peroxide is of importance because the reaction of hydrogen peroxide with ozone is slow compared to its anion (< 1 and 9.6×10^6 $M^{-1}s^{-1}$, respectively) [65].

The determination of rate constants using pseudo-first order conditions can be performed directly, when applying pulse radiolysis as method for generation of hydroxyl radicals. In this study, a different approach is used than the one described above for the determination of rate constants for the reaction with ozone. Instead of monitoring the decay of the oxidant, the decay of the probe compound is measured for several reactions with different excess concentrations of the probe compound. Following a first-order-law, where $k_{obs} = k_{Ox} \times [P]_0$ (k_{obs} in s^{-1}), equation 1.25 is obtained. A plot of k_{obs} versus [P] yields a regular second-order rate constant k_{Ox} as the slope [54].

$$k_{Ox} \times [Ox] \times [P] = k_{obs} \times [P] \qquad (1.25)$$

Another approach for determination of rate constants for the reaction with hydroxyl radicals was competition kinetics. Competition kinetics are generally applied when rate constants are > 1000 [67]. In competition kinetics, a competitor (C) with a well known rate constant has to be available. The occurring reactions are presented in equations 1.26-1.27.

$$P + Ox \xrightarrow{k_{Ox,P}} P_{Ox} \quad (1.26)$$

$$P + Ox \xrightarrow{k_{Ox,C}} C_{Ox} \quad (1.27)$$

P_{Ox} = Oxidation products of the probe compound

C_{Ox} = Oxidation products of the competitor

$k_{Ox,\,P}$ = Reaction rate constant of the oxidation of the probe compound

$k_{Ox,\,C}$ = Reaction rate constant of the oxidation of the competitor

The degradation of both compounds is described by the following equation:

$$\ln\frac{[P]}{[P]_0} = \ln\frac{[C]}{[C]_0} \times \frac{k_{Ox,P}}{k_{Ox,C}} \quad (1.28)$$

$[P]_0$ = Initial concentration of the probe compound

$[C]_0$ = Initial concentration of the competitor

By plotting $\ln([P]/[P]_0)$ versus $\ln([C]/[C]_0)$ a slope of $k_{Ox,P} / k_{Ox,C}$ is obtained. However, another approach was used in this study, to avoid gadolinium species determination. At a ratio of [Ox] << [P] and [C] the following equation is valid:

$$\frac{[C_P]}{[C_{-P}]} = \frac{k_c[C]}{k_C[C] + k_P[P]} \quad (1.29)$$

$$\frac{[C_{-P}]}{[C_P]} = \frac{k_c[C] + k_P[P]}{k_C[C]} = 1 - \frac{k_P[P]}{k_C[C]} \quad (1.30)$$

$[C]_P$ = Concentration of competitor in presence of probe compound

$[C]_{-P}$ = Concentration of competitor in absence of probe compound

By plotting $([C_{-P}]/[C_P])$ versus $([P]/[C])$ the slope $k_{Ox,P} / k_{Ox,C}$ is obtained, from which $k_{Ox,P}$ can be calculated [54].

1.4.3 Adsorption processes in water treatment

In drinking water production Adsorption on activated carbon is mainly used for the removal of dissolved organic carbon (DOC), color, taste, and odor. The great advantage of this method is the elimination of the substance from the water matrix without formation of any by-products, as the removed substances are bound to the carbon surface.

For the description of sorption processes in general it is necessary to differentiate between adsorption and absorption [68]. In the case of sorption to activated carbon, in general, adsorption to the sorbent surface dominates and one generally applies the term adsorption [68]. The efficiency of the adsorption process may be described by determination of sorption isotherms. Sorption isotherms describe the equilibrium of sorption and desorption at constant temperature, i.e. the relationship of sorbed probe compound and dissolved probe compound [69]. The experimentally determined isotherms may have different shapes (cf. Figure 1.4), dependent on the types of sorbent and sorbate as well as on the concentration ratios [69]. The simplest type is a linear isotherm. This type applies to situations where partitioning into a homogeneous organic phase is dominating and/or at low sorbate concentrations where the strongest adsorption sites are by far not saturated [69]. More complicated are the Langmuir isotherm and the Freundlich isotherm, which apply both to a situation in which the extent of sorption is limited (cf. Figure 1.4).

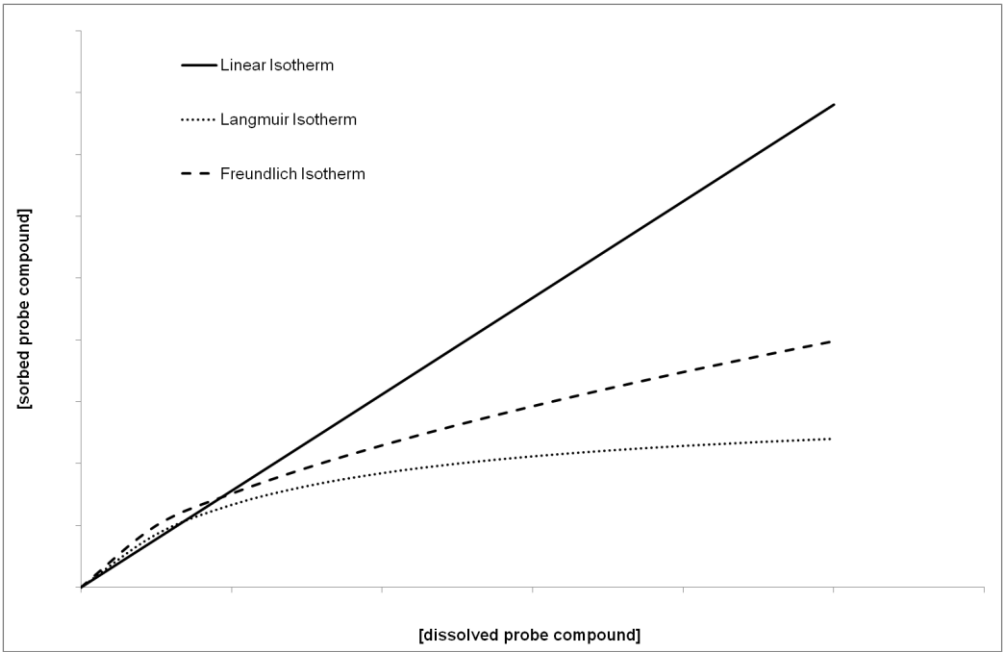

Figure 1.4: Examples for different shapes of isotherms, in detail, the Linear isotherm, Langmuir isothem and Freundlich isotherm

The Langmuir isotherm is based on the assumption that free energy, enthalpy and entropy change due to sorption is constant for all solid-phase concentrations, which is usually only the case for homogeneous surfaces [70]. Furthermore, sorption in monolayers is assumed [71]. Both assumptions are not fulfilled in adsorption processes on activated carbon in water treatment [69-71]. The equation of the Langmuir isotherm is presented in equation 1.31. The Freundlich isotherm (cf. eq. 1.32) may be derived from the Langmuir isotherm by taking a logarithmic decrease of the differential adsorption enthalpy with decreasing sorbent concentration in the liquid phase into account [72].

$$[P]_s = \frac{q_{max} \times K_L \times [P]_W}{1 + K_L \times [P]_W} \qquad (1.31)$$

$$[P]_s = K_F \times ([P]_w)^n \qquad (1.32)$$

$[P]_s$ = Concentration of the probe compound sorbed on solid phase
$[P]_w$ = Concentration of the probe compound in liquid phase
K_L = Langmuir coefficient
q_{max} = Maximal concentration of the sorbent on the solid phase
K_F = Freundlich coefficient
n = Freundlich exponent

The exponent in the Freundlich equation is a measure for diversity of free energy associated with sorption of the sorbate on a heterogeneous surface [69]. The Freundlich coefficient (K_F) is a measure for sorption strength [71]. The Freundlich isotherm is widely used for description of adsorption processes on activated carbon in water treatment. Experimental data are often better described by the Freundlich approach than by the Langmuir isotherm, as the assumptions on which the Langmuir isotherm is based are not valid for sorption on activated carbon, in particular, energetic homogeneity of sorption sites and monomolecular coverage [70, 71]. However, in some cases the Langmuir isotherm was applicable, even though, the basic assumptions were clearly not fulfilled [71]. In fact, the Freundlich isotherm has become some type of standard equation for the characterization of adsorption processes [71]. Furthermore, the K_F is often used for modeling of diverse sorption processes, e.g. the breakthrough behavior of filters [71].

1.5 Scope

The behavior of gadolinium chelates throughout the water cycle is rather unknown. It is assumed that during environmental processes the chelates remain intact and none of the processes decreases the gadolinium concentration during the transport. These assumptions have not been validated sufficiently. Also, the influence of processes during water treatment has not been studied sufficiently up to date.

This work is therefore focusing on two main goals:

- Significance of gadolinium in the water cycle
- Behavior during water treatment processes

To investigate gadolinium chelates in water treatment it is important to develop a reliable analytical method. Factors which may influence analysis and speciation methods are discussed in chapter 2.

The anthropogenic gadolinium in the environment may be best described by the so called gadolinium anomaly. Hence, a short introduction on the anomaly, its occurrence and its use as a pseudo-natural tracer is given in chapter 3. For a basic overview of occurrence of gadolinium throughout the watercylce two monitoring campaigns were carried out. One considered the input of gadolinium into the water cycle. To this end, samples from 75 European WWTPs effluents have been taken. In addition, drinking water samples have been taken in an urban agglomeration. This has been done in order to evaluate how much of the anthropogenic gadolinium reaches consumers' tap water. Results of these monitoring campaigns are presented in chapter 3.

Treatment steps which are of importance for both, drinking water treatment and wastewater treatment are of special interest for evaluation of behavior during water treatment. The focus was on ozonation as energetically and economically feasible oxidation process (cf. chapter 5) and adsorption on activated sorbents (cf. chapter 4). Wastewater treatment is of special interest as the concentration of the gadolinium chelates is higher than in raw water for drinking water production, e.g. due to dilution effects (if taking surface water as raw water). The concentration of the chelates approaches zero when ground water is used as raw water. Yet one has to consider that both advanced wastewater treatment steps are also applied for a long time in drinking water production. For waste water treatment and drinking water

treatment the same physico-chemical processes will take place. However, process parameters as, e.g., concentration of adsorbent / oxidant or matrix constitution and concentration differ and are strongly influencing the retention / oxidation of the substances.

The advanced wastewater treatment steps are designed for the removal of organic trace substances. However, also other compounds will be affected as well. Up to date studies on organo-metallic compounds are very rare. However, ozonation, which is one of the favored steps for advanced wastewater treatment, is of special interest as a destruction of the gadolinium chelates may lead to a release of toxic, free Gd(III) ions. The oxidation of gadolinium chelates via ozone and hydroxyl radicals, which are generated by reactions of ozone with the matrix, is described in chapter 5.

The application of activated carbon or other adsorbents for the removal of trace substances is proposed as an alternative to ozonation. Research on adsorption characteristics of chelates is rare. It is known, that these substances are in general poor adsorbable on activated carbon. Yet, knowledge on the specific behavior of gadolinium chelates in this treatment process has not been investigated up to date. The evaluation of gadolinium chelates adsorption on activated carbon and on an activated material based on spherical polymers is shown in chapter 4. The presented study includes adsorption behavior on powdered material as well as adsorption in fixed-bed filters. Furthermore, the breakthrough behavior was modeled to gain information on the relevant parameters influencing the adsorption in filters.

1.6 Supplement

Table S 1.1: Comparison of thermodynamic and conditional stability constants for gadolinium chelates

Chelate	Thermodynamic stability constant log K_{thern}	Conditional stability constant (pH 7) log K_{cond}
Gd-EDTA	17.4 [22]	14.7 [5]
Gd-DTPA	22.5 [22]	17.7 [10]
Gd-DTPA-BMA	16.9 [32]	14.9 [10]
Gd-DTPA-BMEA	16.6 [10]	15.0 [10]
Gd-EOB-DTPA	23.8 [10]	18.7[10]
Gd-DOTA	24.0 [26]	18.3 [5]
Gd-BT-DO3A	21.8 [31]	14.7 [10]
Gd-HP-DO3A	23.8 [10]	17.1 [10]
Gd-MS-325	22.1 [10]	18.9 [10]
Gd-BOPTA	22.6 [32]	18.4 [32]

1.7 References

1. Idee, J.M., M. Port, I. Raynal, M. Schaefer, S. Le Greneur, and C. Corot, Clinical and biological consequences of transmetallation induced by contrast agents for magnetic resonance imaging: A review. *Fundamental and Clinical Pharmacology*, 2006. **20**(6): 563-576.
2. Giersig, D., 2009: personal communication.
3. Angerer, G., L. Erdmann, F. Marscheider-Weidemann, M. Scharp, A. Lüllmann, V. Handke, and M. marwed, *Rohstoffe für Zukunftstechnologien - Einfluss des branchenspezifischen Rohstoffbedarfs in rohstoffintensiven Zukunftstechnologien auf die zukünftige Rohstoffnachfrage*, in *Inovationspotenziale*. 2009, Frauenhofer Institut für System- und Inovationsforschung ISI: Stuttgart.
4. Künnemeyer, J., L. Terborg, B. Meermann, C. Brauckmann, I. Möller, A. Scheffer, and U. Karst, Speciation analysis of gadolinium chelates in hospital effluents and wastewater treatment plant sewage by a novel HILIC/ICP-MS method. *Environmental Science and Technology*, 2009. **43**(8): 2884-2890.
5. Caravan, P., J.J. Ellison, T.J. McMurry, and R.B. Lauffer, Gadolinium(III) chelates as MRI contrast agents: Structure, dynamics, and applications. *Chemical Reviews*, 1999. **99**(9): 2293-2352.
6. Lawrence, M.G., J. Keller, and Y. Poussade, Removal of magnetic resonance imaging contrast agents through advanced water treatment plants. *Water Science and Technology*, 2010. **61**(3): 685-692.
7. Kümmerer, K. and E. Helmers, Hospital effluents as a source of gadolinium in the aquatic environment. *Environmental Science and Technology*, 2000. **34**(4): 573-577.
8. Chang, C.A., Magnetic resonance imaging contrast agents. Design and physicochemical properties of gadodiamide. *Investigative Radiology*, 1993. **28** (Suppl 1): S21-27.
9. Broome, D.R., Nephrogenic systemic fibrosis associated with gadolinium based contrast agents: a summary of the medical literature reporting. *European Journal of Radiology*, 2008. **66**(2): 230-234.

10. Port, M., J.M. Idée, C. Medina, C. Robic, M. Sabatou, and C. Corot, Efficiency, thermodynamic and kinetic stability of marketed gadolinium chelates and their possible clinical consequences: A critical review. *BioMetals*, 2008. **21**(4): 469-490.

11. Chopra, T., K. Kandukurti, S. Shah, R. Ahmed, and M. Panesar, Understanding nephrogenic systemic fibrosis. *International Journal of Nephrology*, 2012. **2012**.

12. Cowper, S.E. and P.J. Boyer, Nephrogenic systemic fibrosis: An update. *Current Rheumatology Reports*, 2006. **8**(2): 151-157.

13. Grobner, T., Gadolinium - A specific trigger for the development of nephrogenic fibrosing dermopathy and nephrogenic systemic fibrosis? *Nephrology Dialysis Transplantation*, 2006. **21**(4): 1104-1108.

14. Ting, W.W., M. Seabury Stone, K.C. Madison, and K. Kurtz, Nephrogenic fibrosing dermopathy with systemic involvement. *Archives of Dermatology*, 2003. **139**(7): 903-906.

15. Haemel, A.K., E.A. Sadowski, M.M. Shafer, and A. Djamali, Update on nephrogenic systemic fibrosis: Are we making progress? *International Journal of Dermatology*, 2011. **50**(6): 659-666.

16. Que, E.L. and C.J. Chang, Responsive magnetic resonance imaging contrast agents as chemical sensors for metals in biology and medicine. *Chemical Society Reviews*, 2010. **39**(1): 51-60.

17. Schwedt, G., *Analytische Chemie - Grundlagen, Methoden und Praxis*. 2001, Weinheim: Wiley-VCH.

18. Neubert, C., *Umweltverhalten und Ökotoxikologie von gadoliniumhaltigen Magnetresonanztomographie-Kontrastmitteln*.2008, Dissertation at Institut für Technischen Umweltschutz: Prozesswissenschaften TU Berlin.

19. Lauffer, R.B., Paramagnetic metal complexes as water proton relaxation agents for NMR imaging: Theory and design. *Chemical Reviews*, 1987. **87**(5): 901-927.

20. Raymond, K.N. and V.C. Pierre, Next generation, high relaxivity gadolinium MRI agents. *Bioconjugate Chemistry*, 2005. **16**(1): 3-8.

21. Martell, A.E. and R.M. Smith, *Critical Stability Constants: Amino Acids*. Vol. 1. 1974, New York: Plenum Press. 338.

22. Smith, R.M. and A.E. Martell, Critical stability constants, enthalpies and entropies for the formation of metal complexes of aminopolycarboxylic acids and carboxylic acids. *Science of the Total Environment*, 1987. **64**(1-2): 125-147.

23. Perrin, D.D., *Stability Constants of Metal-ion Complexes, Part B: Organic ligands*. IUPAC chemical data series, International Union of Pure and Applied Chemistry, ed. I.U.P.A.C. Analytical Chemistry Division Commision on Equilibrium Data. Erik Högfeldt. 1982: Pergamon Press Ltd.

24. Martell, A.E. and R.M. Smith, *Critical Stability Constants: First Supplement*. Vol. 5. 1982, New York: Plenum Press.

25. Byegård, J., G. Skarnemark, and M. Skålberg, The stability of some metal EDTA, DTPA and DOTA complexes: Application as tracers in groundwater studies. *Journal of Radioanalytical and Nuclear Chemistry*, 1999. **241**(2): 281-290.

26. Martell, A.E., R.J. Motekaitis, E.T. Clarke, R. Delgado, Y. Sun, and R. Ma, Stability constants of metal complexes of macrocyclic ligands with pendant donor groups. *Supramolecular Chemistry*, 1996. **6**(3-4): 353-363.

27. Von Gunten, U., Ozonation of drinking water: Part I. Oxidation kinetics and product formation. *Water Research*, 2003. **37**(7): 1443-1467.

28. Stemmler, K., G. Glod, and U. Von Gunten, Oxidation of metal-diethylenetriamine-pentaacetate (DTPA) - Complexes during drinking water ozonation. *Water Research*, 2001. **35**(8): 1877-1886.

29. Munoz, F. and C. von Sonntag, The reactions of ozone with tertiary amines including the complexing agents nitrilotriacetic acid (NTA) and ethylenediaminetetraacetic acid (EDTA) in aqueous solution. *Journal of the Chemical Society. Perkin Transactions 2*, 2000(10): 2029-2033.

30. Cacheris, W.P., S.C. Quay, and S.M. Rocklage, The relationship between thermodynamics and the toxicity of gadolinium complexes. *Magnetic Resonance Imaging*, 1990. **8**(4): 467-481.

31. Frenzel, T., P. Lengsfeld, H. Schirmer, J. Huetter, and H.-J. Weinmann, Stability of gadolinium-based magnetic resonance imaging contrast agents in human serum at 37 °C*. Investigative Radiology*, 2008. **43**(12): 817-828.

32. Khurana, A., V.M. Runge, M. Narayanan, J.F. Greene Jr, and A.E. Nickel, Nephrogenic systemic fibrosis: A review of 6 cases temporally related to gadodiamide injection (Omniscan)*. Investigative Radiology*, 2007. **42**(2): 139-145.

33. Bohrer, D., P. Cicero do Nascimento, P. Martins, and R. Binotto, Availability of aluminum from glass and an Al form ion exchanger in the presence of complexing agents and amino acids*. Analytica Chimica Acta*, 2002. **459**(2): 267-276.

34. Yuchi, A., K. Ueda, H. Wada, and G. Nakagawa, Equilibrium study on the masking of aluminum ion in the determination of fluoride with ion-selective electrodes*. Analytica Chimica Acta*, 1986. **186**: 313-18.

35. Achour, B., J. Costa, R. Delgado, E. Garrigues, C.F.G.C. Geraldes, N. Korber, F. Nepveu, and M. Isabel Prata, Triethylenetetramine-N,N,N',N'',N''',N'''-hexaacetic acid (TTHA) and TTHA-Bis(butanamide) as chelating agents relevant to radiopharmaceutical applications*. Inorganic Chemistry*, 1998. **37**(11): 2729-2740.

36. Kodama, M. and E. Kimura, Complexation of aluminium ions with polyamino polycarboxylic macrocycles in an aqueous-solution*. Bulletin of the Chemical Society of Japan*, 1995. **68**(3): 852-857.

37. Mori, Y., R. Watanabe, S. Sakamoto, N. Endo, S. Nakano, K. Kanaori, H. Takashima, M. Ohkawa, and K. Tajima, Flow-injection EPR investigation on OH radical scavenging activity of Gd(III) containing MRI contrast media*. Journal of Medicine*, 2004. **35**(1-6): 49-61.

38. Oecd, *Test No. 201: Freshwater Alga and Cyanobacteria, Growth Inhibition Test*. OECD Guidelines for the Testing of Chemicals, Section 2 - Effects on Biotic Systems. 2011: OECD Publishing.

39. Schmitt-Willich, H., Stability of linear and macrocyclic gadolinium based contrast agents [1]*. British Journal of Radiology*, 2007. **80**(955): 581-583.

40. Chatterton, N., C. Gateau, M. Mazzanti, J. Pécaut, A. Borel, L. Helm, and A. Merbach, The effect of pyridinecarboxylate chelating groups on the stability and electronic relaxation of gadolinium complexes. *Dalton Transactions*, 2005(6): 1129-1135.

41. Weinmann, H.J., M. Laniado, and W. Mützel, Pharmacokinetics of GdDTPA/dimeglumine after intravenous injection into healthy volunteers. *Physiological chemistry and physics and medical NMR*, 1984. **16**(2): 167-172.

42. Wedeking, P., K. Kumar, and M.F. Tweedle, Dissociation of gadolinium chelates in mice: Relationship to chemical characteristics. *Magnetic Resonance Imaging*, 1992. **10**(4): 641-648.

43. Choppin, G.R. and K.M. Schaab, Lanthanide(III) complexation with ligands as possible contrast enhancing agents for MRI. *Inorganica Chimica Acta*, 1996. **252**(1-2): 299-310.

44. Uggeri, F., S. Aime, P.L. Anelli, M. Botta, M. Brocchetta, C. De Haen, G. Ermondi, M. Grandi, and P. Paoli, Novel contrast agents for magnetic resonance imaging. Synthesis and characterization of the ligand BOPTA and its Ln(III) complexes (Ln = Gd, La, Lu). X-ray structure of disodium (TPS-9-145337286-C-S)-[4-carboxy-5,8,11-tris(carboxymethyl)-1-phenyl-2-oxa-5,8, 11-triazatridecan-13-oato(5-)]gadolinate(2-) in a mixture with its enantiomer. *Inorganic Chemistry*, 1995. **34**(3): 633-642.

45. Neubert, C., R. Länge, and T. Steger-Hartmann, *Gadolinium containing contrast agents for magnetic resonance imaging (MRI) investigations on the environmental fate and effects*, in *Fate of pharmaceuticals in the environment and in water treatment systems*, D.S. Aga, Editor. 2008, CRC Press Taylor & Francis Group: Boca Raton, Fl.

46. Joss, A., H. Siegrist, and T.A. Ternes, Are we about to upgrade wastewater treatment for removing organic micropollutants? *Water Science and Technology*, 2008. **57**: 251-255.

47. Hollender, J., S.G. Zimmermann, S. Koepke, M. Krauss, C.S. McArdell, C. Ort, H. Singer, U. Von Gunten, and H. Siegrist, Elimination of organic micropollutants in a municipal wastewater treatment plant upgraded with a full-scale post-ozonation followed by sand filtration. *Environmental Science and Technology*, 2009. **43**(20): 7862-7869.

48. Ternes, T., *Assessment of technologies for the removal of pharmaceuticals and personal care products in sewage and drinking water facilities to improve the indirect potable water reuse*, in *Poseidon report*. 2005.

49. Ternes, T.A., M. Stumpf, J. Mueller, K. Haberer, R.D. Wilken, and M. Servos, Behavior and occurrence of estrogens in municipal sewage treatment plants - I. Investigations in Germany, Canada and Brazil. *Science of the Total Environment*, 1999. **225**(1-2): 81-90.

50. Huber, M.M., S. Canonica, G.Y. Park, and U. von Gunten, Oxidation of pharmaceuticals during ozonation and advanced oxidation processes. *Environmental Science and Technology*, 2003. **37**(5): 1016-1024.

51. Routledge, E.J. and J.P. Sumpter, Structural features of alkylphenolic chemicals associated with estrogenic activity. *Journal of Biological Chemistry*, 1997. **272**(6): 3280-3288.

52. Tyler, C.R., S. Jobling, and J.P. Sumpter, Endocrine disruption in wildlife: a critical review of the evidence. *Critical Reviews in Toxicology*, 1998. **18**(4): 319-316.

53. Buffle, M.O., J. Schumacher, S. Meylan, M. Jekel, and U. Von Gunten, Ozonation and advanced oxidation of wastewater: Effect of O_3 dose, pH, DOM and $HO^{\bullet}$-scavengers on ozone decomposition and $HO^{\bullet}$ generation. *Ozone: Science and Engineering*, 2006. **28**(4): 247-259.

54. von Sonntag, C. and U. von Gunten, *Chemistry of ozone in water and wastewater treatment: From basic principles to applications*. 2012, London / New York: IWA.

55. Hoigne, J. and H. Bader, Ozonation of water: selectivity and rate of oxidation of solutes. *Ozone: Science and Engineering*, 1979. **1**(1): 73-85.

56. Buxton, G.V., C.L. Greenstock, W.P. Helman, and A.B. Ross, Critical review of rate constants for reactions of hydrated electrons, hydrogen atoms and hydroxyl radicals in aqueous solution. *Journal of Physical and Chemical Reference Data*, 1988. **17**(2): 513-886.

57. Glaze, W.H., J.-W. Kang, and D.H. Chapin. *Chemistry of water treatment processes involving ozone, hydrogen peroxide and ultraviolet radiation*. in *Ozone: Science and Engineering*. 1987.

58. Raju, C.S.K., D. Luck, H. Scharf, N. Jakubowski, and U. Panne, A novel solid phase extraction method for pre-concentration of gadolinium and gadolinium based MRI contrast agents from the environment. *Journal of Analytical Atomic Spectrometry*, 2010. **25**(10): 1573-1580.

59. Ulanski, P., E. Bothe, K. Hildenbrand, J.M. Rosiak, and C. von Sonntag, Hydroxyl-radical-induced reactions of poly(acrylic acid); a pulse radiolysis, EPR and product study. Part I. Deoxygenated aqueous solutions. *Journal of the Chemical Society, Perkin Transactions 2*, 1996(1): 13-22.

60. Pignatello, J.J., E. Oliveros, and A. MacKay, Advanced oxidation processes for organic contaminant destruction based on the fenton reaction and related chemistry. *Critical Reviews in Environmental Science and Technology*, 2006. **36**(1): 1-84.

61. Fenton, H.J.H., LXXIII. - Oxidation of tartaric acid in presence of iron. *Journal of the Chemical Society, Transactions*, 1894. **65**: 899-910.

62. Sein, M.M., A. Golloch, T.C. Schmidt, and C. von Sonntag, No marked kinetic isotope effect in the peroxone (H_2O_2/D_2O_2 + O_3) reaction: Mechanistic consequences. *ChemPhysChem*, 2007. **8**(14): 2065-2067.

63. Von Sonntag, C., *The chemical basis of radiation biology*. 1987, London: Taylor & Francis.

64. Jarocki, A., M.M. Sein, J. von Sonntag, S. Naumov, A. Golloch, T.C. Schmidt, and C. von Sonntag, The •OH Radical Yield in the Peroxone (H_2O_2 + O_3) Reaction. *Journal of the American Chemical Society*, 2008. **to be submitted**.

65. Staehelin, J. and J. Hoigne, Decomposition of ozone in water - Rate of initiation by hydroxide ions and hydrogen-peroxide*. Environmental Science and Technology*, 1982. **16**(10): 676-681.

66. von Sonntag, C., Advanced oxidation processes: Mechanistic aspects*. Water Science and Technology*, 2008. **58**: 1015-1021.

67. Huber, M.M., *Elimination of pharmaceuticals during oxidative treatment of drinking water and waste water: Application of ozone and chlorine dioxide*.2004, Dissertation at Swiss federal institut of technology Zurich

68. Endo, S., P. Grathwohl, S.B. Haderlein, and T.C. Schmidt, Compound-specific factors influencing sorption nonlinearity in natural organic matter*. Environmental Science and Technology*, 2008. **42**(16): 5897-5903.

69. Schwarzenbach, R.P., P.M. Gschwend, and D.M. Imboden, *Environmental organic chemistry*. 2nd ed. 2003, Hoboken, New Jersey: John Wiley & Sons.

70. Sontheimer, H., J.C. Crittenden, R.S. Summers, B.R. Frick, J. Fettig, G. Hörner, C. Hubele, and G. Zimmer, *Activated carbon for water treatment*. 1988, Karlsruhe: AWWA Research Foundation.

71. Worch, E., *Adsorption technology in water treatment: Fundamentals, processes, and modeling*. 2012, Berlin / Boston: De Gruyter.

72. Adamson, A.W., *Physical chemistry of surfaces* 4th ed. 1985, New York: Wiley.

2 Important aspects in the determination of gadolinium in aquatic samples

2.1 Introduction

For the determination of gadolinium in aquatic samples several aspects are of importance. The determination of total gadolinium or Gd(III) ions may be accomplished by elemental analysis, e.g.

- atomic absorption spectroscopy (AAS) [1]
- inductively coupled plasma (ICP) - optical emission spectrometry (OES) [2-4],
- ICP - mass spectrometry (MS) [5, 6].
- total reflection X-ray fluorescence (TXRF) [7],

The method of choice for samples with high concentrations is TXRF as sample preparation is very fast [7]. However, ICP-MS methods are generally preferable in environmental analysis due to their very low limit of quantification (LOQ). Yet, if analyzing non-aquatic samples, sample preparation may be more extensive [8]. For drinking water or environmental samples, as well as those from wastewater treatment plants (WWTPs) ICP-MS is the method of choice. Nevertheless, it has to be considered that the methods presented above are only able to determine the total gadolinium concentration in a sample, whereas a separation and identification of single species is impossible. For determination of gadolinium species, several methods have been published, among others these are:

- Capillary electrophoresis (CE) - (electrospray ionization) ESI-MS [9, 10]
- High-performance liquid chromatography (HPLC) with Ultraviolet (UV) / visible light (VIS) detection [2, 11]
- Hydrophobic Interaction Liquid Chromatography (HILIC) – ICP - MS [4, 12, 13]
- HILIC – ESI - MS [14, 15]
- HPLC – ICP - MS [16]
- HPLC – ICP - OES [17, 18]
- Ion chromatography (IC) – ICP - MS [19-21]
- Micellar electrokinetic chromatography (MEKC) - UV/VIS [22]
- Size-exclusion chromatography (SEC) – ICP - MS [23]

In many of the methods presented above, a determination of only one gadolinium species was published, e.g., for CE-ESI-MS [10] and HPLC-UV/VIS [2] and sometimes separation of only two or three gadolinium species is possible, e.g., by HILIC-ESI-MS [15] and HPLC-UV/VIS [11].

Furthermore, it has to be noted that most published methods have been developed to investigate gadolinium species in biological samples to evaluate medical issues. An exception are the new HILIC-ICP-MS methods by Künnemeyer [4] and Raju [12]. In principle all other methods are also applicable for environmental, wastewater or drinking water samples. However, the LOQs of the methods are rather high and hence, quantification in such samples will not be accomplished without further improvements. The sensitive determination of the gadolinium species achieved by hyphenation of HILIC to ICP-MS is up to date the only method that provides LOQs which are low enough for analysis of samples from wastewater treatment and environment.

Methods involving HILIC have been described by some authors for determination of metal species in trace amounts [24-26]. The retention mechanism of this chromatographic method is not fully characterized. However, it is assumed that different species can be separated according to partitioning between an immobilized water layer on the surface of the stationary phase and the mobile phase. Interactions between analyte and surface groups of the stationary phase contribute also to the retention mechanisms. In this regard ZIC-HILIC columns offer great selectivity due to their zwitterionic sulfobetaine surface groups bearing surface charges at high and low pH. These allow weak interactions with charged species [27, 28]. One disadvantage of the HILIC technique for ICP-MS is the need of a high organic content within the mobile phase, requiring addition of oxygen to the plasma gas to avoid carbon deposits within the interior of the MS device.

A method for determination of gadolinium species by HILIC-ICP-MS was first published by Künnemeyer et al. [4] in 2009 and allowed the separation of:

- Gadovist® / Gd-BT DO3A (macrocyclic, non-ionic)
- Dotarem® / Gd-DOTA (macrocyclic, ionic)
- Magnevist® / Gd-DTPA (linear, ionic)
- Multihance® / Gd-BOPTA (linear, ionic)
- Omniscan® / Gd-DTPA-BMA (linear, non-ionic)

The reported limit of detection (LOD) was 1 nM (determined by signal-to-noise method s/n = 3) and the corresponding LOQ was 3.3 nM (determined by signal-to-noise method s/n = 10). This method was adapted and modified by Raju et al. [12]. Their modifications allowed LODs of 0.14 ± 0.03 nM (determined by signal-to-noise method s/n = 3) and correspondingly also lower LOQs (for Gd-BOPTA, Gd-DTPA, Gd-DOTA, Gd-DTPA-BMA and Gd-BT DO3A 71 nM, 92 nM, 57 nM, 60 nM and 81 nM, respectively; determined by signal-to-noise method s/n = 10). In comparison to the method of Künnemeyer et al. [4], the flow rate was lower (0.1 mL min^{-1} instead of 0.3 mL min^{-1}), injection volume was higher (5 µL instead of 4 µL) and pH was higher (pH 5.8 instead of 3.75). Furthermore, the composition of the eluent was modified, instead of using a 76/24 ratio of acetonitrile (ACN) / water with a 12.5 mM formate buffer, a 60/40 ratio of ACN / water with a 20 mM acetate buffer was applied. Total analysis time of the method presented by Raju et al. [12] was 25 min which is 5 min less than the one of Künnemeyer et al. [4]. Both methods and combinations of both were tested in this study, to determine best operation parameters for the available HPLC-ICP-MS system.

Concentrations of total gadolinium are in the lower ng L^{-1} range in environmental samples [29-31] as well as in drinking water (cf. chapter 3), [32]. In samples from wastewater treatment plants the concentration of total gadolinium is in the lower µg L^{-1} to medium ng L^{-1} range, depending on the sampling location (location of the WWTP and sampling point in the WWTP) (cf. chapter 3, [4, 6, 19]).

Due to these low concentrations, preconcentration might be necessary for analysis of such samples. In addition to separation and quantification methods, also preconcentration methods for gadolinium species are described in literature. These involve solid phase extraction (SPE) [13, 33, 34] or simple evaporation approaches [12]. Preconcentration approaches are suitable for both, elemental analysis and species analysis. In methods based on SPE it has to be differentiated between methods which are only suitable for enrichment of ionic gadolinium based on ion exchange [33] and those that are also suitable for organic gadolinium species [13, 35]. Depending on the purpose of analysis both techniques might be suitable. SPE methods are faster than evaporation. However, these experiments are labor-intensive. Furthermore, SPE methods based on ion exchange might eliminate a relevant species. Only for the method described by Raju et al. [13]

it is possible to preconcentrate both, organic gadolinium species (neutral or ionic) and free Gd(III) ions. The method described by Möller et al. [35] has not been evaluated regarding this differentiation. For the overall aim of the studies presented in this work, all preconcentration methods are of interest.

The development of a reliable analysis method (including preconcentration) for gadolinium (and its chelates) is presented in the following. Furthermore tests on suitability of equipment for such analysis are shown. These studies have been performed, to support the investigations of the overall scope of the work.

2.2 Methods

2.2.1 Chemicals and Materials

The chemicals used for the experiments are described in the following. As standard for ICP-MS measurements, a rare earth elements standard (ICP-Working Calibration Standard 4 from High Purity Standards, 10 mg L^{-1}) and iridium (Iridium standard solution, CetriPur from Merck, 1000 mg L^{-1}) as an internal standard have been used. For quality assurance, high purity single substance standards were used (gadolinium ICP-Standard (1000 mg L^{-1}, CertiPur from Merck), cerium ICP-Standard (1000 mg L^{-1}, High Purity Standards) and for quality assurance of the measurement method and indium ICP-Standard (1000 mg L^{-1}, CetriPur from Merck) for quality assurance of the enrichment method via evaporization).

For preconcentration experiments gadolinium chloride hexahydrate (99%, Sigma Aldrich) was used. The $GdCl_3$ powder was dryed in a drying chamber (120°C) and afterwards stored until use in a desiccator. The gadolinium chelate standards were medical solutions (Gadovist® (Gd-BT-DO3A, 1.0 M, Bayer Schering Pharma AG); Omniscan® (Gd-DTPA-BMA, 0.5 M, GE Healthcare Buchler); Dotarem® (Gd-DOTA, 0.5 M, Guerbet), Multihance® (Gd-BOPTA, 0.5 M, Nycomed GmbH)), except for Gd-DTPA which was purchased as diethylenetriaminepentaacetic acid gadolinium(III) dihydrogen salt hydrate (97%) from Sigma-Aldrich.

Formic acid (98-100% p.a., Merck), ammonium formate (p.a., Fluka), ammonium hydroxide solution (28% AnalaR NORMAPUR, VWR) and ammonium acetate (puriss., Merck) were used for buffer preparation for HILIC-ICP-MS. ACN (Rotisolv®, Ultra LC-MS, Roth, Germany) was used as eluent.

Ultra pure water (Millipore: MilliQ Gradient / Elga: Purelab ultra; for both used ultra pure waters: R ≥ 18.2 MΩ) was used for experiments. HPLC water was further purified by filtration through a PP syringe filter (0.45 µm × 0.45 µm PP membrane). Nylon syringe filters (25 mm × 0.45 µm, nylon membrane) were used for filtration of the HILIC eluent and buffer.

Stock and standard solutions were always prepared in PP-vials, if not stated elsewise, to avoid surface effects on glass, which will be described in the following (cf. chapter 2.2.4). PP-autosampler vials were used for HILIC-ICP-MS measurements.

2.2.2 ICP-MS

For determination of rare earth element concentrations, measurements were performed with a Perkin Elmer ELAN DRC II ICP-MS equipped with an AS90 autosampler. The ICP-MS instrument parameters are presented in Table 2.1. The integrated peristaltic pump (24 rpm) controlled the flow of washing solution (inlet tube PVC $d_{i\,=}$ 1.143 mm, wall = 0.86 mm), sample solution (inlet tube: PVC $d_{i\,=}$ 0.76mm, wall = 0.86 mm) and flow of the nebulizer waste (discharge tube: PVC d_i = 3.17 mm, wall = 0.86 mm). It is only necessary to determine REE* (rare earth elements excluding gadolinium) if the gadolinium anomaly has to be determined (cf. chapter 3). If not stated elsewise only two gadolinium isotopes (^{158}Gd, ^{160}Gd) and the corresponding internal standard (iridium, ^{192}Ir) were measured. The devices were continuously rinsed between the single measurements with ultrapure water, acidified with 12.5 mL nitric acid (65% Suprapur®, Merck KGaA) and 45mL hydrochloric acid (30% Suprapur®, Merck KGaA) per liter (refered to as washing solution), to avoid any metal salt precipitation. The LOQs for all REEs were determined according to the US EPA guidelines [36] (cf. chapter 3). For gadolinium the LOQ was 1.2 ng L^{-1}.

Table 2.1: Parameters for ICP-MS measurement of gadolinium and REE* (e.g., for calculation of the gadolinium anomaly), including the internal standard iridium and the quality assurance standard indium

Injector tube:	Quartz glass, d_i = 1.85 mm (ball- and socket joint to spray chamber)
Spray chamber:	Cyclone, quartz glass
Nebulizer:	Meinhard, quartz glass
Nebulizer gas flow:	0.9 L min^{-1}
ICP RF power:	1100 W
Skimmer / sampler cone material:	Nickel
Analysed mass traces [m/z]:	^{140}Ce; ^{141}Pr; ^{142}Nd; ^{143}Nd; ^{144}Nd; ^{147}Sm; ^{149}Sm; ^{152}Sm; ^{153}Eu; **^{158}Gd**; ^{159}Tb; **^{160}Gd**; ^{161}Dy; ^{163}Dy; ^{165}Ho; ^{166}Er; ^{169}Tm; ^{173}Yb; ^{174}Yb; ^{175}Lu; ^{115}In; ^{192}Ir
Plasma / auxiliary / nebulizer gas:	Argon (purity min. 4.6; inlet pressure = 7 bar)
Software:	Perkin Elmer Elan V 3.4 software

2.2.3 Spectral data

For the three diagnostics, which were available as “pure substance” spectral absorbance was monitored from 190-800 nm. For this, stock solutions containing 10 mM of the probe compound in pure water (Milli-Q (Elga)) were prepared. The diagnostics Gadovist (Gd-BT-DO3A) and Omniscan (Gd-DTPA-BMA) were medical solutions without addition of substances other than small quantities of NaCl (5% and 0.1% respectively [37]) and Gd-DTPA (Magnevist) was available in 99% purity from Sigma Aldrich. The solutions were measured in 1 cm quartz glass cuvettes by a UV-1650PC UV-VIS Spectrophotometer from Shimadzu.

2.2.4 Interactions with glass

To determine interactions of the chelates with sample vessels, stock solutions containing different concentrations of gadolinium as Gd-DTPA (100 ng L^{-1}, 10 µg L^{-1} and 1 mg L^{-1} as Gd) were stored in different types of vessels (PP, and glass vessels). Several replicates of low concentrated solutions (10 µg L^{-1} and 100 ng L^{-1} as Gd) have been prepared in the respective vessel type to yield sufficient sample volume for the complete sampling period. The 1 mg L^{-1} sample was prepared only once. Hence, for this concentration, samples were taken from one vessel over the whole sampling period. This was possible, as a 10^{-3} dilution previous to measurement had to be made. In contrast, sampling for other concentration levels had to be performed by taking solutions from different sampling vessels of the same material.

Glass vials were tested without treatment and after a conditioning which is described in the following. To ensure that the glass was free of any complex forming agent which might interfere determination of gadolinium chelates, the glass was soaked for 24 h with sodium hypochlorite solution (10 mM) and afterwards cleaned with ultrapure water. Then the vials were heated (550°C) for at least 12 h, to burn organic residues in the vessels.

The gadolinium stock solutions were stored for 4 weeks. Samples were taken at least every second day. On the first day, samples were taken every hour, on the second to fifth day samples were taken every two hours. The samples were measured by ICP-MS. For a detailed measurement description cf. chapter 2.2.2. To shorten analysis time, only gadolinium isotopes have been analyzed, as for this purpose no determination of any other REE was necessary.

2.2.5 HILIC-ICP-MS

For determination and quantification of gadolinium species, in this case the MRI diagnostics, two different methods, both HILIC-ICP-MS methods and combinations of both have been tested. These methods recently published by Künnemeyer et al. [14] and Raju et al. [12] differ mainly in the buffers' pH and eluent solvent (cf. chapter 2.1) used.

For chromatographic separations a Perkin Elmer Series 200 was used. In detail: autosampler, pump, vacuum degaser and a peltier column oven of this product line were coupled to a Perkin Elmer ELAN DRC II ICP-MS. Switching between the ICP-MS autosampler and chromatographic instruments to the inlet of the nebulizer was performed via a 6-way Rheodyne® valve (Index Science & Health). The coupled system was operated by Chromera Version 2.1.2.1752 software which controlled the Perkin Elmer Elan V 3.4 software, responsible for operation of the ICP-MS.
The ICP-MS (details given in chapter 2.2.2) was configured for coupling to the HPLC. As in this case high concentrations of organic solvents had to be used, a PFA micro flow nebulizer and a spray chamber made of quartz glass in a cooling device (Peltier Cooled Cyclonic Chamber Model PC3, Elemental Scientific Inc. Omaha, U.S.) were connected via a ball- and socket joint to the injector tube (d_i = 0.9 mm). Furthermore, Platinum sampler- and skimmer cones (eSpec Sampler WE027802 and eSpec Skimmer WE027803 for Perkin Elmer Elan, Spectron Inc.) were used. To avoid carbon deposition of the organic solvents used in HPLC, oxygen (0.15 L min^{-1} (15% of plasma gas flow) was fed to the nebulizer gas stream and nebulizer gas flow was regulated to 0.6 L min^{-1}. The speed of the peristaltic pump was kept.

For separation of gadolinium species a zwitterionic ZIC-HILIC (SeQuant GmbH, Marl, Germany) was used, with d_i 2.1 mm, length 150 mm, particle size 3.5 µm and pore size 200 Å. A suitable ZIC-HILIC precolumn (SeQuant GmbH, Marl, Germany) with same inner diameter and pore size (length shortened to 20 mm and larger particle size (5 µm)) was used. Furthermore, a pre column filter (Supelco Pre Column Filter 1/16" Peek, 2 µm frit) was tested. Regeneration of the column was achieved by rinsing it with 30 column volumes (, which is 15.6 ml) of ultrapure water, followed by 30 column volumes of a 0.5 M NaCl solution. Afterwards rinsing with 30 column volumes of ultrapure water was repeated.

2.2.6 Sample preconcentration

For preconcentration of the samples different methods have been tested.

- Evaporation: Simple preconcentration method, without any further advantages
- SPE: For preconcentration of gadolinium and for a differentiation of complexed gadolinium and Gd(III) ions

The preconcentration of the samples is necessary as in most environmental samples and especially in drinking water samples the concentration of the rare earth elements including gadolinium is very low. Hence, to be able to get a reliable result, e.g., in the case of a gadolinium anomaly determination, it is necessary to preconcentrate the sample to be within the working range of the analytical method.

2.2.6.1 Preconcentration via evaporation

Preconcentration of the samples by evaporation is a very easy, however, time consuming approach. Samples in the PP vessels were heated up to 65°C in an aerated drying chamber. Higher temperatures were avoided due to limited long-term thermal stability of the vessels. Sample volume was decreased from 40 mL to 10 mL within 5 d.

The initial sample was spiked with indium, to evaluate the enrichment process. Furthermore, to verify the results a certified standard (SPS-SW2, Batch 24 from Spectrapure Standards: [La], [Ce], [Pr], [Nd], [Sm], [Eu], [Gd], [Tb], [Dy], [Ho], [Er], [Tm], [Yb], [Lu] each 2.5 µg L^{-1}) was used. After enrichment the samples were measured as described in chapter 2.2.2.

2.2.6.2 Preconcentration via SPE

For preconcentration via SPE different methods were discussed:

- SPE cartridges for removal of organic moieties (cartridges with Poly(styrenedivinylbenzene-comethylmethacrylate as base material with benzene rings as functional groups)
- Anion exchangers
- Cation exchangers
- Chelation of cations

Methods based on chelation for preconcentration were rejected, as potentially the ligands may be exchanged during this process and hence, a differentiation between chelated cations and free cations is not possible.

Cation exchange is only possible for preconcentration of free Gd(III) ions. Even though focus was on enrichment of the organic species this method was tested, to be able to enrich Gd(III) which might be liberated from ligands, e.g. due to transmetallation or oxidation. As pH of the sample might influence the binding sites of the SPE material, a strong ion exchanger (sulfonic acid) was chosen, as in these materials the speciation of the binding sites is functional for exchanging purposes at $pH \leq pK_a$ [38].

Anion exchange is only possible for negatively charged species. Also, for this method, a strong ion exchanger (alkyl trimethyl ammonium chloride) was chosen. The extraction methods for both ion exchange SPEs have been adapted from manufacturer's information (SCP Science). They are presented in the following.

For conditioning, anion SPE cartridges (DigiSep Red (500 mg / 6 mL cartridges from SCP Science) were rinsed with 1.5 mL 2 M HNO_3 solution. After a vacuum drying step the cartridge was rinsed with 2.5 mL ultra pure water, then dryed again and rinsed with 2.5 mL NaOH (1 M NaOH). After another vacuum drying step, the cartridge was rinsed with 2.5 mL ultra pure water and finally vacuum dried again. After these conditioning steps, the sample was applied (10 mL) and subsequently the cartridge vacuum dried. This sample flushed through the SPE was kept for analysis ("sample flush" in the following). For removal of positively charged (in this case Gd(III) ions) or neutral substances, the cartridge was rinsed with 2.5 mL ultrapure water and vacuum dried This impurity removal flush was kept for analysis as well

(“impurity removal” in the following). For elution of the analyte, the cartridge was rinsed with 0.5 mL HNO_3-solution and vacuum dried. This step is repeated 3 times. The flow rates for all steps described above were set to 1 mL min^{-1}. For regeneration, the same steps are repeated with the same flow rates as for initial conditioning.

As samples for anion exchange, Gd-DOTA and Gd(III) solutions were prepared in ultrapure water. The following sample compositions have been tested: 50, 5 and 0.5 µM Gd as Gd-DOTA, 50 µM Gd as $GdCl_3$ and a mixture of 50 µM Gd as $GdCl_3$ and 50 µM Gd as Gd-DOTA.

For conditioning, cation SPE cartridges (DigiSep Green (500 mg / 6 mL cartridges from SCP Science) were rinsed with 1.5 mL of 2 M HNO_3 solution and after a vacuum drying step rinsed with 2.5 mL ultra pure water. As last step for conditioning the cartridge was vacuum dried again. The sample was applied (10 mL) and afterwards the cartridge was vacuum dried again. The sample flushed through was kept for analysis (again referred to with “sample flush”). For removal of impurities, the cartridge was rinsed with 2.5 mL ultrapure water and vacuum dried afterwards. Also, this flush was kept for further analysis (sample is named “impurity removal”). For analyte elution, rinsing with 0.5 mL HNO_3 solution and vacuum drying was repeated 3 times. The flow rates for all steps were 1 mL min^{-1}. For regeneration, the conditioning steps were applied with the same flow rates.

For cation exchange Gd-DTPA and Gd-BT-DO3A samples were prepared in ultrapure water and drinking water, to detect matrix effects. The tested concentrations of the samples (spiked with only a single substance) were 10 ng $L^{-1}$and 1 µg L^{-1}.

All samples for cation and anion exchange were tested in triplicate and measured with ICP-MS as described in chapter 2.2.2.

2.3 Results and discussion

2.3.1 Spectral data

The spectral data obtained are presented in Figure 2.1.The absorbance maxima of the chelates are 195 nm for Gd-BT-DO3A, 200 nm for Gd-DTPA: 200 nm and 210 nm for Gd-DTPA-BMA. Due to the maxima in the middle to lower UV range, it is not possible to determine gadolinium species in trace concentrations by HPLC-UV methods using organic solvents, as the absorbance maxima of these solvents are usually in the same range. The detection of high concentrations of gadolinium species is possible and also in experiments where no organic solvents are necessary, e.g. pulse radiolysis experiments (cf. chapter 5), it is possible to determine species concentrations via absorbance monitoring.

2.3.2 Interactions with glass

Experimental results for determination of interactions with glass are shown in Figure 2.2. The concentration of total gadolinium in the sample in relation to the total gadolinium concentration at the start of the experiment is increasing step wise over time for 10 µg L^{-1} in PP vials and decreasing step wise for 10 µg L^{-1} in glass vessels (cf. Figure 2.2 b) and d)). This is concluded to be due to measurement of samples from different original preparations, which were made to obtain sufficient sampling volume for the whole monitoring period (cf. chapter 2.2.4) and comparison of the result to the one preparation which was measured at the beginning of the sampling period. Hence, the stepwise increase / decrease may be an artifact due to differences in concentrations in the single original preparations rather than due to a chemical processes over time. For the other tested samples such a trend is not detectable (cf. Figure 2.2 a) and c)). Hence, it is concluded, that the changes in total concentration are negligible. If interactions with glass are due to sorption processes, as described previously for gadolinium chelates [4] a decrease of total gadolinium should have been observed. If interactions with glass are due to transmetalation effects as described for other chelates [39], no change in total gadolinium concentration should be measurable. From the presented results it is concluded, that the described interactions [4, 12] are more likely to be based on transmetalation processes. However, to verify this statement, further experiments would be necessary that are beyond the scope of this study.

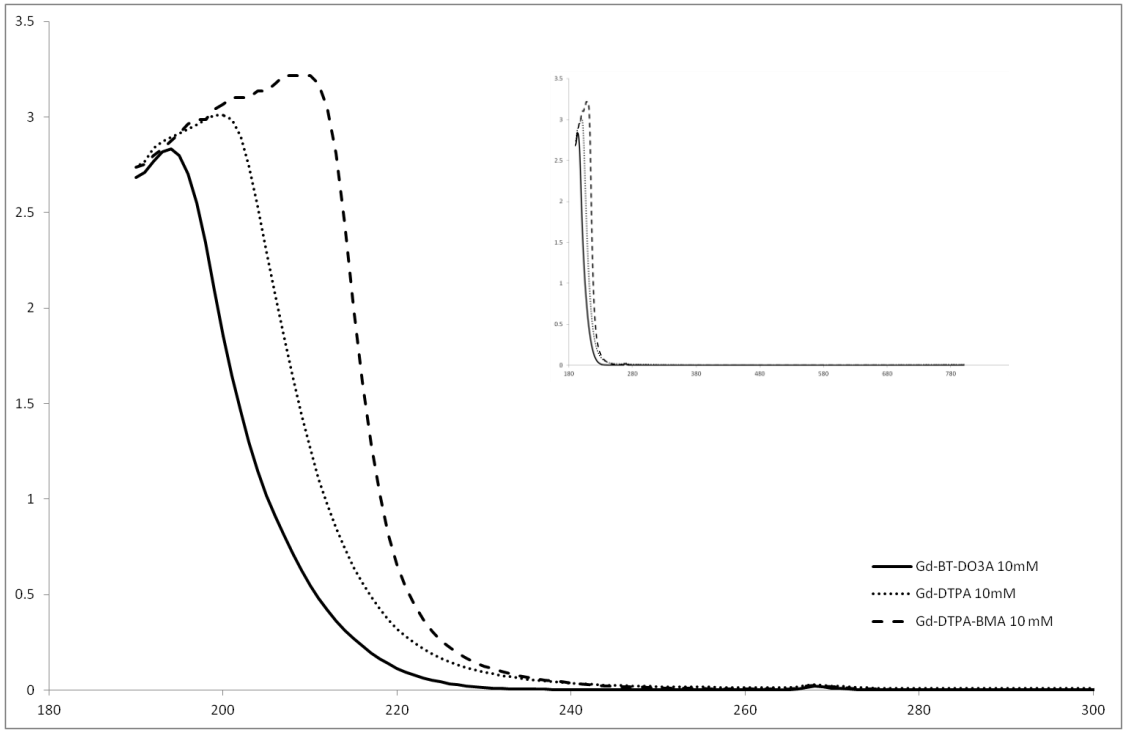

Figure 2.1: UV/VIS-spectra of gadolinium diagnostics (10mM), which were available as "pure" substances, in the relevant wavelength range. The insert displays the full spectra

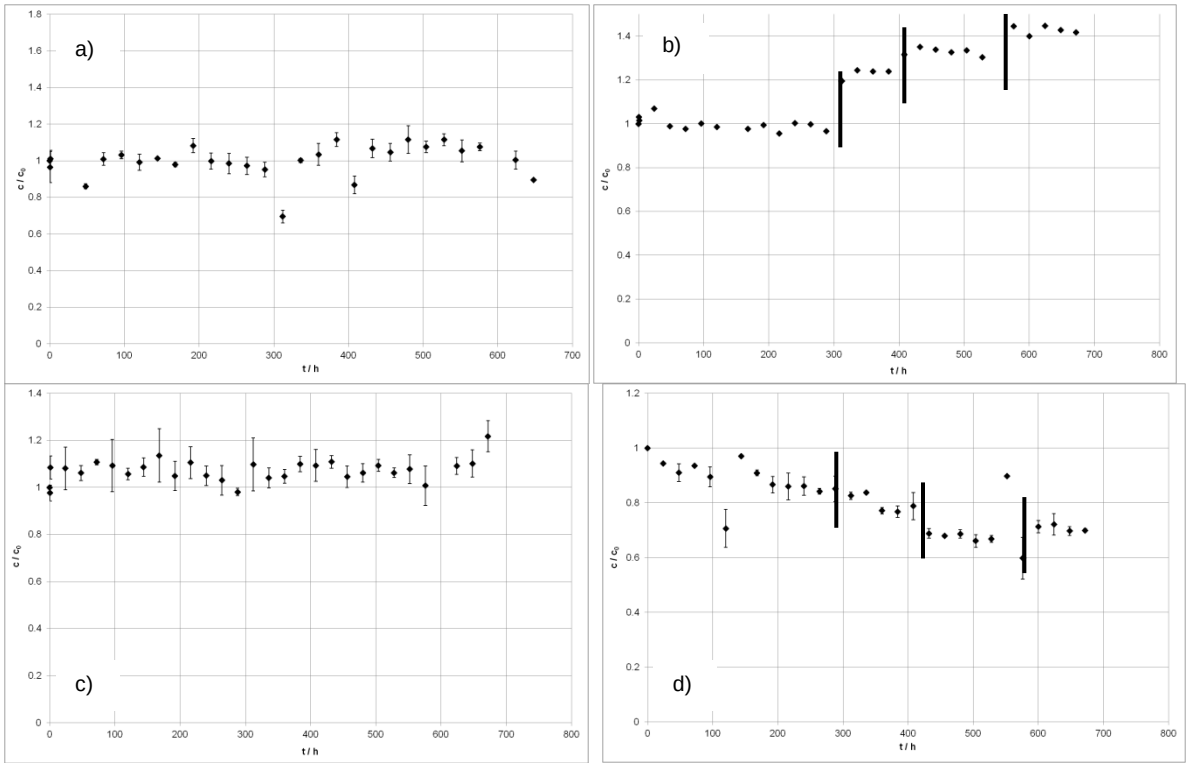

Figure 2.2: Behaviour of Gd-DTPA in different concentrations during storage in different materials, [Gd] = 1 mg L^{-1} for a) and c), [Gd] = 10 µg L^{-1} for b) and d), storage vessel material was PP for c) and d) and glass for a) and b); marked by black bars: Change of sampling vessels

2.3.3 Determination of complexes with HILIC-ICP-MS

For the application of a HILIC separation, prior to ICP-MS analysis, a complete modification of the sample introduction system is necessary. Hence, a first test has been performed to check the quality of hyphenation for the different devices.

For this test, a validated method for platinum species analysis (for method description cf. chapter 2.5) was used. To this end, the ZIC-HILIC column was exchanged by a Discovery HS F5 (Supelco) and to avoid high background noises by platinum the cones, sampler and skimmer cones of the ICP-MS were substituted by nickel cones. Beside these minor necessary changes for a validation of the instrument setup, the instrumental setup for use of HILIC remained identical. A modification compared to the validated method was the injector tube size. The one used for the HILIC method featured an inner diameter of 0.9 mm instead of 1.85 mm in the validated method. This injector tube was kept for the test. The achieved chromatogram (cf. Figure 2.3) showed the same retention times as in the validated method. However, lower intensities were observed which is due to the smaller inner diameter of the injector tube. This gave evidence of successful hyphenation. Thus, method development for determination of gadolinium species via HILIC-ICP-MS was continued.

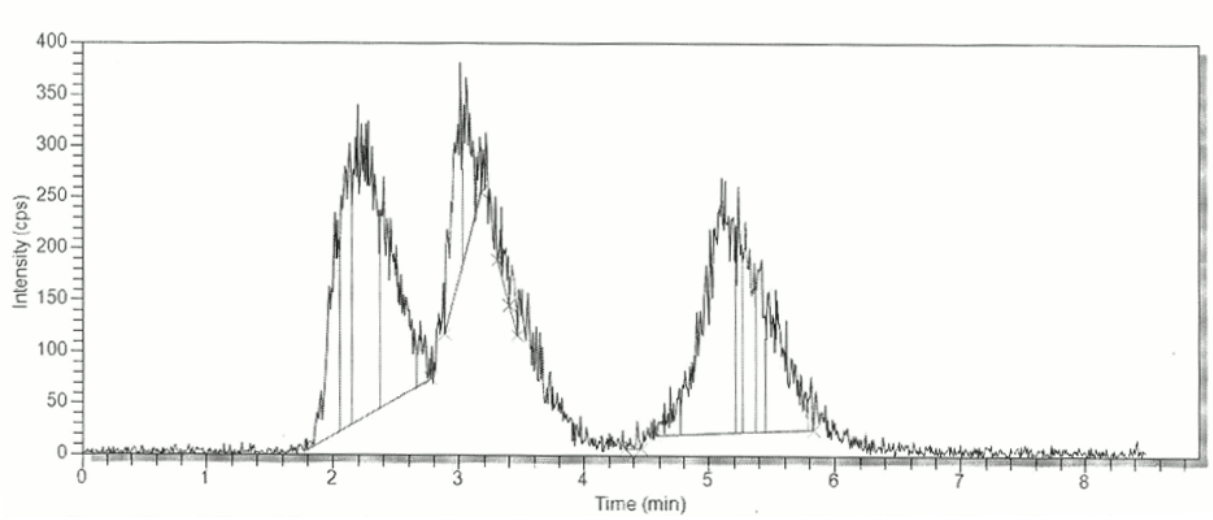

Figure 2.3: Separation of cis-, carbo- and oxali-platin using the LC-ICP-MS system setup for organic solvents as eluents (same setup used as for HILIC-ICP-MS measurements)

First qualitative tests for hyphenation of HILIC to the ICP-MS were performed for the use of the method described by Künnemeyer et al. [4] (cf. chapter 2.1). These involved injection of a single gadolinium species (Gd-BT-DO3A), to verify if signal detection with the instrument setup was possible. For this, 5 µL Gd-BT-DO3A solution ([Gd] = 10^{-8} M) was injected with an eluent flow of 0.1 mL min^{-1} which is less than the 0.3 mL min^{-1} used by Künnemeyer et al. [4], to avoid high pressure and leakage in the sensitive system. The ACN / water ratio of the eluent was 76/24 ACN / water, formiate buffer concentration was 12.5 mM and pH set to 3.5, which are the same conditions used by Künnemeyer et al. [4]. By application of this method a signal for the injected gadolinium species was detectable. However, no reproducible results could be obtained. This effect may not be explained by the lowered flow rate. However, it may be due to hardware problems which ocured throughout the whole period of method development. The same effect was observed for the method published by Raju et al. [12]. Adjustments to both methods (flow rates, buffer strength and pH and ACN / water ratio) were made and combinations of both methods have been tested to identify the suitable method for the available, sensitive system.

An adjustment of both flow rate and ACN / water ratio was necessary to obtain narrower peaks and a reproducible retention time. The flow was increased gradually from 0.1 mL min^{-1} to 0.3 mL min^{-1}, which was the flow rate stated by Künnemeyer et al. [4]. Furthermore, the ACN / water ratio was increased from 60/40 to 80/20 at buffer strength of 10 mM formiate yielding a pH of 3.5. Increasing ACN content led to delayed elution and increasing water content to a significant narrowing of the peaks. By a variation of the Künnemeyer method to a ACN / water ratio of 70/30 at a buffer strength of 15 mM (formiate buffer), a pH = 3.5 and a flow rate of 0.3 mL min^{-1}, sufficient retention and narrow peaks without coelution were obtained (cf. Figure 2.4). Furthermore, the influence of the buffer has been tested, as Raju et al. [12] used higher buffer concentrations and higher pH than Künnemeyer et al. [4] (20 mM acetate buffer at pH = 5.8 and 12.5 mM formiate buffer at pH =3.8, respectively). Three different buffers were applied, as gadolinium species are charged differently and hence, ionic strength as well as pH are of importance. Two formic acid / formiate buffer systems adjusted to pH = 3.5 and pH = 3.8 (buffer strength varied for both pHs between 5 and 50 mM), respectively and an acetic acid / acetate buffer at pH = 5.1 (buffer strength varied between 1 and 30 mM) were tested. The long-term use of formiate buffers resulted in hardware problems (pressure

increase, clogging at different places of the system) and higher gadolinium background concentration, due to lower purity of these buffer reagents. Using the acetate buffer fewer problems occurred and reproducible signal intensities and retention times were obtained. Additionally, the background concentration of gadolinium was lower, when using the acetate buffer.

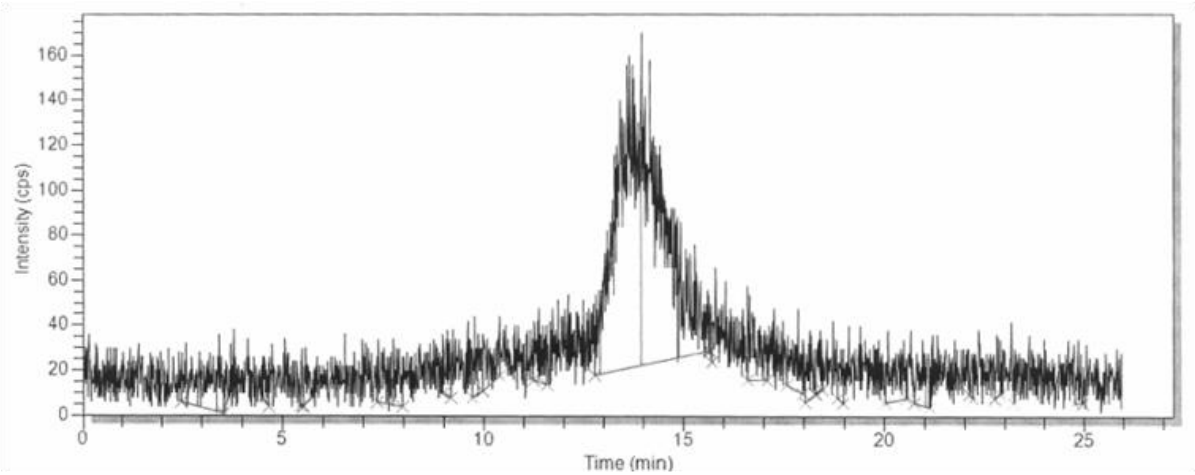

Figure 2.4: Chromatogram of 5×10^{-8} M Gd-BT-DO3A in ultrapure water (70/30 ACN / water, 15 mM formiate buffer, flow rate: 0.3 mL min^{-1})

Changing buffer concentration led to different behaviour of gadolinium species. The neutral species Gd-BT-DO3A and Gd-DTPA-BMA showed no buffer concentration dependency in the tested concentration range, but for the negatively charged Gd-DTPA significant changes in retention time were observable, due to modifications in buffer strength. This effect has been reported by Raju et al. as well [12]. For all tested buffer systems (acetate and formiate buffer) higher concentrations of the buffer led to earlier elution of Gd-DTPA. Furthermore, Gd-DTPA peaks were sharper, with less tailing, when higher acetate buffer concentrations were used.

The best separation has been obtained for the buffer-independent species Gd-BT-DO3A and the buffer-dependent species Gd-DTPA at an ACN / water ratio of 70/30 with a flow rate of 0.2 mL min^{-1} in an acetate buffered system (30 mM, pH = 5.1) (cf. Figure 2.5). In this case Gd-DTPA was eluted earlier than Gd-BT-DO3A. Quality of the separation is mainly influenced by buffer strength. A higher buffer concentration led to a better separation of the two peaks. A separation using the same LC conditions except exchange of buffer (formiate buffered system, c = 30 mM, pH = 3.81) was not possible (cf. Figure 2.6) which corroborated the hypothesis that the separation also depends on pH. The order of elution was the

same as for the method published by Raju et al. [12] (Gd-DTPA is eluted before Gd-BT-DO3A). Künnemeyer et al. [4] stated another order of elution. For comparison, the elution order described by Raju et al [12] is Gd-BOPTA > Gd-DTPA > Gd-DOTA > Gd-DTPA-BMA > Gd-BT-DO3A, whereas the elution order described by Künnemeyer et al. [4] is Gd-BOPTA > Gd-DTPA-BMA > Gd-BT-DO3A > Gd-DOTA > Gd-DTPA. The change in the order of elution is proposed to be due to the increased buffer strength in the method used by Raju et al. [12], as this leads to an earlier elution of ionic gadolinium species.

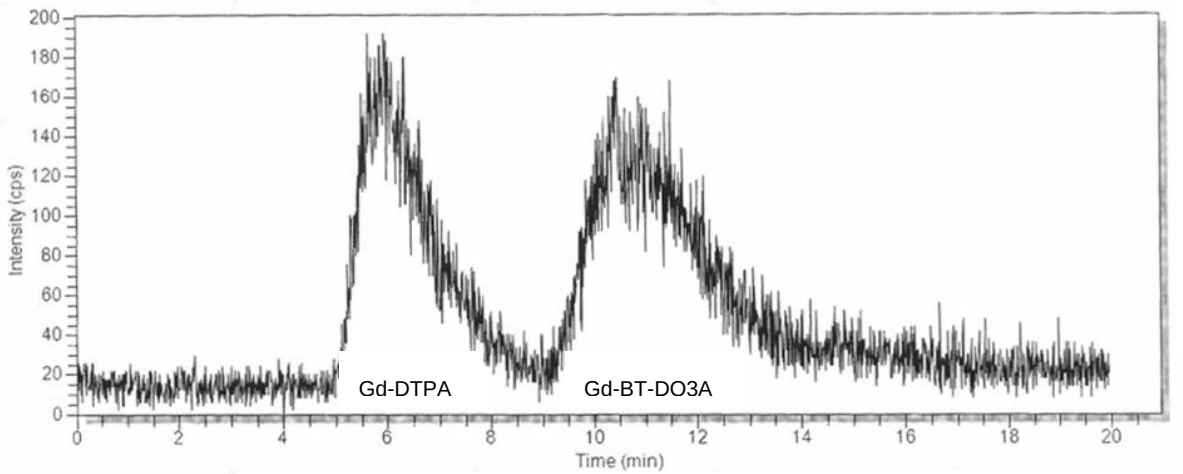

Figure 2.5: Signals for a 10^{-7} M Gd-DTPA and 10^{-7} M Gd-BT-DO3A sample (70/30 ACN / water, 30 mM acetate buffer, flow rate: 0.2 mL min^{-1})

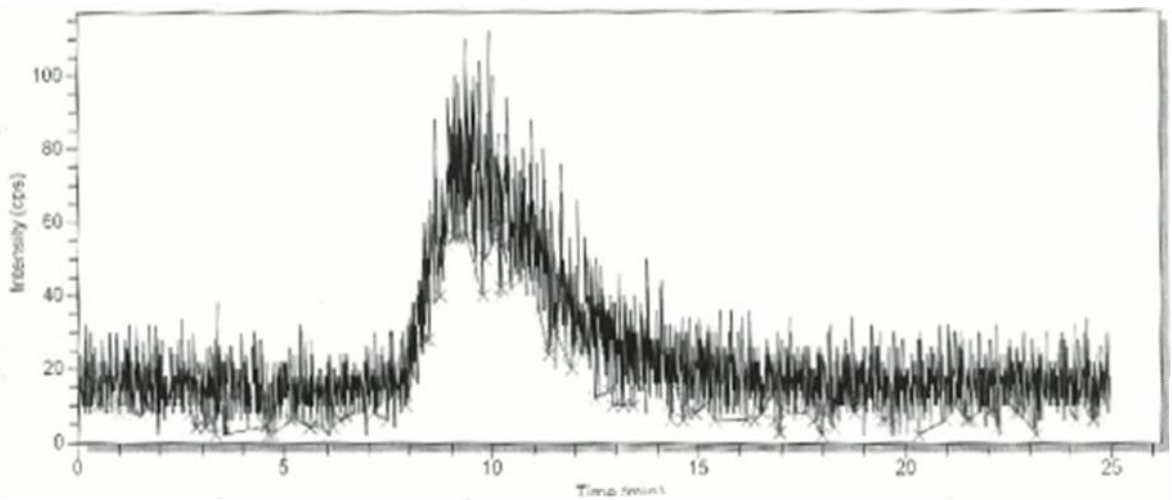

Figure 2.6: Chromatogram for a mixed 10^{-7} M Gd-DTPA and 10^{-7} M Gd-BT-DO3A sample (70/30 ACN / water, 30 mM formiate buffer, flow rate: 0.2 mL min^{-1})

2.3.4 Sample preconcentration

For preconcentration two different methods were tested. An evaluation of this method is simply obtained by calculation of the recovery rate, which is defined as deviation of the measured concentration from the target value.

A very simple approach for preconcentration is evaporation of the sample. For this, tap water samples, spiked with indium as internal quality standard have been investigated. The samples were enriched by a factor of 4. For comparison, a synthetic sample in pure water was tested as well.

The recovery rates of a synthetic sample (1.5 µg L^{-1} REE standard solution with 4 µg L^{-1} indium standard in ultrapure water) for REE isotopes and indium as internal quality control standard are presented in Table 2.2. The resulting recovery rates were excellent. Hence, further tests were performed with drinking water samples. The resulting recovery rates are presented in Table 2.3. Also, with these samples good recovery rates could be achieved, with exception of cerium. However, cerium analysis is interfered by oxide generation (cf. chapter 3). For analysis of the total element concentration of REEs this enrichment method is reliable and easily applicable.

Table 2.2: Recovery rates of the measured analytes after preconcentration via evaporation for a synthetic sample in ultra pure water

Isotope	Recovery rate	Isotope	Recovery rate
^{115}In	103%	^{158}Gd	107%
^{139}La	108%	^{159}Tb	109%
^{140}Ce	109%	^{160}Gd	109%
^{141}Pr	111%	^{161}Dy	111%
^{142}Nd	112%	^{163}Dy	112%
^{143}Nd	110%	^{165}Ho	111%
^{144}Nd	111%	^{166}Er	112%
^{147}Sm	111%	^{169}Tm	111%
^{149}Sm	112%	^{173}Yb	113%
^{152}Sm	112%	^{174}Yb	111%
^{153}Eu	112%	^{175}Lu	111%

Table 2.3: Recovery rates for the determination of REE after preconcentration via evaporation; mean of 10 drinking water samples

Isotope	Recovery rate		Isotope	Recovery rate
^{140}Ce	70%		^{159}Tb	105%
^{141}Pr	96%		^{160}Gd	97%
^{142}Nd	92%		^{161}Dy	95%
^{143}Nd	84%		^{163}Dy	102%
^{144}Nd	88%		^{165}Ho	91%
^{147}Sm	86%		^{166}Er	99%
^{149}Sm	86%		^{169}Tm	96%
^{152}Sm	104%		^{173}Yb	108%
^{153}Eu	104%		^{174}Yb	99%
^{158}Gd	97%		^{175}Lu	101%

As an alternative to the slow evaporation method SPE methods were tested. The advantage of SPE is that additional to preconcentration, a separation of ionic gadolinium species from other gadolinium species is possible. Furthermore enrichment factors of max. 200 may be achieved for the tested SPE cartridges.

For anion exchange, solutions with an anionic gadolinium species (Gd-DOTA) in different concentrations, a solution containing only Gd(III) and a solution with a mixture of both have been tested. The recovery rates for the respective samples are presented in Table 2.4. The obtained recovery rates are > 90% for Gd-DOTA samples. These recovery rates are excellent for an SPE method. Yet it has to be considered that the tested matrix was pure water, with no competition effect by any other ions. For a mixture of anionic and cationic gadolinium species a lower recovery rate was achieved. Nevertheless, this method is a very promising approach for differentiation and preconcentration of anionic gadolinium species.

Table 2.4: Recovery rates for SPE samples, using an anion exchange resin

Gadolinium species	[Gd] / µM	Recovery rate
Gd-DOTA	50	98%
Gd-DOTA	5	93%
Gd-DOTA	0.5	98%
Gd-DOTA and Gd(III)	50 both	79%

For cation exchange, solutions with an anionic gadolinium species (Gd-DTPA) and a non-ionic species have been tested in different concentrations and matrices. For evaluation of this method a mass balance has been performed (cf. equation 2.1). In this equation (cf. eq. 2.1) the mass of gadolinium in the eluate should be equal to zero as no analyte is supposed to be retarded by the SPE material. Hence, equation 2.2 is resulting.

$$Mass_{sample} = Mass_{sample\ flush} + Mass_{impurity\ removal} + Mass_{Eluate} \quad (2.1)$$

$$Mass_{sample} = Mass_{sample\ flush} + Mass_{impurity\ removal} \quad (2.2)$$

The results are presented in Table 2.5. The recovery of gadolinium species in sample flush and the flush for impurity removal is quite well, with exception for low concentrations of Gd-DTPA. Yet the presented results are only triplicate experiments in used and regenerated SPE cartridges. For a comprehensive study, further experiments are necessary.

Table 2.5: Mass balance results for cation exchange experiments; different concentrations of Gd-DTPA (anionic) and Gd-BT-DO3A (neutral) in ultrapure water and a drinking water matrix

Matrix	Gadolinium species	[Gd] / µg L^{-1}	$Mass_{sample}$ / ($Mass_{sample\ flush}$ + $Mass_{impurity\ removal}$) in %	$Mass_{sample}$ / ($Mass_{sample\ flush}$ + $Mass_{impurity\ removal}$ + $Mass_{Eluate}$) in %
Ultrapure water	Gd-DTPA	0.01	75	122
	Gd-DTPA	1	107	109
	Gd-BT-DO3A	0.01	124	197
	Gd-BT-DO3A	1	98	109
Drinking water	Gd-DTPA	0.01	68	94
	Gd-DTPA	1	95	94
	Gd-BT-DO3A	0.01	97	98
	Gd-BT-DO3A	1	103	104

2.4 Conclusions

From experiments presented in this chapter important aspects for the further proceeding have been revealed. The absorbance spectra of gadolinium chelates have been determined for application in further experiments, e.g. pulse radiolysis experiments for the determination of reaction rate constants.

In literature, a decrease of gadolinium species concentration is described, when glass ware is used for storage [4, 12]. It has been proposed, that this effect is due to sorption [4]. However, a sorption processes would lead to a decrease of the total gadolinium concentration. In the presented experiments no significant decrease of the total gadolinium concentration has been detected. Hence, it is assumed, that transmetalation processes occur. Transmetalation processes have been proposed for other chelates when using glass ware [39]. However, for a final elucidation whether sorption effects or transmetalation is responsible for the decrease of gadolinium species, further experiments are necessary. Yet use of glassware for other experiments is omitted.

Preconcentration of gadolinium via evaporation of the sample is a feasible, but a time consuming method with low enrichment factors. The separation of Gd-DOTA from other gadolinium species by anion exchange SPE is also feasible. However, this method is in comparison to the simple evaporation method very work intensive. Furthermore, by this method it is only possible to preconcentrate anionic gadolinium species and a separation of these from the matrix is possible. Other gadolinium species are also charged negatively, such as Gd-DTPA^{-2}, Gd-BOPTA^{-2}, Gd-EOB-DTPA^{-2} and Gd-MS-325^{3-}, hence, a preconcentration of at least those four and Gd-DOTA is possible via this method. Other SPE methods might be used to preconcentrate the cationic and neutral gadolinium species. However, these SPE methods are only able to discriminate between charged and neutral species and not between the single species. Hence, it is not possible to perform SPE previous to ICP-MS measurements for determination of single gadolinium species.

HILIC-ICP-MS is able to discriminate and quantify single gadolinium species. The coupling of HILIC to ICP-MS is extensive and involves a complete modification of the sample introduction system. This is only feasible for an ICP-MS system which is used in long term for determinations, that require such a sample introduction system. Hence, further developments of the very promising method have been restricted. Yet

a system in which a single species has to be detected is only necessary for evaluation of processes in real water samples. Previous experiments under laboratory conditions do not necessarily need a separation method for evaluation since they are carried out with single substances.

The information gained from the results presented in this chapter give necessary information and tools for successful analysis applications in the further proceeding of the study.

2.5 Supplement

The method for determination of platinum species, which was used to test hyphenation of the HILIC system to ICP-MS, is described in the following. The described method is validated according to the standards given in DIN EN ISO/IEC 17025.

For analysis of platinum species, instrumental setup is changed only minor compared to the one used for gadolinium species analysis (cf. chapter 2.3.3). However, in the validated reference method, a larger injector tube (d_i = 1.85 mm) is used and a glass nebulizer in a non-cooled spray chamber. The separation column is a Discovery HS F5 HPLC Column 15 cm × 2.1 mm, 3 µm (Supleco) with a Discovery HS F5 Guard Column (2 cm × 2.1 mm, 3 µm (Supleco)). Furthermore, a Pre-Column Filter (1/16'' Peek 2 µm Frit Sigma Aldrich) is used. The eluent is ammonium formiate buffer (20 mM in 4 vol% methanol, pH = 3.75) /water (50/50). Flow rate is set to 0.3 ml min^{-1} with a total run time of 8 min. LOQ of the validated method is 0.3 µg L^{-1} for all three species (cis-, carbo- and oxali-platin).

2.6 Literature

1. Kimura, J., T. Ishiguchi, J. Matsuda, R. Ohno, A. Nakamura, S. Kamei, K. Ohno, T. Kawamura, and K. Murata, Human comparative study of zinc and copper excretion via urine after administration of magnetic resonance imaging contrast agents. *Radiation Medicine - Medical Imaging and Radiation Oncology*, 2005. **23**(5): 322-326.
2. Weinmann, H.J., M. Laniado, and W. Mützel, Pharmacokinetics of GdDTPA/dimeglumine after intravenous injection into healthy volunteers. *Physiological chemistry and physics and medical NMR*, 1984. **16**(2): 167-172.
3. Hagan, J.J., S.C. Taylor, and M.F. Tweedle, Fluorescence detection of gadolinium chelates separated by reversed-phase high-performance liquid chromatography. *Analytical Chemistry*, 1988. **60**(6): 514-516.
4. Künnemeyer, J., L. Terborg, B. Meermann, C. Brauckmann, I. Möller, A. Scheffer, and U. Karst, Speciation analysis of gadolinium chelates in hospital effluents and wastewater treatment plant sewage by a novel HILIC/ICP-MS method. *Environmental Science and Technology*, 2009. **43**(8): 2884-2890.
5. Bau, M. and P. Dulski, Anthropogenic origin of positive gadolinium anomalies in river waters. *Earth and Planetary Science Letters*, 1996. **143**(1-4): 245-255.
6. Lawrence, M.G., J. Keller, and Y. Poussade, Removal of magnetic resonance imaging contrast agents through advanced water treatment plants. *Water Science and Technology*, 2010. **61**(3): 685-692.
7. Telgmann, L., M. Holtkamp, J. Künnemeyer, C. Gelhard, M. Hartmann, A. Klose, M. Sperling, and U. Karst, Simple and rapid quantification of gadolinium in urine and blood plasma samples by means of total reflection X-ray fluorescence (TXRF). *Metallomics*, 2011. **3**(10): 1035-1040.
8. Telgmann, L., M. Sperling, and U. Karst, Determination of gadolinium-based MRI contrast agents in biological and environmental samples: A review. *Analytica Chimica Acta*, 2013.

9. Künnemeyer, J., L. Terborg, S. Nowak, L. Telgmann, F. Tokmak, B.K. Krämer, A. Günsel, G.A. Wiesmüller, J. Waldeck, C. Bremer, and U. Karst, Analysis of the contrast agent Magnevist and its transmetalation products in blood plasma by capillary electrophoresis/electrospray ionization time-of-flight mass spectrometry. *Analytical Chemistry*, 2009. **81**(9): 3600-3607.

10. Campa, C., M. Rossi, A. Flamigni, E. Baiutti, A. Coslovi, and L. Calabi, Analysis of gadobenate dimeglumine by capillary zone electrophoresis coupled with electrospray-mass spectrometry. *Electrophoresis*, 2005. **26**(7-8): 1533-1540.

11. Vora, M.M., S. Wukovnig, R.D. Finn, A.M. Emran, T.E. Boothe, and P.J. Kothari, Reversed-phase high-performance liquid chromatographic determinationof gadolinium-diethylenetriaminepentaacetic acid complex. *Journal of Chromatography A*, 1986. **369**(C): 187-192.

12. Raju, C.S.K., A. Cossmer, H. Scharf, U. Panne, and D. Lueck, Speciation of gadolinium based MRI contrast agents in environmental water samples using hydrophilic interaction chromatography hyphenated with inductively coupled plasma mass spectrometry. *Journal of Analytical Atomic Spectrometry*, 2010. **25**(1): 55-61.

13. Raju, C.S.K., D. Luck, H. Scharf, N. Jakubowski, and U. Panne, A novel solid phase extraction method for pre-concentration of gadolinium and gadolinium based MRI contrast agents from the environment. *Journal of Analytical Atomic Spectrometry*, 2010. **25**(10): 1573-1580.

14. Künnemeyer, J., L. Terborg, S. Nowak, A. Scheffer, L. Telgmann, F. Tokmak, A. Günsel, G. Wiesmüller, S. Reichelt, and U. Karst, Speciation analysis of gadolinium-based MRI contrast agents in blood plasma by hydrophilic interaction chromatography/electrospray mass spectrometry. *Analytical Chemistry*, 2008. **80**(21): 8163 - 8170.

15. Telgmann, L., C.A. Wehe, J. Künnemeyer, A.C. Bülter, M. Sperling, and U. Karst, Speciation of Gd-based MRI contrast agents and potential products of transmetalation with iron ions or parenteral iron supplements. *Analytical and Bioanalytical Chemistry*, 2012: 1-9.

16. Frenzel, T., P. Lengsfeld, H. Schirmer, J. Huetter, and H.-J. Weinmann, Stability of gadolinium-based magnetic resonance imaging contrast agents in human serum at 37 °C*. Investigative Radiology*, 2008. **43**(12): 817-828.

17. Kahakachchi, C.L. and D.A. Moore, Speciation of gadolinium in gadolinium-based magnetic resonance imaging agents by high performance liquid chromatography inductively coupled plasma optical emission spectrometry*. Journal of Analytical Atomic Spectrometry*, 2009. **24**(10): 1389-1396.

18. Mazzucotelli, A., V. Bavastello, E. Magi, P. Rivaro, and C. Tomba, Analysis of gadolinium polyaminopolycarboxylic complexes by HPLC-ultrasonic nebulizer-ICP-AES hyphenated technique*. Analytical Proceedings including Analytical Communications*, 1995. **32**(5): 165-167.

19. Telgmann, L., C.A. Wehe, M. Birka, J. Künnemeyer, S. Nowak, M. Sperling, and U. Karst, Speciation and isotope dilution analysis of gadolinium-based contrast agents in wastewater*. Environmental Science and Technology*, 2012. **46**(21): 11929-11936.

20. Pfundstein, P., D. Flottmann, C. Martin, W. Schulz, K.M. Ruth, A. Wille, T. Moritz, and A. Steinbach, Gadolinium-based MRI contrast agents: IC-ICP/MS analysis*. G.I.T. Laboratory Journal Europe*, 2011. **15**(7-8): 31-33.

21. Pfundstein, P., C. Martin, W. Schulz, K.M. Ruth, A. Wille, T. Moritz, A. Steinbach, and D. Flottmann, IC-ICP-MS analysis of gadolinium-based MRI contrast agents*. LC-GC Europe*, 2011: 16-18.

22. Andra¡si, M., A. Gaspar, O. Kovacs, Z. Baranyai, A. Klekner, and E. Brücher, Determination of gadolinium-based magnetic resonance imaging contrast agents by micellar electrokinetic capillary chromatography*. Electrophoresis*, 2011. **32**(16): 2223-2228.

23. Loreti, L. and J. Bettmer, Determination of the MRI contrast agent Gd-DTPA by SEC–ICP–MS*. Analytical and Bioanalytical Chemistry*, 2004. **379**: 1050-1054.

24. Falta, T., G. Koellensperger, A. Standler, W. Buchberger, R.M. Mader, and S. Hann, Quantification of cisplatin, carboplatin and oxaliplatin in spiked human plasma samples by ICP-SFMS and hydrophilic interaction liquid chromatography (HILIC) combined with ICP-MS detection. *Journal of Analytical Atomic Spectrometry*, 2009. **24**(10): 1336-1342.

25. Hemström, P., Y. Nygren, E. Björn, and K. Irgum, Alternative organic solvents for HILIC separation of cisplatin species with on-line ICP-MS detection. *Journal of Separation Science*, 2008. **31**(4): 599-603.

26. Nygren, Y., P. Hemstroem, C. Astot, P. Naredi, and E. Bjoern, Hydrophilic interaction liquid chromatography (HILIC) coupled to inductively coupled plasma mass spectrometry (ICPMS) utilizing a mobile phase with a low-volatile organic modifier for the determination of cisplatin, and its monohydrolyzed metabolite. *Journal of Analytical Atomic Spectrometry*, 2008. **23**(7): 948-954.

27. Hao, Z., B. Xiao, and N. Weng, Impact of column temperature and mobile phase components on selectivity of hydrophilic interaction chromatography (HILIC). *Journal of Separation Science*, 2008. **31**(9): 1449-1464.

28. Ikegami, T., K. Tomomatsu, H. Takubo, K. Horie, and N. Tanaka, Separation efficiencies in hydrophilic interaction chromatography. *Journal of Chromatography A*, 2008. **1184**(1-2): 474-503.

29. Kulaksiz, S. and M. Bau, Contrasting behaviour of anthropogenic gadolinium and natural rare earth elements in estuaries and the gadolinium input into the North Sea. *Earth and Planetary Science Letters*, 2007. **260**(1-2): 361-371.

30. Lawrence, M.G. and D.G. Bariel, Tracing treated wastewater in an inland catchment using anthropogenic gadolinium. *Chemosphere*, 2010. **80**(7): 794-799.

31. Verplanck, P.L., H.E. Taylor, D.K. Nordstrom, and L.B. Barber, Aqueous stability of gadolinium in surface waters receiving sewage treatment plant effluent Boulder Creek, Colorado. *Environmental Science and Technology*, 2005. **39**(18): 6923-6929.

32. Kulaksiz, S. and M. Bau, Anthropogenic gadolinium as a microcontaminant in tap water used as drinking water in urban areas and megacities. *Applied Geochemistry*, 2011. **26**(11): 1877-1885.

33. Hennebrüder, K., R. Wennrich, J. Mattusch, H.J. Stärk, and W. Engewald, Determination of gadolinium in river water by SPE preconcentration and ICP-MS. *Talanta*, 2004. **63**(2): 309-316.

34. Möller, P., P. Dulski, M. Bau, A. Knappe, A. Pekdeger, and C. Sommer-Von Jarmersted, Anthropogenic gadolinium as a conservative tracer in hydrology. *Journal of Geochemical Exploration*, 2000. **69-70**: 409-414.

35. Möller, P., P. Dulski, and J. Luck, Determination of rare earth elements in seawater by inductively coupled plasma-mass spectrometry. *Spectrochimica Acta Part B: Atomic Spectroscopy*, 1992. **47**(12): 1379-1387.

36. *Analytical detection limit guidance & laboratory guide for determining method detection limits*, in *PUBL-TS-056-96*, Wisconsin Department of Natural Resources. 1996.

37. Idee, J.M., M. Port, I. Raynal, M. Schaefer, S. Le Greneur, and C. Corot, Clinical and biological consequences of transmetallation induced by contrast agents for magnetic resonance imaging: A review. *Fundamental and Clinical Pharmacology*, 2006. **20**(6): 563-576.

38. Camel, V., Solid phase extraction of trace elements. *Spectrochimica Acta Part B: Atomic Spectroscopy*, 2003. **58**(7): 1177-1233.

39. Ulanski, P., E. Bothe, K. Hildenbrand, J.M. Rosiak, and C. von Sonntag, Hydroxyl-radical-induced reactions of poly(acrylic acid); a pulse radiolysis, EPR and product study. Part I. Deoxygenated aqueous solutions. *Journal of the Chemical Society, Perkin Transactions 2*, 1996(1): 13-22.

3 Occurrence of gadolinium in the water cycle

3.1 Introduction

The gadolinium anomaly was first discovered by Bau and Dulski in 1996 [1]. It was the first time that anthropogenic gadolinium had been detected in the environment. The anomaly describes elevated concentrations of gadolinium which have been found in environmental aquatic samples all over the world by now.

The anomaly is calculated as the ratio of the expected total gadolinium concentration in a sample and the measured concentration. The geogenic gadolinium concentration, which is the expected concentration, can be derived from an interpolation of normalized concentrations of other REEs (cf. chapter 3.2). Hence, the anomaly describes the factor by which the non-geogenic fraction of gadolinium is higher than the geogenic one.

The anomaly is assumed to be originated from gadolinium chelates [1-3] which are extremely stable ($\log K > 16$) and used as diagnostics in Magnetic Resonance Imaging (MRI) (cf. chapter 1). This assumption was made, because no other application is introducing gadolinium in relevant concentrations to water bodies [1]. It is assumed that they are excreted unmetabolized by the patients [4]. Hence, the chelates reach wastewater treatment plants (WWTPs) via the sewage system. There, the chelates are retained insufficiently [5].

The chelates are classified as not readily biodegradable [6]. This is explained by their chemical stability (cf. chapter 4.2.2.1). Microbial degradation of gadolinium chelates is not of any importance in the aquatic environement [6]. This is an important factor for the persistence of the chelates during wastewater treatment. The chelates which are not retained in the wastewater treatment plant reach the recipient waters without any modification [5]. The soluble and stable chelates differ strongly from natural gadolinium in their reactivity and hence, an amplification and transfer of the gadolinium anomaly has been proposed [1]. This statement has been corroborated by subsequent studies on the gadolinium anomaly [7, 8]. An summary of important studies reporting on the anomaly in different water bodies is presented in Table 3.1.

Table 3.1: Occurrence of the gadolinium anomaly; MUQ is Mud from Queensland, PAAS is Post Archaean Australian shale, NASC is North American Shale Composite; concentrations of $Gd_{anthropogenic}$ and values for the anomaly are not given, due to the varity of the sampling locations (amongst others to avoid comparison of river water data which are differently influenced by WWTP plumes)

Place	Water bodies	Year	Reference material	Author
Australia	River, semi-enclosed shallow bay	2009	MUQ	Lawrence [3]
Australia	River, WWTP	2009	MUQ	Lawrence and Bariel [9]
Australia	WWTP, surface water, tap water	2009	MUQ	Lawrence et al. [10]
Austria	River, WWTP	2005, 2007	PAAS	Kulaksiz and Bau [8]
Czech Republic	WWTP, river, tap water, spring	2002	PAAS	Möller et al. [11]
Czech Republic	WWTP, river, raw water, tap water, spring,	2006	PAAS	Morteani et al. [12]
England	River, tap water	2009	PAAS	Kulaksiz and Bau [8]
France	River, lagoon	2002	NASC	Elbaz-Poulichet et al. [13]
France	River, wells and springs for drinking water supply, WWTP effluent	2003 - 2004	NASC	Rabiet et al. [14]
France	River, wells for drinking water supply, WWTP effluent	2004	NASC	Rabiet et al. [14]
Germany	River, tap water, WWTP	1996	PAAS	Bau und Dulski [1]
Germany	River	2000	PAAS	Möller et al. [2]
Germany	River, groundwater, tap water	2004 - 2011	PAAS	Kulaksiz and Bau [8]
Germany	Lake, river, WWTP	2005	PAAS	Knappe et al. [15]
Germany	WWTP, river, estuary, sea	2007	PAAS	Kulaksiz and Bau [7]
Germany	River, wells for drinking water supply	2009	PAAS	Schwesig and Bergmann [16]
Germany	Hyporheic zone water of a river, groundwater	2010	PAAS	Lewandowski et al. [17]
Italy	River	2003	PAAS	Möller et al. [18]
Japan	River	1996	PAAS	Bau und Dulski [1]
Japan	River, estuaries	1996	PAAS	Nozaki et al. [19]
Japan	River	2000	PAAS	Möller et al. [2]
Japan	River, coastal sea water	2001	PAAS	Zhu et al. [20]
Japan	River, surface sea water,	2006	Local silicic rock	Ogata and Terakado [21]
Luxembourg	River, wells for drinking water supply	2009	PAAS	Schwesig and Bergmann [16]
Sweden	Lake, coastal semi-closed basin	1996	PAAS	Bau und Dulski [1]
Sweden	River	2000	PAAS	Möller et al. [2]
USA	WWTP	2005-2007	NASC	Verplanck et al. [22]
USA	River, WWTP effluent	2005	NASC	Verplanck et al. [23]
USA	River	2006	NASC	Barber et al. [24]
USA	River, lake	2006	PAAS	Bau et al. [25]

Soon after the first detection of the gadolinium anomaly, it has been proposed to use the anomaly as pseudo-natural tracer for the anthropogenic influence on a water body [2]. To investigate if, e.g., a deep well is contaminated with water originated from a WWTP, it is possible to determine the anomaly. Furthermore, it may be determined, how great such an influence is. In detail, by determination of the anomaly not only in the water body of interest, but also in surrounding water bodies, the mixing ratio may be determined [2, 9, 16]. The gadolinium anomaly has also been used for verification of biodegradation studies [17]. In this study [17], water samples from the hyporheic zone of a eutrophic river have been taken in different depths and concentrations of different micropollutants, such as ibuprofen and diclofenac, have been determined. These concentrations were decreasing with sampling depth. However, also the concentration of borate and the gadolinium anomaly which were used as indicators for wastewater contact were decreasing. By the determination of these tracers a wrong interpretation of the data has been prevented. It has been possible to distinguish between samples that were in contact with wastewater and in which a biodegradation took place and such samples that have never been in contact with wastewater.

For the application of the gadolinium anomaly as tracer it is not necessary to know the speciation of the gadolinium present in the sample, as only the total concentration of gadolinium has to be determined [1]. Natural gadolinium which is ionic or weakly inorganic chelated binds to particles and is affected by mixing and sedimentation processes, or by environmental flocculation processes [3, 7]. Organic and highly stable chelates like the medical diagnostics are not affected by such processes [3, 7]. Hence, the transfer and amplification of the anomaly is based on different environmental behavior of the geogenic gadolinium and anthropogenic gadolinium [3, 7]. Consequential, if the speciation of the anthropogenic gadolinium is changed, this will also influence the gadolinium anomaly.

However, to use gadolinium as tracer it is necessary to determine the gadolinium anomaly and not only the total gadolinium concentration [1, 11, 13, 16, 19, 20, 23, 25, 26]. The determination of the anomaly is required as high total gadolinium concentrations are not necessarily only due to anthropogenic gadolinium but may also be caused by a high geogenic background, which will be described in the following. The gadolinium anomaly describes how much higher the concentration of

the measured gadolinium is compared to the one expected from the distribution pattern of other rare earth elements (REE). To determine the anomaly, the concentration of the relevant REEs in a sample is measured and normalized to a reference material. This normalized concentration is plotted versus the atomic number of the elements, and the resulting graph is fitted with a (linear or exponential) function. If the sample contains only geogenic gadolinium, the data point of the normalized gadolinium concentration is close to the interpolated function. Yet, if a sample contains non-geogenic gadolinium (e.g. from wastewater), the normalized gadolinium concentration will be higher than the expected one. The gadolinium anomaly can be calculated by dividing the normalized measured gadolinium concentration by the normalized expected concentration (cf. chapter 3.2.3). Consequently, the gadolinium anomaly describes the factor by which the actual gadolinium concentration is above the geogenic level.

The relevance of the anomaly determinations for description of anthropogenic influence is presented in the following. It is not possible to identify an anthropogenic influence by determination of the total elemental concentration of gadolinium only. A complete determination of the gadolinium anomaly has to be performed as shown in the following examples. In Figure 3.1 the calculation of the anomaly for a sample from a deep well is presented. In this sample, the total elemental concentration of gadolinium is extremely high ($[Gd]_{total}$ = 4470 ng L^{-1}), even higher as one might expect in wastewater treatment plants (, which is usually ≤ 1 µg L^{-1}). Hence, one might falsely conclude that this sample is influenced by human activity, if only considering the total element concentration. However, based on the determination of the gadolinium anomaly (, which is in this case < LOQ), this conclusion has to be rejected. The gadolinium concentration is not any higher than one might expect by comparing it to other REE concentrations. The high concentrations of REEs in this sample are probably due to the acidity of the water (pH = 4.7). The acidic water must have leached the metals from the surrounding bedrock.

The importance of the anomaly calculation can be supported by an example of another extreme (cf Figure 3.2). The sample was taken from a wastewater plant in Finland.

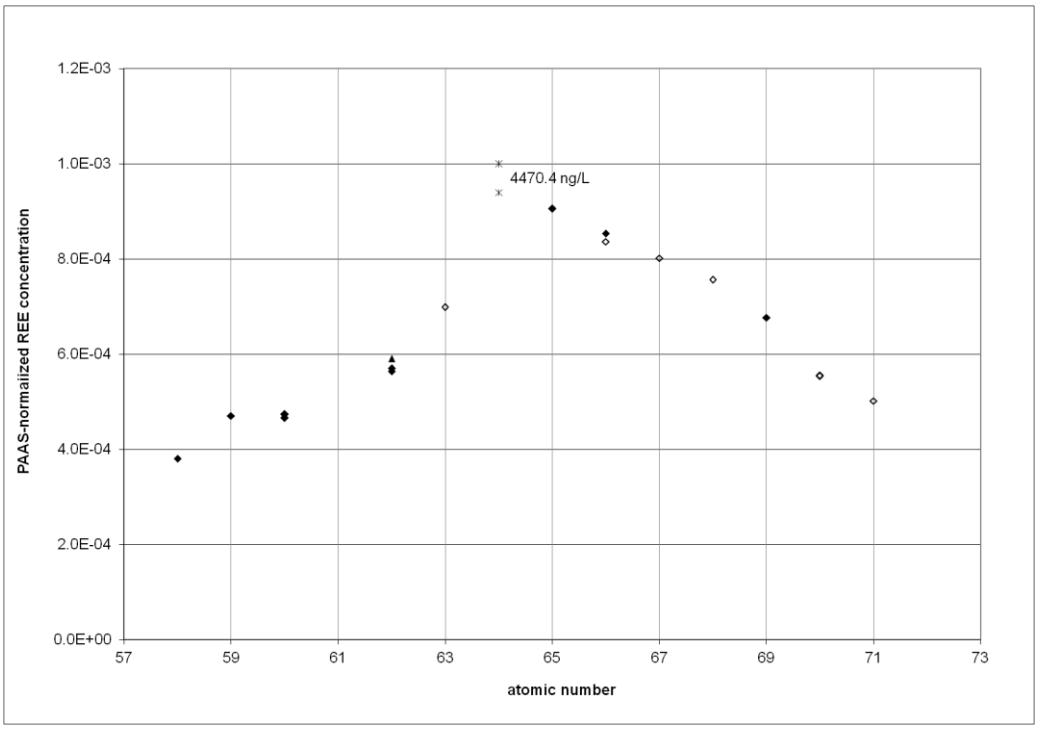

Figure 3.1: Plot of the concentration of the REEs normalized to PAAS (as reference material) vs. the atomic number for the determination of the gadolinium anomaly in a deep well sample; filled diamonds: mass traces used for the determination of the anomaly; open triangles: mass traces not used for determination of the anomaly and / or the determination of the isotope is interfered; marked with a star: normalized gadolinium concentration

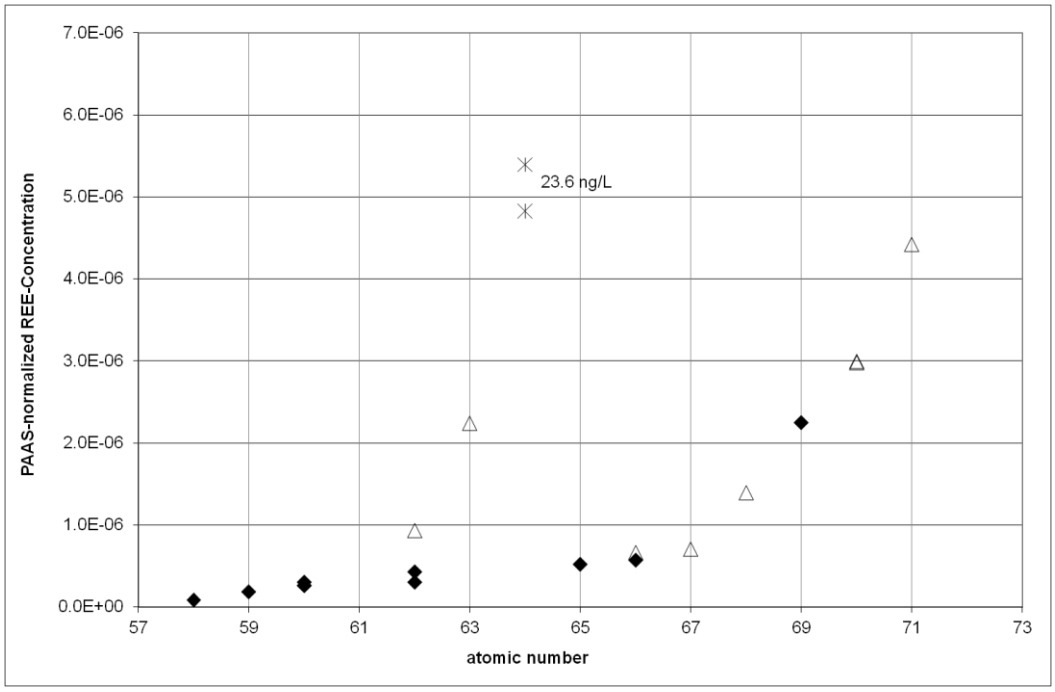

Figure 3.2: Plot of the concentration of the REEs normalized to PAAS (as reference material) vs. the atomic number for the determination of the gadolinium anomaly in a sample from a wastewater treatment plant effluent in Finland; filled diamonds: mass traces used for the determination of the anomaly; open triangles: mass traces not used for determination of the anomaly and / or the determination of the isotope is interfered; marked with a a star: normalized gadolinium concentration

Even though the gadolinium concentration seems to be rather low (23.6 ng L^{-1}), by determination of the anomaly (gadolinium anomaly = 8.3) it is evident that a large fraction of this gadolinium is of non-geogenic origin and as there are no relevant applications of gadolinium other than MRI contrast agents which may have an influence on the gadolinium concentration in water, the determined gadolinium must derive from such applications.

Since the end of the 1990ies gadolinium anomalies have been detected in natural water systems and attributed to the influence of wastewaters from medical applications of gadolinium compounds (cf. Table 3.1). In this chapter, the extent of gadolinium emission and its relevance in the water cycle from wastewater treatment to tap water is described. This was done to verify that gadolinium chelates are present in notable high concentrations, making it necessary to investigate the effects of water treatment on the chelates.

3.2 Experimental

The relevance of anthropogenic gadolinium in the water cycle was determined by identification of the gadolinium anomaly in two different water matrices. WWTPs effluents were studied to investigate the impact of gadolinium on surface waters, as well as the spatial distribution of the anomaly in Europe to verify that the emission of gadolinium has become by now a problem, independent from the countries development status. As gadolinium emissions are generally originated by health care, a correlation of gadolinium data and data from a health care systems ranking has been performed, to verify not only a qualitative, but also a semi-quantitative dependency.

Tap water samples have been taken to study how great the impact of anthropogenic gadolinium on drinking water is which implies how great the uptake of gadolinium is by drinking tap water. Furthermore these investigations give a hint on the removal rates during water treatment.

3.2.1 Sampling

Tap water samples in households in the Ruhr area in Germany were collected according to German drinking water standards for metal ion determinations [28]. Prior to sampling the tap water was run until a constant temperature of approx. 10-15°C was reached. Then samples were taken in Vials (PP) and acidified when they arrived in the laboratory (4 ml HNO_3 (65%, ultrapure) per liter).

Deep well samples were taken according to the DIN 38402-13 [29] and also acidified when they arrived in the laboratory (4 ml HNO_3 (65%, ultrapure) per liter).

The samples from the waste water treatment plants were taken as random samples according to DIN 38402-11 [30]. Samples were cooled during transport and acidified when they arrived in the laboratory (4 ml HNO_3 (65%, ultrapure) per liter).

3.2.2 Instrumentation

For the determination of the rare earth elements' concentrations, measurements were performed with a Perkin Elmer ELAN DRC II ICP-MS that was equipped with an AS90 autosampler. The ICP-MS method parameters are presented in Table 2.1 (cf. chapter 2). It is necessary to determine also other REEs to be able to differentiate between geogenic and non-geogenic gadolinium). The limit of quantification for all REEs was determined according to the US EPA guidelines [27] (cf. Table 3.2).

Table 3.2: Limit of quantification for each measured m/z in the gadolinium anomaly method and possible interferences in the determination

Isotoppe	LOQ [ng L^{-1}]	Abundance [%]	Isobaric interferences (abundance [%])	Molecule interferences (abundance of Ba isotope [%])
^{140}Ce	2	88.5	-	-
^{141}Pr	2	100.0	-	-
^{142}Nd	3	27.1	^{142}Ce (11.1)	-
^{143}Nd	3	12.2	-	-
^{144}Nd	5	23.8	^{144}Sm (3.1)	-
^{147}Sm	4	15.0	-	-
^{149}Sm	5	13.8	-	-
^{152}Sm	5	26.7	^{152}Gd (0.2)	^{136}BaO (7.9)
^{153}Eu	2	52.2	-	^{137}BaO (11.2)
^{158}Gd	1	24.8	^{158}Dy (0.1)	
^{159}Tb	1	100.0	-	
^{160}Gd	1	21.9	^{160}Dy (2.3)	
^{161}Dy	3	18.9	-	
^{163}Dy	3	24.9	-	
^{165}Ho	1	100.0	-	
^{166}Er	3	33.6	-	
^{169}Tm	1	100.0	-	
^{173}Yb	3	16.1	-	
^{174}Yb	1	31.8	^{174}Hf (0.2)	
^{175}Lu	1	97.4	-	

3.2.3 Calculation of the anomaly

The calculation of the anomaly is performed according to Bau and Dulski [1]. As reference material the Post Achaean Australian Shell (PAAS) was chosen as well. The calculation of the anomaly is presented in the following. First molar concentrations of the REEs are normalized to the PAAS:

$$\text{normalized REE concentration} = \frac{\text{measured REE concentration [M]}}{\text{REE concentration in PAAS [M]}} \qquad (3.1)$$

The normalized concentrations are ploted vs. the atomic number (cf. Figure 3.3). The resulting plot is fitted to an (usually) exponential curve.

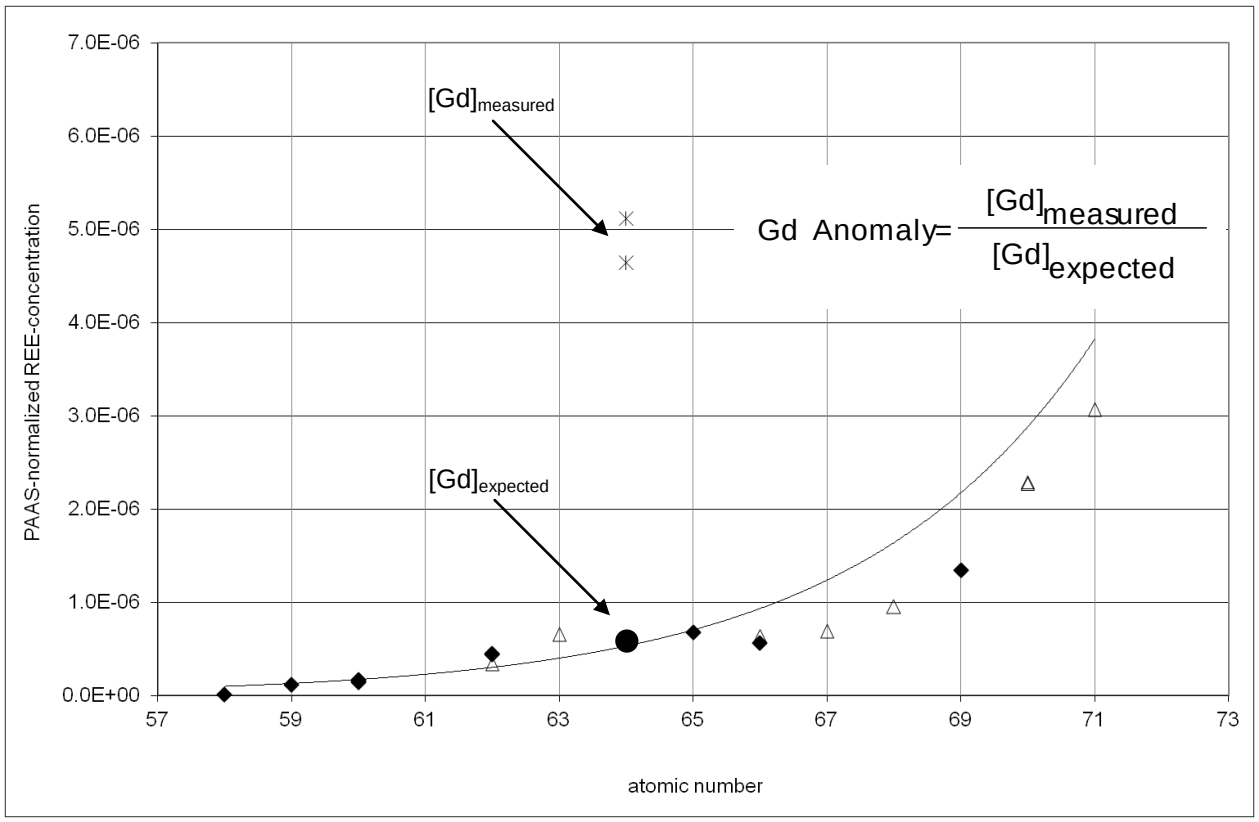

Figure 3.3: Determination of the gadolinium anomaly; PAAS-normalized REE concentration vs. the atomic number; filled diamonds: isotopes used for calculation of the anomaly; open triangles: determination of isotopes interfered and / or isotopes not used for calculation; measured gadolinium isotopes marked with a star; gadolinium concentration which would be expected marked with a dot; sample type: Tap water from a household in Kerken, Germany

The normalized geogenic gadolinium concentration is defined by this fitted function. Hence, it is possible to calculate this “expected” normalized gadolinium concentration by use of the function.

Once the expected normalized gadolinium concentration is known, as well as the measured normalized gadolinium concentration, one is able to calculate the gadolinium anomaly:

$$\text{gadolinium anomaly} = \frac{\text{measured normalized gadolinium concentration}}{\text{expected normalized gadolinium concentration}} \quad (3.2)$$

3.3 Results

The determination of the gadolinium anomaly in the effluent of wastewater treatment plants in Europe has shown that there is an enormous input of non-geogenic gadolinium to water resources all across Europe. The results are presented in Figure 3.4 (detailed results are presented in Table S 3.1).

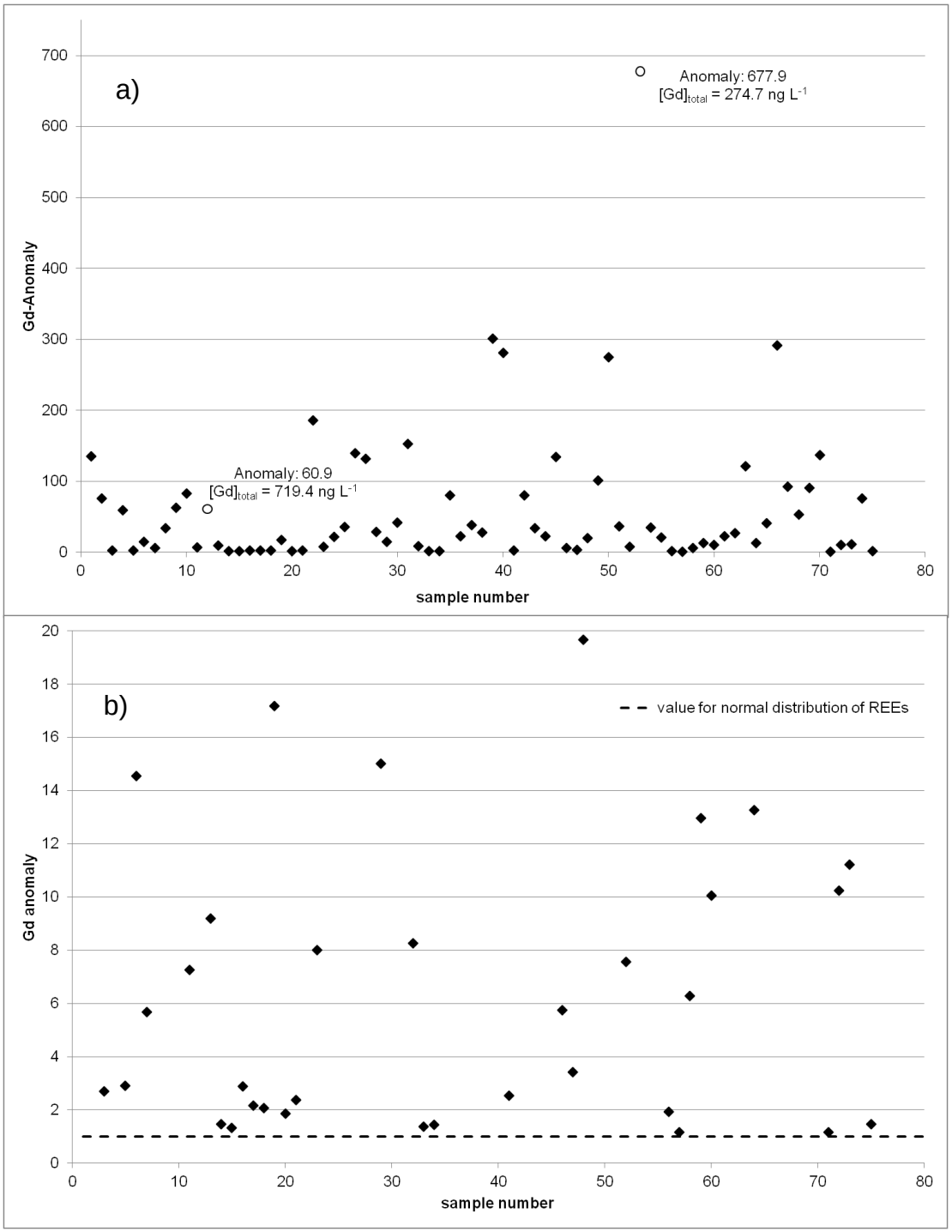

Figure 3.4: Results of a pan-European monitoring study: gadolinium anomaly plotted vs. the sample number; b) Zoom, to show the value for a normal distribution of the rare earth elements in a water sample

The gadolinium anomaly is independent on the economic development status of the country (cf. Figure S 3.1). Non-geogenic gadolinium may be found in any wastewater treatment plant receiving water from a hospital or doctor's office applying gadolinium based contrast agents or from patient's households.

Interestingly, the gadolinium anomaly may be correlated with the performance of the health care system of the specific country (cf. Figure 3.5). The quartile average (average of the first and third quartile) was taken to reduce the influence of the lowest anomalies, as no or very low anomalies may be found in wastewater treatment plants which do not receive water from any MRI using facility.

DALE and independent from this, expenditure (both taken from the WHO ranking "performance of the health system" [31]), were also correlated with gadolinium anomaly. Best fit ($r^2 = 0.87$) was obtained vs. the complete ranking (performance of the health system).

The ranking of the health system in 2000 was performed by the World Health Organization (WHO). The performance of a health care system is a combination of two factors:

- health (here, expressed in disability-adjusted life expectancy (DALE))
  which is established by several factors, also by such which are not manageable by a health system (good nutrition, work, climate, war, etc) and
- expenditure (private and public) for the health care system
  (, including costs for MRI diagnostics as one factor) [31]

The DALY (disability-adjusted life year) which is usually used for burden of disease estimation, was not used as more parameters are necessary for its calculation than for calculation of DALE [32]. For estimation of the DALE following information is necessary:

- fraction of the population surviving certain age (calculated using birth and death rates);
- prevalence disability types at all ages;
- Type of disability is weighted sometimes with age (dependents on the type of disability). [32]

Gadolinium in diagnostic is not directly linked to the health of a population. Yet, good diagnostics are necessary to find correct cures for the specific disability and hence, to decrease the mortality assigned to the specific disability. However, the correlation between those data sets (DALE and gadolinium anomaly) is rather poor. The interdependency between expenditure and gadolinium data did not lead to a better correlation, as one might have expected. The expenditure for the health care systems is very complex and diagnostics are only a small part of the complete system. Eventhough MRI diagnostics are considered as one factor in overall expenditure, it is composed of several different parameters which contributing to different (larger) extend to the overall expenditure [31].

Considering the remarks above (health is not dependent on the use of MRI contrast agents, nor are MRI contrast agents influencing costs as single most factor,) it is comprehensible that the best correlation is found when considering the complete ranking.

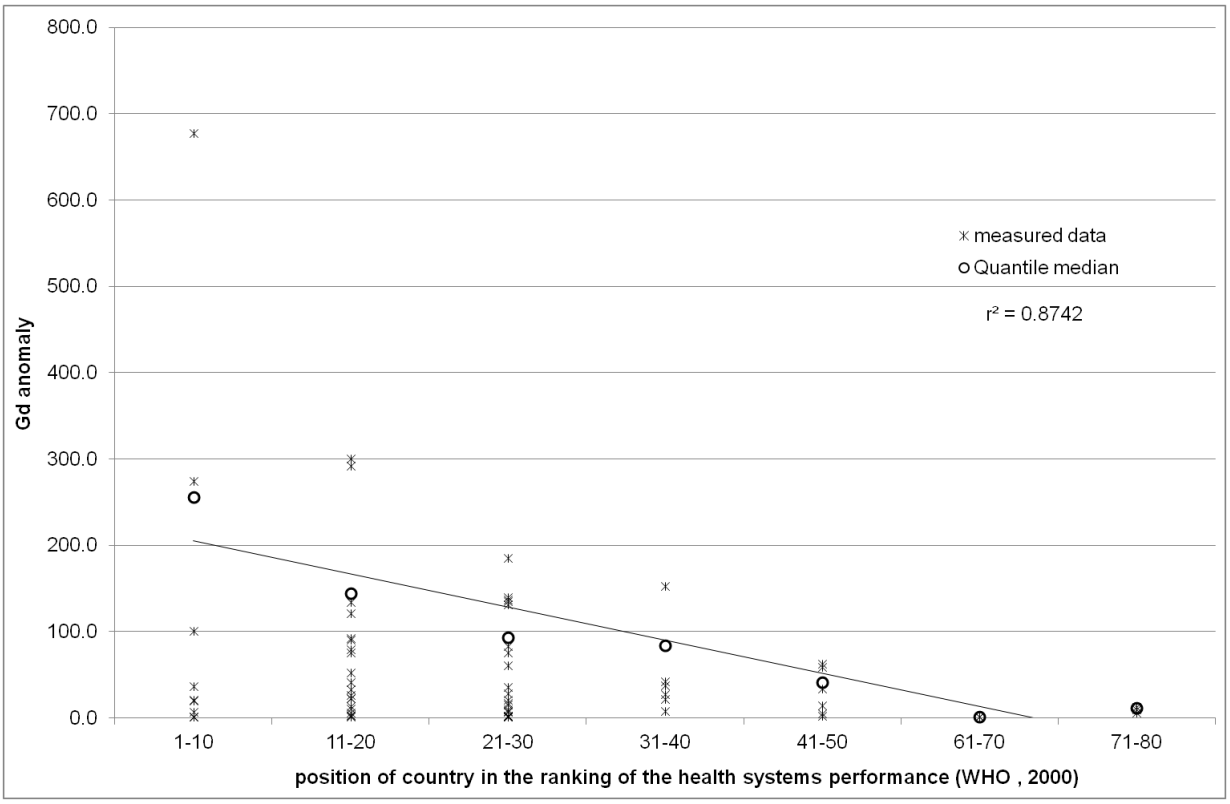

Figure 3.5: Results of the pan-European study: Gadolinium anomaly in the effluent of 75 European wastewater treatment plants plotted vs. the position of the specific country in the 2000 WHO ranking of the performance of the health system (rank 1-10: Italy, Spain, Austria (n = 10), rank 11-20: Portugal, Greece, Netherlands, Ireland, Switzerland (n = 22), rank 21-30: Belgium, Cyprus, Germany (n = 24), rank 31-40: Finland, Slovenia (n = 7), rank 41-50: Czech republic (n = 7), rank 51-60: Hungary (n = 2), rank 71-80: Lithuania (n = 3)); circled quartile average was used for linear regression

Results from a drinking water monitoring campaign in the densely populated Ruhr area (5.15 million inhabitants [33]) are presented in Figure 3.6 (detailed results in chapter 3.5.2). In the Ruhr area a great proportion of the drinking water supply is based on bank filtration from the Ruhr River and also most of the wastewater treatment plants discharge their effluent into the Ruhr River. The area surrounding Ruhr River is very densely populated (cf. Figure 3.6) and hence, the wastewater load in the river is higher than in the Lippe River, which is used for drinking water production in the northern part of the Ruhr area. Due to high population density also hospital density is higher. Centralization of the health system is a factor contributing to increased influence of pharmaceuticals in the Ruhr River. Patients are referred to specialists in hospitals in urban centers, for special examinations and therapies. Hence, pharmaceuticals, which are used for these special treatments, are discharged into the urban wastewater. This applies also for gadolinium diagnostics, as there are remarkably fewer MRI facilities in less densely populated regions.

Next page:

Figure 3.6: Results from drinking water monitoring in the Ruhr area; orange bars: $[Gd]_{total}$, value above is the concentration in ngL^{-1}; yellow (and bright yellow) bars: $[Gd]_{geogenic,}$; < LOQ = $[Gd]_{total}$ < LOQ; n.d. = not determined ([REE] too low); n.q. = not quantified (anomaly < 1.5), for both cases (n.d. and n.q.) it is assumed that $[Gd]_{total} = [Gd]_{geogenic}$; brown circles: wastewater treatment plant; blue squares: drinking water treatment plant; red circles: city center with population > 100000; grey area: building covered area; black lines: drinking water distribution area (2012, LANUV NRW) NOTE: drinking water distribution areas may be variable and drinking water is not necessarily from one specific supplier, only a certain water quality is described by the drinking water distribution area

N

Gadolinium anomaly in drinking water in the Ruhr area

Herne City Center > 100.000 cit.

Waterworks

WWTP

Ruhr Surface water

Drinking water distribution area (source: LANUV NRW 2012)

$[Gd]_{total}$ / ng L^{-1}

$fGd_{geogenic}$

urban district

n.d. = not determined (REE* < LOQ)

n.q. = not quantified (Gd-Anomaly < LOQ)

Lippe

Emscher

Rhein

Ruhr

Wupper

Marl-Sinsen 27.1

Recklinghausen 26.3 n.d.

Recklinghausen

Ge-Buer 17.4

Ge-Horst 17.9

Herne-Mitte 32.9

Her-Horsthausen 22.1

Herne

Ob-Sterkrade 26.9 n.d.

Bot-Mitte < LOQ n.d.

Bot-Boy 22.7

Bot-Batenbrock 22.5

Bottrop

Gelsenkirchen

Bot-Wattenscheid 31.3

Do-Mitte 22.5

Do-Buschei 15.2

Dortmund

Du-Meidereich 23.0

Oberhausen 30.4

Alt-Oberhausen 30.7

E-Altenessen 35.8

E-Frohnhausen 28.0

Bo-Ehrenfeld 28.5

Bochum

Witten 22.4

Moers 4.3 n.q.

Du-Homberg 23.5

Du-Duissern 4.5

Du-Dellviertel 5.6

Mh-Broich 37.2

Mh-Styrum n.d.

Mh-Mitte 34.2

Mülheim

Essen

E-Steele 24.0

E-Heisingen 29.5

E-Kettwig 34.5

Hattingen 36.5

Schwerte 20.9

Hagen

Velbert 14.4

Ratingen-Mitte < LOQ n.d.

Krefeld

Wuppertal

5 0 5 10 Kilometer

Yet, in the northern part of the region water supply is provided by the Lippe River and to a greater extent (compared to the southern and central Ruhr Area) ground water is used. The anthropogenic influence on the Lippe River is less pronounced than on the Ruhr River. Hence, it has been assumed, that the non-geogenic fraction of gadolinium should be higher in the region close to the Ruhr River and lower in the northern part of the Ruhr area. The results shown in Figure 3.6 corroborate this assumption. Only few exceptions have been found, which may be explained by the variable sources of the drinking water. This variability of drinking water is described by the drinking water supply areas (also displayed in Figure 3.6) that describe areas in which a certain composition of drinking water is supplied. The samples from Bottrop- Mitte, Mülheim-Styrum and Oberhausen-Sterkrade do not show an anomaly, even though they are directly located in the densely populated region. However, these sampling locations were in other drinking water distribution areas than the neighboring samples, with high gadolinium anomalies.

The sample from Recklinghausen is located in the same drinking water supply area as the samples from Gelsenkirchen-Buer, Gelsenkirchen-Horst and Marl-Sinsen. However, it is the only sample in this area that does not show an anomaly. This might be due to the variability of the drinking water supply areas. The drinking water does not necessarily have to be from one supplier at all times.

Sampling time (samples were taken on different days of the week), has also been assumed to contribute to the variations. This assumption has been disproved by a sampling campaign at three different sampling locations (Duisburg-Duissern, Essen-Steele and Oberhasuen-Sterkrade) over a period of at least 10 days. The results are presented in Figure 3.7. Due to a lower concentration in the samples of Oberhausen-Sterkrade and Duisburg-Duissern it was necessary to preconcentrate the samples to be able to determine not only gadolinium, but also other REEs. The preconcentration by evaporation of the samples (1:4 enrichment (cf. chapter 2.2.6.1) yielded recovery rates of 80%. The low concentration of the REE`s may be explained by lower flow rates (due to seasonal variations) in the river used for bank filtration which leads to less turbulences. These turbulences are responsible for transport of particle-bound REEs [34].

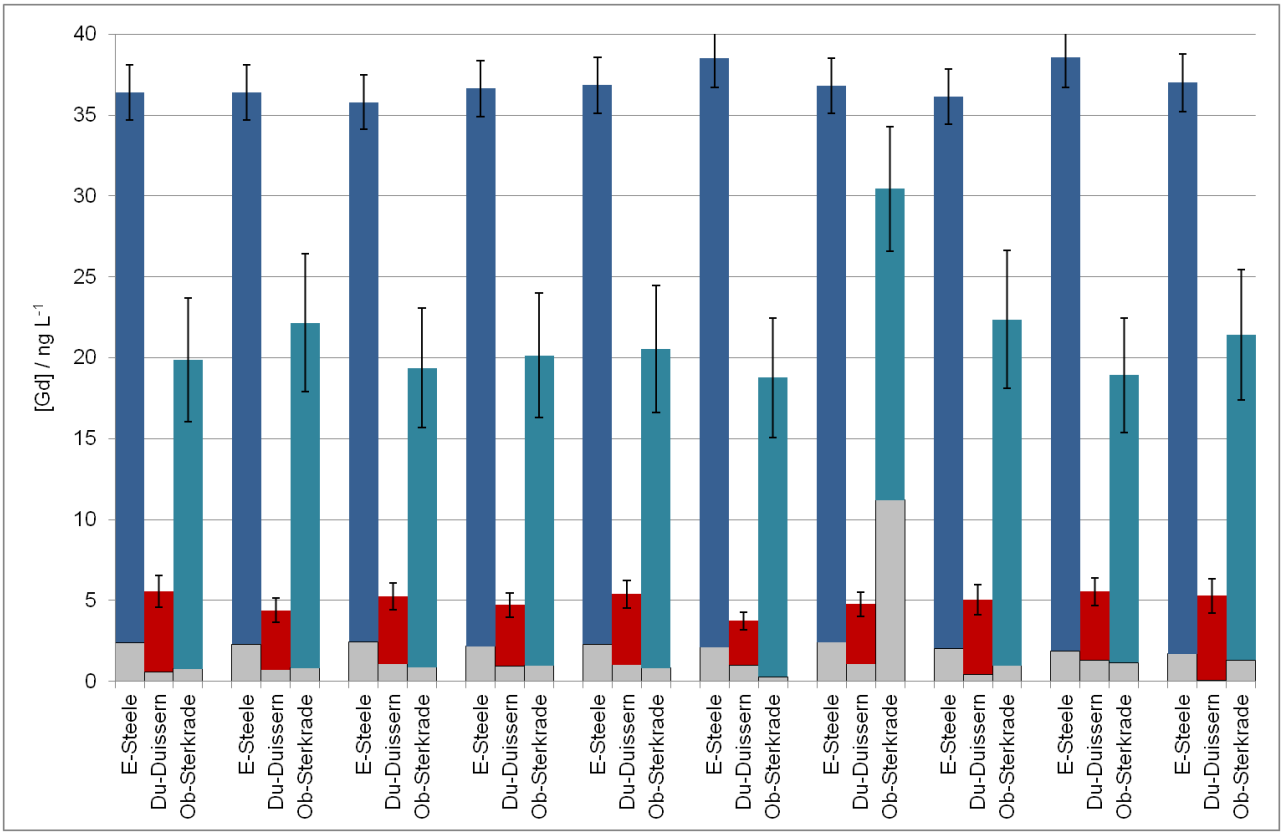

Figure 3.7: Monitoring of the gadolinium anomaly at three sampling locations over a period of 10 days; the geogenic gadolinium concentration in ng L^{-1} is colored; the non-geogenic fraction of the gadolinium concentration is grey; deviation is higher for OB-Sterkrade and Du-Duissern as a preconcentration of the samples by evaporation was necessary to be able to quantify not only gadolinium but also concentrations of the other REEs

The results presented in Figure 3.7 cleary show that a daily variation of the gadolinium anomaly in drinking water is not given. However, a variation might be detectable in a broader time range, e.g. connected to the seasonal variation. The small differences of $[Gd]_{non\text{-}geogenic}$ presented in Figure 3.7 may be explained by other factors. Gadolinium, discharged from a wastewater treatment plant travels different distances until it reaches drinking water production. Every gadolinium discharge into the river increases the gadolinium load in this specific river. However, one has to consider also the dilution by rivers, creeks and wastewater treatment plants not carrying gadolinium. Furthermore, also the ratio of former wastewater in the raw water which is used for the drinking water production for the specific tap water is variable, as well as the residence time in soil. All these factors may contribute to the small variations of the anomaly.

Another important result from this monitoring campaign is the dimension of the anomaly compared to other urban areas. A recent study from Berlin has shown a non-geogenic concentration of 18 ng L^{-1} as maximum (additional to a geogenic background of 0.54 ng L^{-1}), with an average non-geogenic concentration of 3.7 ng L^{-1} (additional: average geogenic background of 2 ng L^{-1}). For the Ruhr area the maximum non-geogenic concentration is 35.1 ng L^{-1} (additional geogenic background = 2.1 ng L^{-1}), with an average non-geogenic concentration of 16.4 ng L^{-1} (additional average geogenic background = 7.3 ng L^{-1}).

Considering only the non-geogenic fraction of the total gadolinium concentration, the concentrations in the Ruhr area are almost twice as high. This may have several reasons:

- Emission of gadolinium diagnostics in the Ruhr area is of importance for the whole area since 1988, in Berlin this is only the case for the western part until the reunion and the following reconstruction years.
- Less inhabitants in Berlin (3.5 million people in Berlin [Amt für Statistik Berlin-Brandenburg, Stichtag 31.12.2011]; 5.15 million people in the Ruhr area [33])
- Higher “re-use-rate” of the water in the Ruhr area: The percentage of wastewater treatment plants in the Ruhr region that use a water body which serves as raw water source for drinking water production is higher than for wastewater treatment plants in Berlin (cf. Figure 3.6 and [8])
- Steady increase in use of gadolinium diagnostics for MRI: campaign in Berlin was in 2010 [8]; results of the Ruhr area in this study are from 2012

3.4 Conclusion

The results of both drinking water monitoring campaigns in urban areas show that anthropogenic gadolinium reaches drinking water. It is concluded, that the anthropogenic gadolinium is not substantially removed by any of the treatment processes. Yet the speciation of gadolinium in the drinking water is unknown. Consumers of drinking water are highly concerned, when even such low concentrations of anthropogenic chemicals are detected in the water. Recently it has been shown that transmetalation occurs during flocculation steps in drinking water treatment (with Fe(III)) [35, 36]. However, the extent of this process and speciation of gadolinium which reaches consumers' tap has not been evaluated. It is possible, however unlikely, that gadolinium is present in its free and toxic form. The LD_{50} of $GdCl_3 \cdot 6\,H_2O$ is 100-200 mg kg^{-1} for mice [37]. For an acute intoxication with gadolinium from drinking water a mice had to drink 100 m^3 (assumptions: 30 ng L^{-1} Gd_{total} in drinking water present as Gd(III), typical house mouse 20 g). Humans would need even higher amounts. Nevertheless, long-term effects of low (chelated or ionic) gadolinium dosages are not known [8].

Even though research in this area has increased in the past years, a great part of the processes in the environment and in water treatment are still unknown [5, 8, 35, 36, 38, 39]. In this study it could be demonstrated, that gadolinium emission via WWTPs into the aquatic environment is relevant all across Europe. The amount of anthropogenic gadolinium is not directly linked to an economic development status of the country, however, to the development status of the health care system in that specific country.

In other studies, it could be shown that non-toxic gadolinium chelates enter the wastewater treatment plants and approx. one third enter the recipient waters [5]. In general it is unknown which processes are important for the removal of the gadolinium species whether in its original (chelated) form or as newly generated chelate or in its free ionic form. However, it is known that the gadolinium concentration (as chelated form and $[Gd]_{total}$) decreases right after a sedimentation step [5]. Hence, it was considered that sorption on organic matter is an important factor [5]. However, this may only apply to ionic, non-chelated gadolinium, as results of adsorption on activated carbon filters have shown no significant removal of $[Gd]_{non\text{-}geogenic}$ in a biologically active filter (cf. chapter 4). It is not known if

transmetalation occurs during transport in the environment, eventhough there are hints that Cu(II) and Ni(II) exchange Gd(III) during soil passage [40]. Sorption processes in the environment are also hitherto poorly studied. It is known that, that anthropogenic gadolinium is not retained by soil passage [39-41]. However, processes during transport in the environment may influence the speciation of gadolinium and may also lead to a reduction of gadolinium in the water phase. A crucial factor for evaluation of these processes is an analytical method for speciation which is highly sensitive [42].

The presence of anthropogenic gadolinium in drinking water, which could be demonstrated in this study analogue to previous studies [8] and its occurrence in WWTPs all across Europe could demonstrate the necessity of research on the behavior of gadolinium chelates during water treatment processes. Due to insufficient removal during the treatment processes for wastewater and drinking water, processes which are of importance for both treatment processes have been investigated. Hence, activated carbon treatment (cf. chapter 4) and oxidative processes (cf. chapter 5) were evaluated to provide insight in their behavior. However, to fully understand the life cycle of gadolinium, further research is necessary.

3.5 Supplement

3.5.1 Detailed results of the pan-European study

Table S 3.1: Detailed results of the pan-European study; gadolinium anomaly in the effluent of wastewater treatment plants

Country	[Gd] / ng L^{-1}	Gd anomaly	Non-geogenic Gd / %	$[Gd]_{non\text{-}geogenic}$ / ng L^{-1}	$[Gd]_{geogenic}$ / ng L^{-1}	Performance of health systems WHO ranking			
						Ranking of health level (DALE)	Ranking of health level performance[1]	Ranking of health expenditure per capita in international dollars[2]	Overall ranking of performance of the health system
Austria	275	678	100	274	0.4	17	15	6	9
Greece	247	301	100	246	0.8	7	11	30	14
Netherlands	237	292	100	237	0.8	13	19	9	17
Greece	204	281	100	204	0.7	7	11	30	14
Austria	58.2	275	100	57.9	0.2	17	15	6	9
Belgium	15.7	186	99	15.6	0.1	16	28	15	21
Finland	711	153	99	706	4.6	20	44	18	31
Belgium	154	140	99	153	1.1	16	28	15	21
Germany	441	137	99	438	3.2	22	41	3	25
Cyprus	52.5	135	99	52.1	0.4	25	22	39	24
Switzerland	66.4	134	99	65.9	0.5	8	26	2	20
Belgium	419	132	99	416	3.2	16	28	15	21
Netherlands	211	121	99	209	1.7	13	19	9	17
Austria	118	101	99	117	1.2	17	15	6	9
Netherlands	227	92.5	99	225	2.4	13	19	9	17
Netherlands	115	90.9	99	114	1.2	13	19	9	17
Belgium	59.3	83.1	99	58.6	0.7	16	28	15	21
Finland	101	80.2	99	99.2	1.2	20	44	18	31
Switzerland	92.0	79.8	99	90.9	1.1	8	26	2	20
Cyprus	41.1	75.8	99	40.5	0.5	25	22	39	24
Netherlands	305	75.8	99	301	4.0	13	19	9	17
Czech Republic	115	63.1	98	113	1.8	35	81	40	48
Germany	719	60.9	98	708	12	22	41	3	25
Czech Republic	43.9	58.8	98	43.2	0.7	35	81	40	48
Netherlands	84.1	53.0	98	82.5	1.6	13	19	9	17
Slovenia	49.6	42.2	98	48.5	1.1	34	62	29	38

[1] Ranking of comparison of actual attainment and attainment which a system should be able to accomplish (best results, which

[2] international dollar: hypothetical currency with the same purchasing power as the U.S. dollar in the United States

Country	[Gd] / ng L^{-1}	Gd anomaly	Non-geogenic Gd / %	$[Gd]_{non\text{-}geogenic}$ / ng L^{-1}	$[Gd]_{geogenic}$ / ng L^{-1}	Performance of health systems WHO ranking			
						Ranking of health level (DALE)	Ranking of health level performance[1]	Ranking of health expenditure per capita in international dollars[2]	Overall ranking of performance of the health system
Netherlands	223	41.2	98	218	5.3	13	19	9	17
Finland	232	38.2	97	227	5.9	20	44	18	31
Austria	24.7	36.6	97	24.0	0.7	17	15	6	9
Belgium	219	35.7	97	213	6.0	16	28	15	21
Spain	19.3	35.1	97	18.7	0.5	5	6	24	7
Czech Republic	56.4	33.7	97	54.7	1.6	35	81	40	48
Switzerland	33.9	33.6	97	32.9	1.0	8	26	2	20
Belgium	390	28.8	97	375	13	16	28	15	21
Finland	208	27.9	97	200	7.2	20	44	18	31
Netherlands	43.7	26.6	96	42.1	1.6	13	19	9	17
Switzerland	10.7	22.5	96	10.2	0.5	8	26	2	20
Netherlands	122	22.4	96	117	5.2	13	19	9	17
Finland	95.0	22.2	96	90.9	4.1	20	44	18	31
Belgium	17.5	21.5	96	16.7	0.8	16	28	15	21
Spain	33.6	20.6	95	32.0	1.6	5	6	24	7
Austria	21.0	19.7	95	19.9	1.0	17	15	6	9
Belgium	59.5	17.2	95	56.2	3.3	16	28	15	21
Belgium	155	15.0	94	145	9.7	16	28	15	21
Czech Republic	5.7	14.6	94	5.3	0.4	35	81	40	48
Netherlands	90.1	13.3	93	83.7	6.3	13	19	9	17
Lithuania	16.8	13.0	93	15.6	1.2	63	93	71	73
Netherlands	146	11.2	92	134	12	13	19	9	17
Germany	58.7	10.2	91	53.5	5.2	22	41	3	25
Lithuania	46.6	10.0	91	42.3	4.2	63	93	71	73
Belgium	105	9.2	90	94.2	10	16	28	15	21
Finland	23.6	8.3	89	21.0	2.5	20	44	18	31
Belgium	219	8.0	89	194	24	16	28	15	21
Austria	25.1	7.6	88	22.1	2.9	17	15	6	9
Belgium	83.6	7.3	88	73.4	10	16	28	15	21
Lithuania	16.1	6.3	86	13.9	2.2	63	93	71	73
Ireland	32.6	5.7	85	27.7	4.8	27	32	117	19
Czech Republic	91.3	5.7	85	77.6	14	35	81	40	48
Ireland	3.0	3.4	77	2.3	0.7	27	32	117	19

Country	[Gd] / ng L^{-1}	Gd anomaly	Non-geogenic Gd / %	$[Gd]_{non\text{-}geogenic}$ / ng L^{-1}	$[Gd]_{geogenic}$ / ng L^{-1}	Performance of health systems WHO ranking			
						Ranking of health level (DALE)	Ranking of health level performance[1]	Ranking of health expenditure per capita in international dollars[2]	Overall ranking of performance of the health system
Czech Republic	1.8	2.9	74	1.3	0.5	35	81	40	48
Belgium	54.2	2.9	74	40.2	14	16	28	15	21
Czech Republic	2.3	2.7	73	1.7	0.6	35	81	40	48
Switzerland	2.5	2.5	72	1.8	0.7	8	26	2	20
Belgium	34.5	2.4	70	24.3	10	16	28	15	21
Belgium	127	2.2	68	86.8	40	16	28	15	21
Belgium	35.0	2.1	67	23.6	11	16	28	15	21
Belgium	16.9	< 2	≤ 66	0.0	17	16	28	15	21
Belgium	46.1	< 2	≤ 66	0.0	46	16	28	15	21
Belgium	16.1	< 2	≤ 66	0.0	16	16	28	15	21
Hungary	55.6	< 2	≤ 66	0.0	56	62	105	59	66
Hungary	65.1	< 2	≤ 66	0.0	65	62	105	59	66
Italy	231	< 2	≤ 66	0.0	231	6	3	11	2
Italy	15.7	< 2	≤ 66	0.0	16	6	3	11	2
Portugal	49.5	< 2	≤ 66	0.0	50	29	13	28	12
Spain	3.5	< 2	≤ 66	0.0	3.5	5	6	24	7

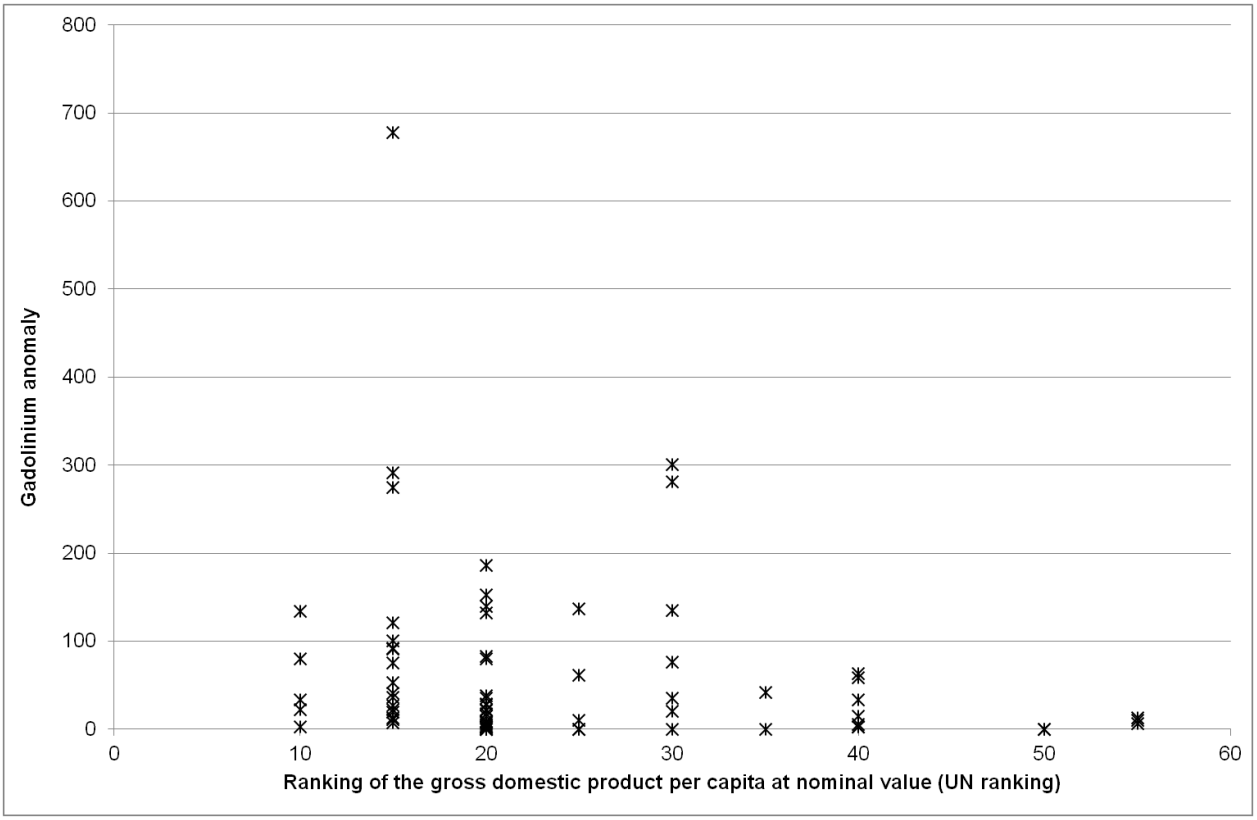

Figure S 3.1: Results of the pan-European study: Gadolinium anomaly in the effluent of 75 European wastewater treatment plants plotted vs. the position of the specific country in the 2011 United Nations (UN) ranking of the gross domestic product per capita at nominal value; rank 1-5: no country; rank 5-10: Switzerland (n = 5); rank 11-15: Netherlands and Austria (n = 17); rank 16-20: Belgium, Finland, and Ireland (n = 27); rank 21-25: Germany and Italy (n = 5); rank 26-30: Spain, Cyprus, and Greece (n = 7); rank 31-35: Portugal and Slovenia (n = 2); rank 36-40: Czech republic (n = 7); rank 41-45: none; rank 50-55: Hungary (n = 2); rank 56-60: Lithuania (n = 3)

3.5.2 Detailed results of the gadolinium anomaly in the Ruhr area

Table S 3.2: Gadolinium anomaly in the Ruhr area, detailed results; geogenic results in grey: Anomaly < LOQ, hence, it is assumed that [Gd]geogenic = [Gd]total

Place	Gd in ng L^{-1}	Gd anomaly	$Gd_{non\text{-}geogenic}$ [%]	$[Gd]_{non\text{-}geogenic}$ in ng L^{-1}	$[Gd]_{geogenic}$ in ng L^{-1}
Bo-Ehrenfeld	29	5.0	80	4.7	24
Bot-Batenbrock	23	19	95	1.2	22
Bot-Boy	23	24	96	0.9	22
Bot-Mitte	< LOQ	n.d.	n.d.	n.d.	n.d.
Bo-Wattenscheid	31	5.4	82	4.9	27
Do-Buschei	15	8.4	88	1.6	14
Do-Mitte	23	7.4	86	2.7	20
Du-Dellviertel	5.6	5.3	81	0.9	4.7
Du-Duissern	4.3	5.1	80	0.7	3.6
Du-Homberg	24	9.4	89	2.3	21
Du-Meidereich	23	5.8	83	3.4	20
D-Wersten	11	4.7	79	1.9	8.8
E-Altenessen	28	11	91	2.4	26
E-Frohnhausen	36	16	94	2.1	34
E-Heisingen	30	12	91	2.3	27
E-Kettwig	35	13	92	2.4	32
E-Steele	24	13	92	1.8	22
Ge-Buer	17	3.6	72	3.8	14
Ge-Horst	18	3.5	71	4.0	14
Hattingen	37	9.9	90	3.4	33
Her-Horsthausen	22	5.6	82	3.4	19
Her-Mitte	33	10	90	3.0	30
Kerken	16	7.1	86	2.0	14
Marl-Sinsen	27	6.5	85	3.6	24
Mh-Broich	37	28	96	1.3	36
Mh-Mitte	34	19	95	1.7	33
Mh-Styrum	31	n.d.	n.d.	0	31
Moers	4.3	< 2	n.q	0	4.3
Alt-Oberhausen	30	25	96	1.2	30
Ob-Sterkrade	27	n.d.	n.d.	0	27
Ratingen-Mitte	< LOQ	n.d.	n.d.	n.d.	n.d.
Recklinghausen	26	4.7	79	4.6	22
Schwerte	21	7.1	86	2.6	18
Velbert	14	4.9	80	2.4	12
Witten	22	5.9	83	3.3	19

3.6 References

1. Bau, M. and P. Dulski, Anthropogenic origin of positive gadolinium anomalies in river waters. *Earth and Planetary Science Letters*, 1996. **143**(1-4): 245-255.
2. Möller, P., P. Dulski, M. Bau, A. Knappe, A. Pekdeger, and C. Sommer-Von Jarmersted, Anthropogenic gadolinium as a conservative tracer in hydrology. *Journal of Geochemical Exploration*, 2000. **69-70**: 409-414.
3. Lawrence, M.G., Detection of anthropogenic gadolinium in the Brisbane River plume in Moreton Bay, Queensland, Australia. *Marine Pollution Bulletin*, 2010. **60**(7): 1113-1116.
4. Caravan, P., J.J. Ellison, T.J. McMurry, and R.B. Lauffer, Gadolinium(III) chelates as MRI contrast agents: Structure, dynamics, and applications. *Chemical Reviews*, 1999. **99**(9): 2293-2352.
5. Künnemeyer, J., L. Terborg, B. Meermann, C. Brauckmann, I. Möller, A. Scheffer, and U. Karst, Speciation analysis of gadolinium chelates in hospital effluents and wastewater treatment plant sewage by a novel HILIC/ICP-MS method. *Environmental Science and Technology*, 2009. **43**(8): 2884-2890.
6. Neubert, C., R. Länge, and T. Steger-Hartmann, *Gadolinium containing contrast agents for magnetic resonance imaging (MRI) investigations on the environmental fate and effects*, in *Fate of pharmaceuticals in the environment and in water treatment systems*, D.S. Aga, Editor. 2008, CRC Press Taylor & Francis Group: Boca Raton, Fl.
7. Kulaksiz, S. and M. Bau, Contrasting behaviour of anthropogenic gadolinium and natural rare earth elements in estuaries and the gadolinium input into the North Sea. *Earth and Planetary Science Letters*, 2007. **260**(1-2): 361-371.
8. Kulaksiz, S. and M. Bau, Anthropogenic gadolinium as a microcontaminant in tap water used as drinking water in urban areas and megacities. *Applied Geochemistry*, 2011. **26**(11): 1877-1885.
9. Lawrence, M.G. and D.G. Bariel, Tracing treated wastewater in an inland catchment using anthropogenic gadolinium. *Chemosphere*, 2010. **80**(7): 794-799.

10. Lawrence, M.G., C. Ort, and J. Keller, Detection of anthropogenic gadolinium in treated wastewater in South East Queensland, Australia. *Water Research*, 2009. **43**(14): 3534-3540.

11. Möller, P., T. Paces, P. Dulski, and G. Morteani, Anthropogenic Gd in surface water, drainage system, and the water supply of the city of Prague, Czech Republic. *Environmental Science and Technology*, 2002. **36**(11): 2387-2394.

12. Morteani, G., P. Möller, A. Fuganti, and T. Paces, Input and fate of anthropogenic estrogens and gadolinium in surface water and sewage plants in the hydrological basin of Prague (Czech Republic). *Environmental Geochemistry and Health*, 2006. **28**(3): 257-264.

13. Elbaz-Poulichet, F., J.-L. Seidel, and C. Othoniel, Occurrence of an anthropogenic gadolinium anomaly in river and coastal waters of Southern France. *Water Research*, 2002. **36**(4): 1102-1105.

14. Rabiet, M., F. Brissaud, J.L. Seidel, S. Pistre, and F. Elbaz-Poulichet, Positive gadolinium anomalies in wastewater treatment plant effluents and aquatic environment in the Herault watershed (South France). *Chemosphere*, 2009. **75**(8): 1057-1064.

15. Knappe, A., P. Moeller, P. Dulski, and A. Pekdeger, Positive gadolinium anomaly in surface water and groundwater of the urban area Berlin, Germany. *Chemie der Erde*, 2005. **65**(2): 167-189.

16. Schwesig, D. and A. Bergmann, Use of anthropogenic gadolinium as a tracer for bank filtrate in drinking water wells. *Water Science and Technology: Water Supply*, 2012. **11**(6): 654-658.

17. Lewandowski, J., A. Putschew, D. Schwesig, C. Neumann, and M. Radke, Fate of organic micropollutants in the hyporheic zone of a eutrophic lowland stream: Results of a preliminary field study. *Science of the Total Environment*, 2011. **409**(10): 1824-1835.

18. Möller, P., G. Morteani, and P. Dulski, Anomalous gadolinium, cerium, and yttrium contents in the Adige and Isarco river waters and in the water of their tributaries (Provinces Trento and Bolzano/Bozen, NE Italy). *Acta hydrochimica hydrobiolica*, 2003. **31**(3): 225-239.

19. Nozaki, Y., D. Lerche, D.S. Alibo, and M. Tsutsumi, Dissolved indium and rare earth elements in three Japanese rivers and Tokyo Bay: Evidence for anthropogenic Gd and In. *Geochimica et Cosmochimica Acta*, 2000. **64**(23): 3975-3982.

20. Zhu, Y., M. Hoshino, H. Yamada, A. Itoh, and H. Haraguchi, Gadolinium anomaly in the distributions of rare earth elements observed for coastal seawater and river waters around Nagoya City. *Bulletin of the Chemical Society of Japan*, 2004. **77**: 1835-1842.

21. Ogata, T. and Y. Terakado, Rare earth element abundances in some seawaters and related river waters from the Osaka Bay area, Japan: Significance of anthropogenic Gd. *Geochemical Journal*, 2006. **40**(5): 463-474.

22. Verplanck, P.L., E.T. Furlong, J.L. Gray, P.J. Phillips, R.E. Wolf, and K. Esposito, Evaluating the behavior of gadolinium and other rare earth elements through large metropolitan sewage treatment plants. *Environmental Science and Technology*, 2010. **44**(10): 3876-3882.

23. Verplanck, P.L., H.E. Taylor, D.K. Nordstrom, and L.B. Barber, Aqueous stability of gadolinium in surface waters receiving sewage treatment plant effluent Boulder Creek, Colorado. *Environmental Science and Technology*, 2005. **39**(18): 6923-6929.

24. Barber, L.B., S.F. Murphy, P.L. Verplanck, M.W. Sandstrom, H.E. Taylor, and E.T. Furlong, Chemical loading into surface water along a hydrological, biogeochemical, and land use gradient: A holistic watershed approach. *Environmental Science and Technology*, 2006. **40**(2): 475-486.

25. Bau, M., A. Knappe, and P. Dulski, Anthropogenic gadolinium as a micropollutant in river waters in Pennsylvania and in Lake Erie, northeastern United States. *Chemie der Erde*, 2006. **66**(2): 143-152.

26. Kümmerer, K. and E. Helmers, Hospital effluents as a source of gadolinium in the aquatic environment. *Environmental Science and Technology*, 2000. **34**(4): 573-577.

27. *Analytical detection limit guidance & laboratory guide for determining method detection limits*, in *PUBL-TS-056-96*, Wisconsin Department of Natural Resources. 1996.

28. DVGW, *Trinkwasserverordnung 2011 vom 3. Mai 2011*, DVGW. 2011.

29. *DIN 38402-13:German standard methods for the examination of water, waste water and sludge; general information (group A); sampling from aquifers (A 13)*. 1985, Beuth.

30. *DIN 38402-11: German standard methods for the examination of water, waste water and sludge - General information (group A) - Part 11: Sampling of waste water*. 2009, Beuth.

31. *The World health report 2000: health systems: improving performance*. 2000, World Health Organization: Geneva

32. Murray, C., J. Salomon, and C.A. Mathers, *Critical examination of summary measures of population health*. 1999, World Healh Organization: Geneva.

33. Horch, C., P. Lessing, and H. Proll, *Kleiner Zahlenspiegel der Metropole Ruhr 2012*. 2012, Regionalverband Ruhr: Essen.

34. Bau, M., October, 2012: personal communication.

35. Pfundstein, P., D. Flottmann, C. Martin, W. Schulz, K.M. Ruth, A. Wille, T. Moritz, and A. Steinbach, Gadolinium-based MRI contrast agents: IC-ICP/MS analysis*. G.I.T. Laboratory Journal Europe*, 2011. **15**(7-8): 31-33.

36. Pfundstein, P., C. Martin, W. Schulz, K.M. Ruth, A. Wille, T. Moritz, A. Steinbach, and D. Flottmann, IC-ICP-MS analysis of gadolinium-based MRI contrast agents*. LC-GC Europe*, 2011: 16-18.

37. Caille, J.M., B. Lemanceau, and B. Bonnemain, Gadolinium as a contrast agent for NMR *American Journal of Neuroradiology*, 1983. **4**(5): 1041-1042.

38. Telgmann, L., J. Künnemeyer, and U. Karst. *Speciation of gadolinium-based MRI contrast media in wastewater treatment plants by HILIC/ICP-MS*. in *International Symposium on Chromatography*. 2010. Valencia.

39. Meyer, S., U. Willme, B. Kuhlmann, and N. Zullei-Seibert, *Orientierende Untersuchungen zum Vorkommen und Verhalten von Gadolinium in*

Oberflächenwasser und angereichertem Grundwasser, in *Wasser 2011*. 2011: Norderney, Germany.

40. Dulski, P., P. Möller, and A. Pekdeger, Comparison of gadopentetic acid (Gd-DTPA) and bromide in a dual-tracer field experiment*. Hydrogeology Journal*, 2011. **19**(4): 823-834.

41. Möller, P., A. Knappe, P. Dulski, and A. Pekdeger, Behavior of Gd-DTPA in simulated bank filtration*. Applied Geochemistry*, 2011. **26**(1): 140-149.

42. Telgmann, L., M. Sperling, and U. Karst, Determination of gadolinium-based MRI contrast agents in biological and environmental samples: A review*. Analytica Chimica Acta*, 2013.

4 Adsorption of gadolinium-based diagnostics in water treatment

4.1 Introduction

New treatment steps for advanced wastewater treatment are discussed for municipal treatment plants [1] and hospital wastewaters [2]. Most promising of currently discussed additional wastewater treatment steps are oxidative treatment by ozone and adsorption on activated carbon (AC) [3]. The advantage of adsorption is that no transformation products or byproducts are formed that may exhibit toxicological relevance [4-6]. A strong disadvantage of activated carbon treatment are costs for removal and / or regeneration. Furthermore, adsorption on activated carbon is very generally speaking, not a suitable process for (very) large substances (if molecular size is so large that pores cannot be entered and hence, available sorption sites are not reached) and very hydrophilic substances. Other factors are influencing adsorption characteristics of a substance as well. A good adsorption of the gadolinium chelates has not been expected. However, gadolinium chelates will be affected simultaneously with other substances, if such an adsorption process is applied in wastewater treatment. Hence, it was investigated to which (small) extend the chelates will be retained in an adsorption step.

The use of activated carbon is a well-known drinking water treatment technology. In Germany it is usually used as granulated activated carbon (GAC) in fixed-bed filters. GAC is also used for the treatment of industrial wastewater, in particular for the removal of dyes.

Generally speaking, the higher the surface of an AC the higher is the Freundlich constant (K_F). Another crucial factor for adsorption efficiency is the character of the surface groups. Competitive adsorption is one of the limiting factors and therefore a challenge especially for removal of micropollutants from wastewater matrices. For wastewater treatment a dosage of 10 - 20 mg L^{-1} powdered activated carbon (PAC) [1, 7] has been proposed. GAC fixed-bed filters may be preferred depending on the specific needs and existent equipment in wastewater treatment plants (WWTPs).

Adsorption equilibrium constants are most relevant for the design of the process in practice [1, 8]. Adsorption on activated carbon is often described by a Freundlich isotherm, as it considers inhomogeneous distribution of binding site energy [9]. Especially for modeling, e.g. of breakthrough behavior in fixed-bed filters, Freundlich constants are necessary [10, 11].

Focus of this study was to evaluate adsorption behavior of gadolinium chelates on different sorbents. The use of gadolinium in magnetic resonance imaging (MRI) for medical diagnostics is increasing [12, 13]. The paramagnetism of gadolinium is used to enhance the contrast of images by reducing the relaxation time [14]. As, the free gadolinium(III) ion is toxic (LD_{50} = 100-200 mg L^{-1} [15]), it is complexed for medical purposes. Gadolinium, in its ionic form, as well as in its chelated form is not regulated by any environmental or waste- / drinking water standard, but its increasing medical use leads to detectable input of these compounds into the aquatic environment via waste water. Hence, the behaviour of these compounds during waste water treatment processes becomes of interest. Some of the most commonly used gadolinium-based diagnostics are presented in Figure 4.1.

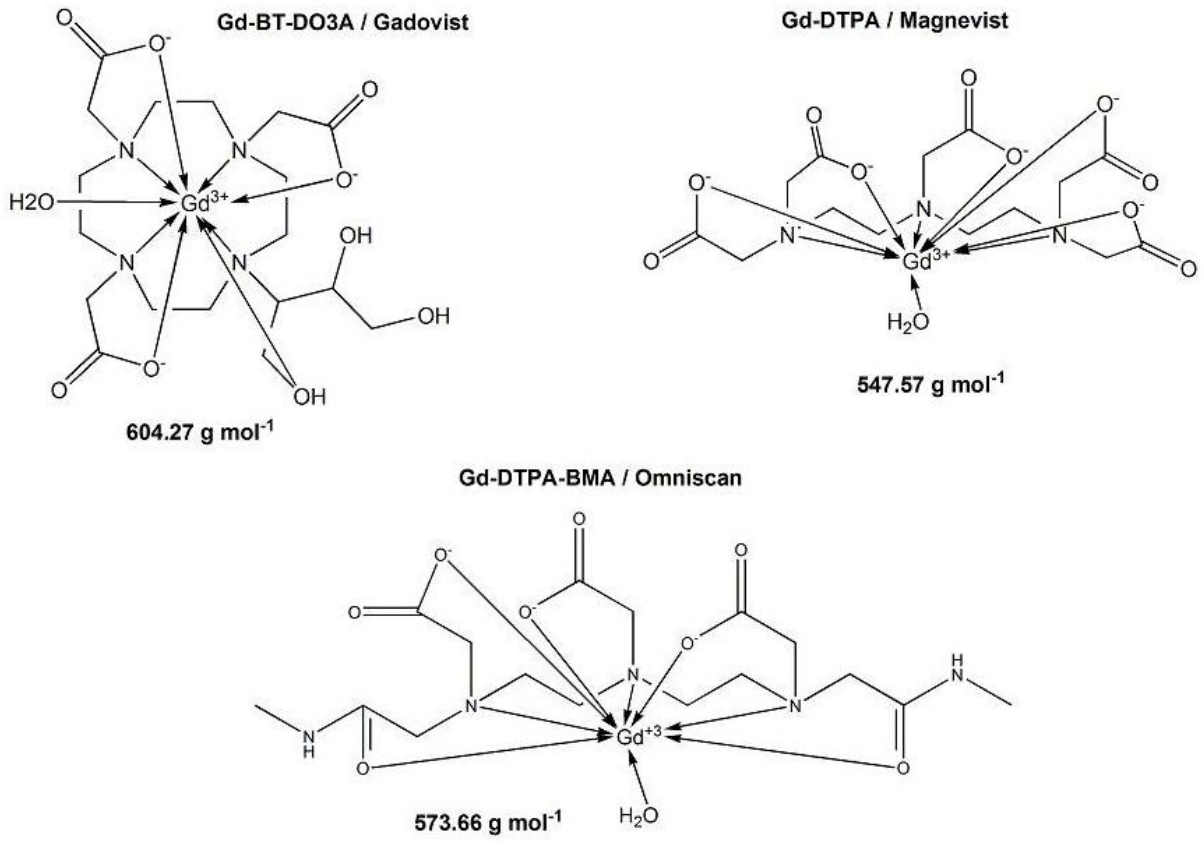

Figure 4.1: Structures of the gadolinium diagnostics investigated and their molar weight

The used gadolinium chelates are very stable (log $K_{[GdL]/[Gd][L]}$ > 15) and it is assumed that these diagnostics are excreted un-metabolized from the human body and hence enter the sewage system unmodified [14]. In WWTPs, these diagnostics are not removed sufficiently [16, 17]. Künnemeyer et al. [16] estimated a reduction of the concentration in the final treated water up to approx. two third of the inflow concentration. Recently, these findings based on random samples have been verified in a follow-up study [17]. A typical effluent concentration of gadolinium from WWTPs in Europe is 120 ng L^{-1} [mean of 75 samples; cf. chapter 3]. Yet a speciation of gadolinium has not been performed. This would be important as transmetalation of the diagosnstics (e.g. exchange of Gd(III) with Fe(III)) may be possible as it has been shown for drinking water [18].

Recently, several investigations revealed elevated concentrations of gadolinium in the aquatic environment [19-21]. It is possible to determine the non-geogenic fraction of the gadolinium concentration in a sample by comparison of concentrations with those of the other rare earth elements (REE) and taking into account the natural abundance of each element [19]. To do this, concentrations of the REEs are normalized to a reference material and plotted versus the atomic number of the elements, and the resulting graph is fitted with a function. The gadolinium anomaly, which is the ratio of the normalized measured gadolinium concentration and the expected normalized concentration, describes the factor by which the gadolinium concentration is above the geogenic level. Hence, gadolinium may be used as a tracer in hydrogeology [21]. It is assumed that adsorption of the chelates on soil is not relevant, yet adsorption behavior of the gadolinium diagnostics on activated carbon and other man-made sorbents has not been studied yet.

As advanced wastewater treatment, with e.g. activated carbon, will increase in the next years, it is important to have a complete view on the behavior of relevant substance classes affected by this treatment. Also, poorly adsorbing substances are retained by application of activated carbon, however, to a minor extent. Especially for the gadolinium-diagnostics it is important to know about the removal efficiency as chelates are generally assumed to be retained poorly. In contrast, metal ions are assumed to adsorb well on AC.

4.2 Experimental

4.2.1 Chemicals and Materials

For determination of adsorption isotherms, two different PACs were used. Norit SA UF® and Chemviron Pul Sorb RD 90®. Both have a small medium particle size (cf. Table 4.1), relatively high capacity and fast adsorption kinetics. Also, adsorption on two different GACs was determined (Norit 830 EN and Jacobi AquaSorb 5000). In comparison to PACs, they exhibit only marginal differences concerning iodine number and BET surface area (cf. Table 4.1). Furthermore, two different synthetic sorbents were tested (Blücher GmbH, Erkrath, Germany: Saratech 1 and Saratech 2). The raw material for these synthetic adsorbents is a spherical polymer which is carbonized and activated in a special procedure. Characteristic for these adsorbents are considerably higher iodine numbers and surface areas than in conventional activated carbons (cf. Table 4.1). As previous experiments have shown [unpublished results], these spherical polymers seem to be able to bind more hydrophilic substances than activated carbons.

Table 4.1: Comparison of the used sorbents (manufacturers' data); [1]for PAC: Particle Size (D_{50}) [µm]; for GAC and synthetic sorbents: Particle size distribution > 95% [µm]

	PAC		GAC		Synthetic sorbents	
Parameter	Norit SA UF	Chemviron Pul Sorb RD 90	Jacobi AquaSorb 5000	Norit 830 EN	Blücher Saratech 1	Blücher Saratech 2
Iodine number [mg g^{-1}]	≥ 1100	≥ 1100	≥ 1100	≥ 1000	1730 – 1780	1380 – 1480
Density (stamped) [kg m^{-3}]	225	250	300	450	408	562
Inner surface (BET) [m^2 g^{-1}]	1200	1100	≥ 1150	1150	1920	1486
Size[1]	5	10	2360 – 600	2380 – 800	315 – 580	315 – 580

For determination of adsorption isotherms the two GACs as well as synthetic sorbents were pulverized with a planetary mill (Pulverisette 7 (Fritsch), Zirconium oxide beakers, 7 zirconium oxide balls (Ø 20 mm), 20 min at 90% power; resulting size ≤ 45 µm). Suspensions were prepared from the pulverized sorbents in drinking water after drying of carbon for at least 24 h at 110°C.

Stock solutions of gadolinium diagnostics ([Gd] = 6.36 µM = 1 mg L^{-1}) were prepared with ultrapure water in polypropylene (PP) vessels. PP-vessels were used to avoid any interaction with glass surfaces (cf. chapter 2). Stock solutions were prepared from Gd-DTPA (powdered, Sigma-Aldrich), Gadovist® (1 M, medical solution from Bayer) and Omniscan® (1 M, medical solution from GE Healthcare).

4.2.2 Adsorption experiments

Adsorption isotherms were determined in triplicate experiments in drinking water (Mülheim tap water for PACs and Duisburg tap water for GACs and synthetic sorbents, for both tap waters ([Gd] < level of quantification (LOQ) and DOC = 0.72 mg L^{-1} (Mülheim), DOC = 0.54 mg L^{-1} (Duisburg)) with an initial concentration of $[Gd]_0 = 6.36 \times 10^{-3}$ µM = 1 µg L^{-1} for PAC isotherms and $[Gd]_0 = 6.36 \times 10^{-2}$ µM = 10 µg L^{-1} for GAC and synthetic sorbents in the water phase. Bottle point isotherms for the determination of isotherms were performed in tap water to take direct competitive adsorption of gadolinium chelates with DOC of the tap water into account [22]. By this it is possible to evaluate general adsorption characteristics of the gadolinium chelates. The concentration of AC and the synthetic sorbents varied between 5 – 50 mg L^{-1} (10 equidistant points). Aliquots of the sorbent suspension (preparation described above) were withdrawn under continuous stirring, to prevent sedimentation of activated carbon, and introduced to the sample solutions in PP-vessels. Samples were shaken continuously with 140 rpm (horizontally). After an equilibration time of at least 24 h, samples (10 mL) were taken with a syringe and filtered through a syringe filter (PP, Ø 25 mm, 0.45 µm PP membrane). The samples were acidified right after filtration with HNO_3 (65% suprapur, Merck) to yield an acid concentration of 0.4 M for stabilization purposes.

Concentration of gadolinium in the aqueous phase was determined by ICP-MS measurements. From this result the load q was calculated and isotherms were determined and evaluated using the Freundlich approach (cf. Equation 4.1).

$$q = K_F \cdot c^n \quad (4.1)$$

K_F → Freundlich coefficient
n → Freundlich exponent

4.2.2.1 Fixed-bed filter experiments

To investigate behavior of gadolinium chelates during filtration processes which may be used as an alternative to the dosage of PAC, lab scale filter experiments were performed. Due to limited resources experiments were carried out in drinking water (same as in the batch experiments for determination of the isotherms) and only for one of the diagnostics. The use of spiked tap water as feed for the filters is feasible and as isotherms for gadolinium chelates and for DOC were determined in the same tap water it should be possible to use these data for description of the breakthrough behavior of gadolinium chelates in a fixed-bed filter with a mathematical model such as the LDF model.

To ensure that effects will be observable, only the diagnostic which revealed the highest affinity to activated carbon was chosen as test adsorbate, in this case Gd-BT-DO3A (cf. Table 4.3).The characteristics of the filters are presented in Table 4.2. As filter media the two GACs and the two synthetic sorbents were used (for characteristics cf. Table 4.1). Gadolinium diagnostics are not readily biodegraded [23]. Generally speaking the more nitrogen atoms substituted with carboxylic groups are present, the more stable is the complex [24, 25]. Gd-BT-DO3A with four amino groups and three carboxy substituents is particularly stable. Even though, one sorbent (Saratech 1) was tested twice, in order to ensure that during the several weeks of experiment duration no microbial activity biased the results of the experiment. To the feed of the second filter with Saratech 1 the biocide sodium azide (50 µg L^{-1}) was added.

Table 4.2: Characteristics of the lab scale filters

Feed	Drinking water
Flow $\dot{v}$	20 L h^{-1}
Filter velocity v_f (filter)	10 m h^{-1}
Layer height	7 cm
Inner diameter d_i	5 cm

Samples from feed and filtrate were taken over a period of 6 weeks (at least one sample per day) to determine the breakthrough of Gd-BT-DO3A.

To gain a first insight on behavior of gadolinium chelates during activated carbon treatment in a wastewater matrix, AC filters in a WWTP (for operation procedure and basic data cf. chapter 4.5.1) were studied. The filter experiment was scaled up from pilot plant (pilot scale filter (PSF)) to full scale (large scale filter (LSF), both PSF and LSF fixed-bed filters were operated with real wastewater). In the WWTP the so called Biofor®-process was used as final treatment step, before establishing the AC filters, and was operated further, parallel to the full scale filter during the monitoring period. In the Biofor®-process the wastewater is filtered through a Biolite™ filter media in bottom-up direction. Particles are retained during the filtration process and biofilms on the surface of the Biolite™ filter material reduce nitrogen and carbon concentration in the filtrate. The lower region of the filter bed is aerated, to enhance aerobic biodegradation.

One of these Biofor®-process basins was modified in such a way that it could be used for the full scale fixed-bed adsorber. This large scale filter (LSF) was operated in upward flow direction. As the Biofor®-process was used in parallel it was possible to compare both treatment steps, the Biofor®-process, which is based on particle removal and biodegradation and the activated carbon filtration, in which as additional removal process adsorption takes place. The LSF (filter area = 40 m^2) consisted of a support layer (0.5 m) of Jacobi AquaSorb 5000 and a 2.0 m fixed-bed consisting of the same type of activated carbon, however, granulated more finely. During the monitoring period, filter velocity was 2 m h^{-1}, to yield high contact time (at v_f = 2 m h^{-1} empty bed contact time = 75 min) and hence maximal adsorption efficiency. Samples were taken at the influent and effluent of the filter bed.

The third filter, a pilot scale filter (PSF), running in the WWTP was the basis for up-scaling to the LSF. The cylindrical filter column (d_i = 190 mm; A_i = 0.0283 m^2) was

operated in downward flow. Bed height was likewise 2.5 m of finely granulated AquaSorb 5000, as the support layer could be omitted. Filter velocity was set to 10 m h^{-1} to yield an empty bed contact time of 15 min. Sampling was also performed at the influent and effluent and of the filter bed. Due to the higher velocity, saturation loading is achieved faster as number of bed volume throughputs per time is increased.

4.2.3 Measurements

Concentration of gadolinium in the aquatic phase was determined by ICP-MS (ELAN DRC II). The detection limit calculated is according to german standard DIN 32645 [26] 0.8 ng L^{-1}. The limit of quantification is as low as 2.4 ng L^{-1} (RSD ≤ 3%). Because of this sensitive analytical method it was possible to determine isotherms in a concentration range which is close to the expected concentrations in WWTPs (< 1 µg L^{-1}, cf. chapter 2 and 3).

Determinations of iopromide and carbamazepine were performed by SPE-HPLC-MS^2 respectively GC-MS. The limit of quantification for both substances is 400 ng L^{-1}.

4.2.4 Modeling of fixed-bed filters

For modeling of fixed-bed filters two programs were used, to confirm the results:

- LDF and AdsAna program, Version 2.6 (© E. Worch 2009); based on the linear driving force model (LDF) and the ideal adsorbed solution theory (IAST) [9]
- FAST 2.0 (© A. Sperlich and S. Schimmelpfennig, 2008 [27]); in this software two different approaches were used: The homogeneous surface diffusion model (HSDM) and the LDF model.

HSDM is a combination of film and surface diffusion and Freundlich equation as equilibrium relationship (incorporating dispersion).

The linear driving force model is considered as valuable alternative to HSDM. It is a simplified surface diffusion model in which instead of Fick`s law a linear driving force (LDF) is used for the mass transfer equation for film diffusion. [9]

For calculations with both programs K_F and n from bottle point isotherm experiments [28] were used and dimensions of the filter as well as operation parameters given above were used. The LDF program provides an estimation tool for the diffusion coefficient (D_L), the liquid-phase mass transfer coefficient (k_F) multiplied with the external adsorbent particle surface area related to the adsorbent volume (a_v) and the surface diffusion coefficient multiplied with a_v. These calculated diffusion coefficients were adopted in the FAST program. In the FAST program only single-solute adsorption modeling is possible.

Modeling was used to gain insight in the characteristics of the adsorption process in fixed-bed adsorbers. Of special interest were competitive adsorption effects of gadolinium chelates with the water matrix, i.e., the natural organic matter which was measured by DOC, as it is assumed to be one of the main factors influencing adsorption processes in wastewater treatment.

The AdsAna model is a mathematical approach to describe adsorption behavior of an unknown mixture of organic substances in water. For this, a DOC isotherm is measured and the DOC is divided into different groups of compounds with different adsorption behavior (different Freundlich parameters). The AdsAna software allows calculation of the competitive adsorption between the different groups of compounds. Variation of the Freundlich coefficients of the different groups allows the fitting of calculated DOC isotherm to the measured values.

4.3 Results and discussion

Adsorption isotherms of the gadolinium diagnostics on the two PAC used are presented in Table 4.3. The Freundlich coefficients of Gd-BT-DO3A on all tested sorbents are presented in Table 4.4.

Table 4.3: Freundlich isotherms of Gd(III) and gadolinium chelates on different PACs ($[Gd]_0 = 6.36 \times 10^{-3}$ µM ; n.d. = not determined)

Substance	Parameter	PAC	
		Norit SA UF	Chemviron® Pul Sorb RD 90
Gd-BT-DO3A (Gadovist®)	K_F [(µmol kg^{-1}) (L $µmol^{-1})^{1/n)}$]	0.256	1.34×10^{-2}
	n	0.376	0.400
	r^2	0.984	0.960
Gd-DTPA-BMA (Omniscan®)	K_F [(µmol kg^{-1}) (L $µmol^{-1})^{1/n)}$]	0.035	5.9×10^{-3}
	n	0.300	0.404
	r^2	0.944	0.959
Gd-DTPA (Magnevist®)	K_F [(µmol kg^{-1}) (L $µmol^{-1})^{1/n)}$]	0.035	7×10^{-6}
	n	0.176	0.245
	r^2	0.827	0.808
$GdCl_3$	K_F [(µmol kg^{-1}) (L $µmol^{-1})^{1/n)}$]	0.282	n.d.
	n	0.690	n.d.
	r^2	0.952	n.d.

Table 4.4: Freundlich coefficients of Gd-BT-DO3A for different sorbents ($[Gd]_0 = 6.36 \times 10^{-6}$ µM)

Sorbent		K_F [(µmol kg^{-1}) (L $µmol^{-1})^{1/n)}$]	n	r^2
GAC	Jacobi® AquaSorb 5000	0.071	0.131	0.894
	Norit® 830 EN	0.016	0.421	0.967
Synthetic sorbent	Blücher® Saratech 1	2.83	0.298	0.959
	Blücher® Saratech 2	0.11	0.395	0.934

K_F values of all diagnostics on all tested sorbents are very low. For instance, the K_F for Gd-DTPA-BMA (, which is sorbing in the middle range of all tested diagnostics) of 1.26 [(mmol kg^{-1}) (L $mmol^{-1})^{1/n)}$] is approximately the same as the one of iopromide (1.92 [(mmol kg^{-1}) (L $mmol^{-1})^{1/n)}$] [28]) on Norit SA UF. Iopromide is considered as a substance insufficiently removable by activated carbon [3]. The results of the experiments show clearly that adsorption of the diagnostics on activated carbon is low with an exemplary removal efficiency of 41% (Gd-DTPA-BMA) for a dosage of 10 mg L^{-1} Norit SA UF.

Adsorption in general depends on several different characteristics of both adsorbates (e.g. structure and size) and adsorbent (e.g. surface characteristics), as well as on different matrix dependent effects (e.g. pH, temperature, concentration and composition). One of the aspects influencing adsorption is water solubility and hydrophilicity of the adsorbate. In general it is assumed that substances with high hydrophilicity, which may be described by the P_{OW}, are adsorbed less efficient than those with a low hydrophilicity. This has been described by Zwiener, who found that substances with a log P_{OW} >10^3 have a removal efficiency of 75 - 100% with activated carbon [29]. Gadolinium chelates are characterized by high water solubility and extremely low P_{OW} values (e.g., log P_{OW} = $10^{-5.4}$ for Gd-BT-DO3A, Gadovist®), like most metal chelates. Hence, a low K_F has been expected.

In literature it is furthermore discussed whether complexation of metals improves or decreases adsorption of metal ions on activated carbon [30]. In general, adsorption of metals increases with increasing pH [30, 31] and chelation with organic ligands decreases adsorption at all pHs relevant for water treatment [32]. Hence, it was assumed that the Gd(III) ion is sorbing better than any of the gadolinium chelates. This assumption has been confirmed by experimental results (cf. Table 4.3).

Another important factor for describing adsorption is the surface of the adsorbent. This has been shown by a comparison of conventional activated carbons with synthetic sorbents. The spherical sorbents are mainly characterized by a very high BET, up to almost 2000 $m^2 g^{-1}$ (for Saratech 1). The higher the surface area of the sorbents the higher is K_F. The results of isotherm determinations (cf. Table 4.4) and a comparison of the results of filter experiments (cf. Figure 4.2) indicate that the surfaces of the spherical synthetic sorbents are better capable of adsorbing these hydrophilic compounds, than the ACs. As shown in Figure 4.2, filter breakthrough for the sorbent with highest inner surface area (Saratech 1) is occurring last.

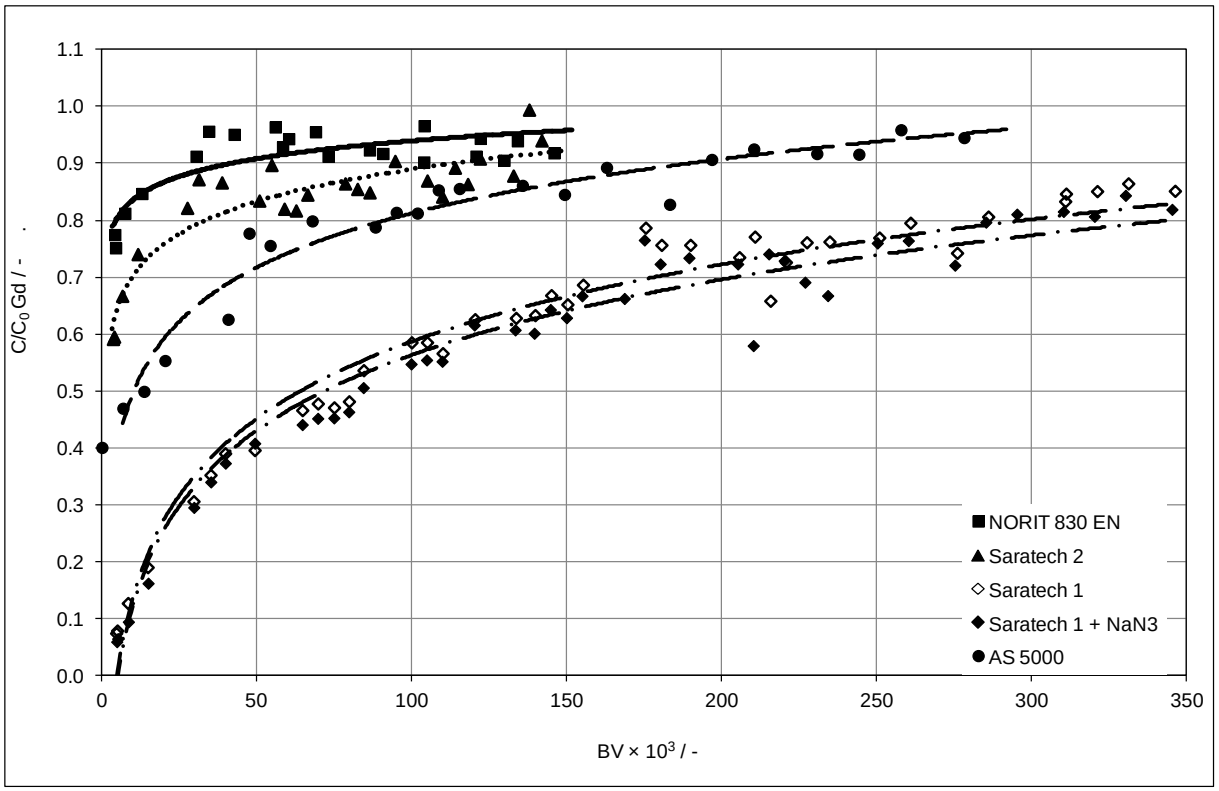

Figure 4.2: Adsorption of Gd BT DO3A, spiked in drinking water on different sorbents in a fixed bed reactor; $[Gd]_{influent} = 6.36 \times 10^{-5}$ mM

Comparing the two synthetic sorbents with the activated carbons, it is clear that breakthrough of the filters is fastest for Norit carbon and slowest for the Saratech sorbent with the highest inner surface. Nevertheless, Jacobi AS 5000 is more efficient for removal of gadolinium chelate from the tested drinking water matrix than Saratech 2. Comparing BET surface area and iodine number, one has to consider that no maximum values are given for Jacobi AS 5000. Nevertheless, BET surface and iodine number are not the only values for a complete characterization of adsorption capacity for an adsorbent. Further properties like wettability, accessibility

of the total pore system, and the kind of surface groups on all surfaces of the adsorbent may influence removal efficiency. However, a more indepth characterization of adsorbents was not in focus of this study.

Calculation of breakthrough curves for Saratech 1, based on both model approaches used (LDF and FAST program) are shown in Figure 4.3 (for input parameters cf. chapter 4.5.2).

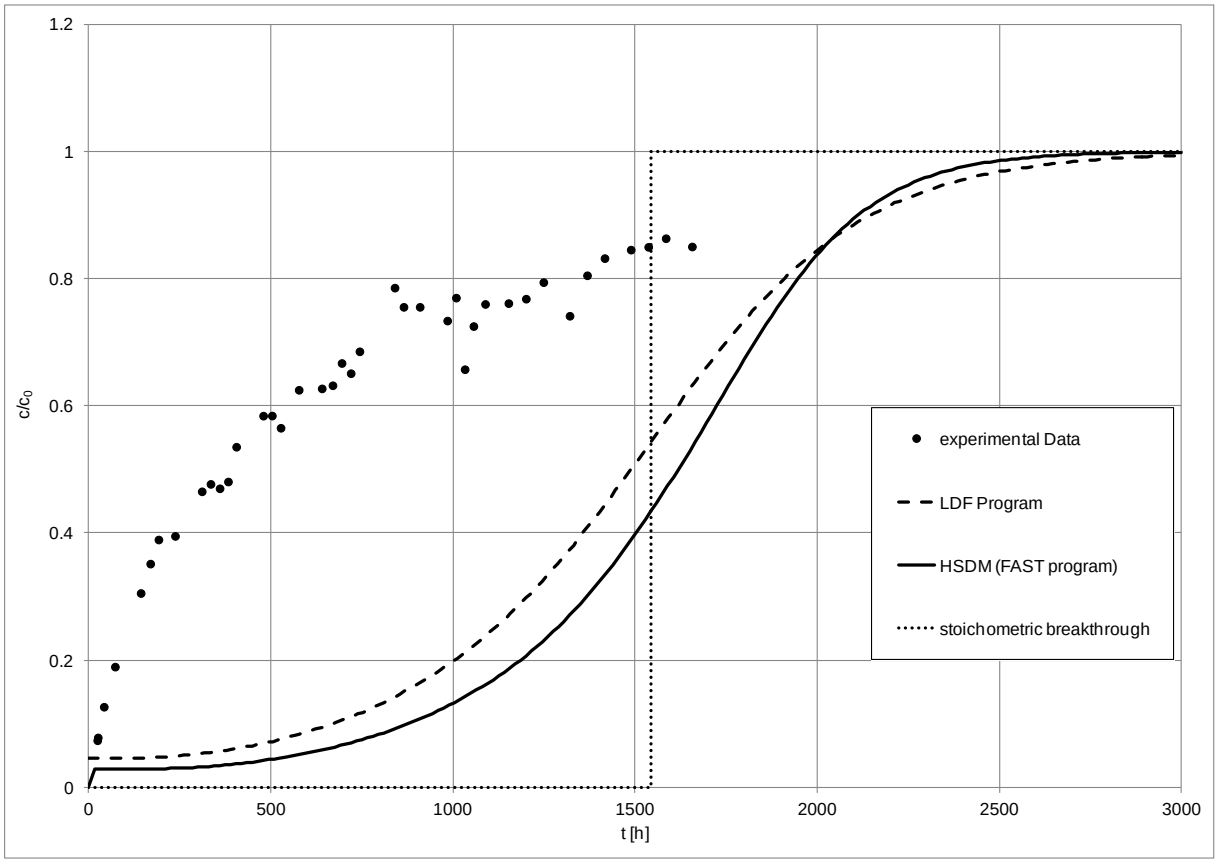

Figure 4.3: Comparison of experimental breakthrough data (lab scale experiments, $[Gd\text{-}BT\text{-}DO3A]_0 = 6.36 \times 10^{-5}$ mM in drinking water matrix without sodium azide) and model predictions (LDF program and FAST program) for Saratech 1

To ensure that the effect of competitive adsorption is considered, all adsorption isotherms were determined in tap water. However, when using data from these batch experiments to model filter breakthrough instead of using isotherm data from single solute experiments, a comparison of fixed-bed experimental data and modeled data shows a clear deviation (cf. Figure 4.3).

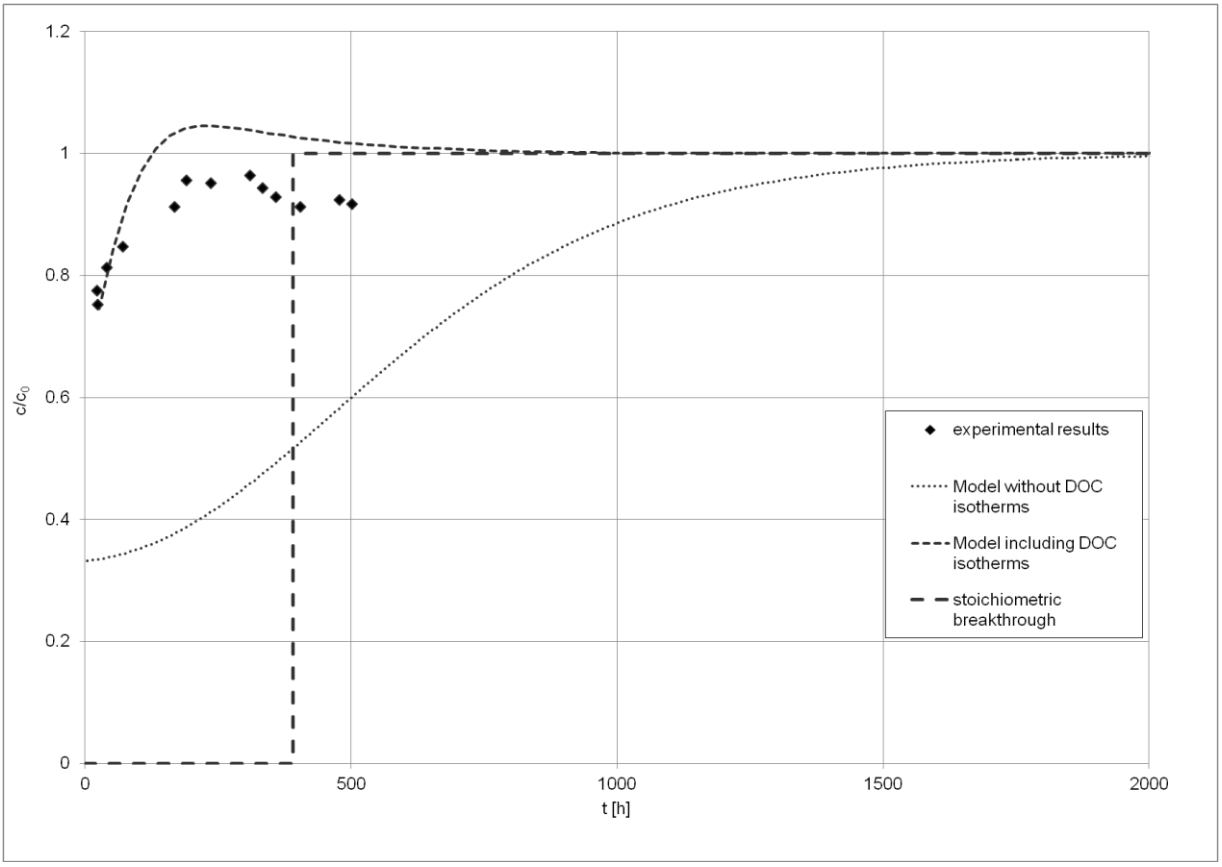

Figure 4.4: Breakthrough curves of Gd BT DO3A (6.36×10^{-5} mM in drinking water matrix); lab scale experiments with Norit 830 EN (model predictions (LDF program, input parameters, c.f. chapter 4.5.2) and experimental data)

Thus, to describe early breakthrough a simple approach was tested. For this, in addition to the Freundlich data for the gadolinium chelate in tap water - taking into account competitive adsorption in batch – Freundlich data for three different groups of virtual DOC compounds resulting from adsorption analysis with the AdsAna Software were used in the LDF model. Results of this calculation are shown in Figure 4.4. It is shown that the calculated breakthrough curve on basis of the mentioned procedure leads to a quite good description of the measured values. Also, desorption after reaching a maximum may be explained by competitive adsorption of DOC and gadolinium chelate. Gadolinium chelates which have already adsorbed can be displaced from adsorption sites by components of the DOC, resulting in a higher effluent than initial concentration.

Filter experiments in a WWTP corroborate results obtained in lab scale experiments and modeling. The results (cf. Figure 4.5) show that adsorption of gadolinium is very low.

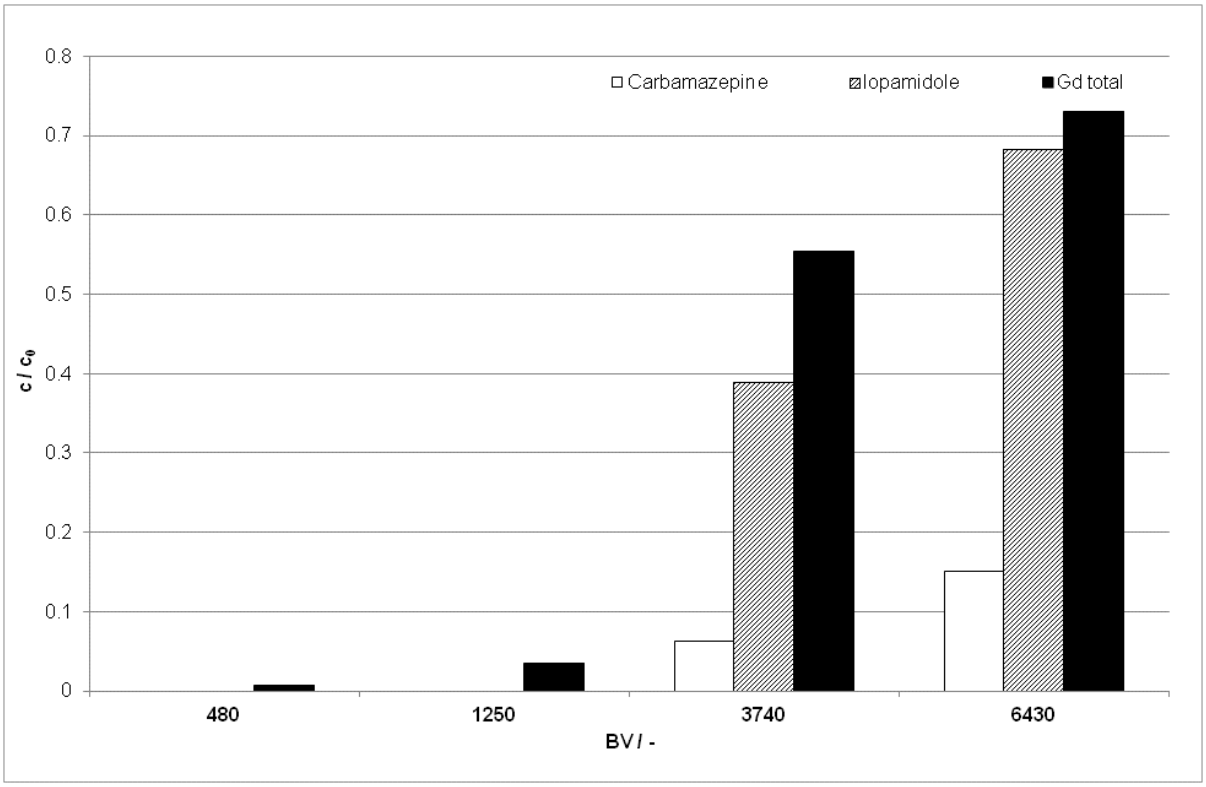

Figure 4.5: Removal of different substances in the PSF in the WWTP; white bars: carbamazepine; hatched bars: iopamidole; black bars: total gadolinium. (Carbamazepine and iopamidole where below limit of quantification (LOQ) (for carbamazepine and iopamidole LOQ = 0.04 µg L^{-1}) in the effluent of the filter until a throughput of 3744 bed volumes (BV), influent concentrations: Carbamazepine = 1.3 µg L^{-1}; iopamidole = 0.2 µg L^{-1}; $gadolinium_{total}$ = 0.5 µg L^{-1}

As it can be seen in Figure 4.5, gadolinium will be one of the first substances which can be detected in the filter effluent. The effluent concentration of iopamidole, which is supposed to adsorb very poorly on activated carbon [3], is reduced to a greater extent than the one of gadolinium. Information of a differentiation of anthropogenic and geogenic gadolinium removal during the filtration process is given in the supplement (cf. chapter 4.5.3).

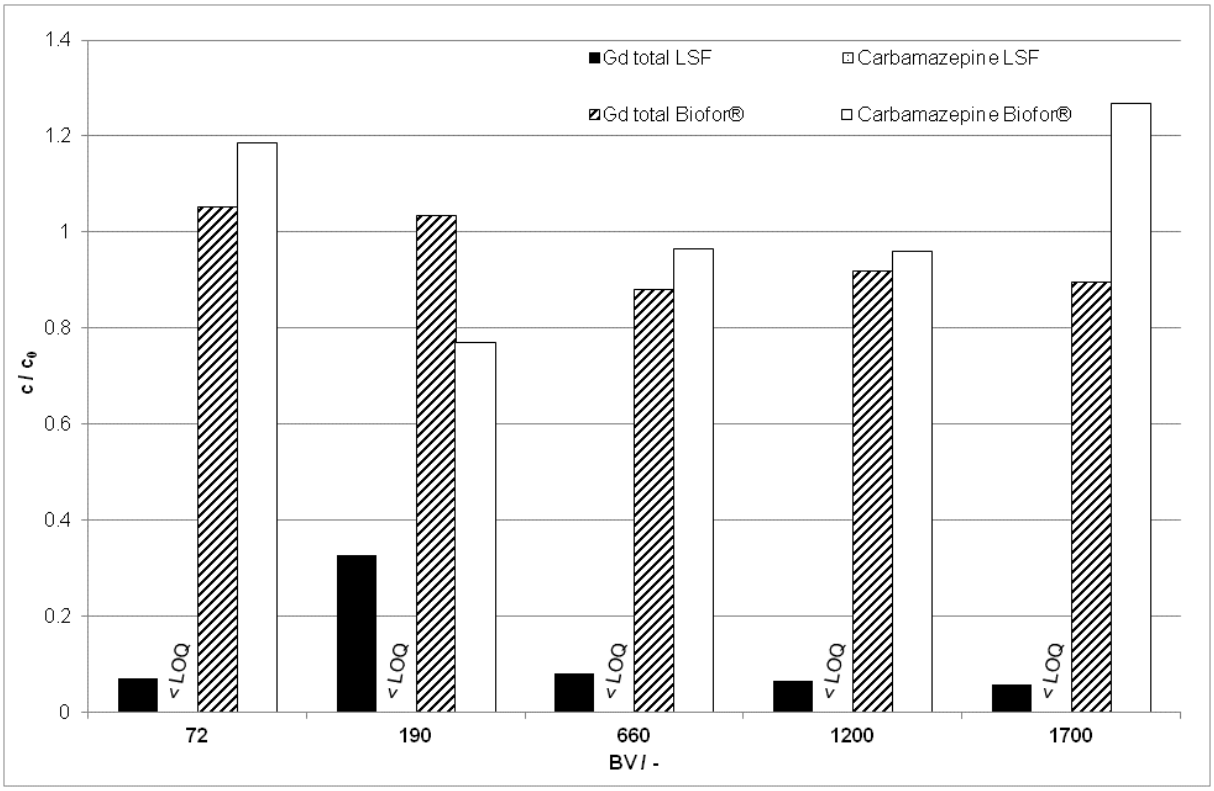

Figure 4.6: Comparison of the removal of carbamazepine and gadolinium in the Biofor® process and the large scale filter ($LOQ_{carbamazepine}$ = 400 ng L^{-1}) in a WWTP

The comparison of the Biofor®-process and adsorption on activated carbon shows that the reduction of carbamazepine is not possible by biological degradation. However, adsorption on activated carbon eliminates carbamazepine completely. Gadolinium is also not reduced by biological treatment. Adsorption in the activated carbon filter is reducing gadolinium by more than 90% in this short operating period. In a worst case scenario for operating fixed-bed filters in wastewater treatment (i.e. removal of 70% of diclofenac, a poorly adsorbing substance, and a median removal of 80% for all other substances from a hospital wastewater matrix with c(DOC) = 10 mg L^{-1}), up to 7500 BV can be treated before the carbon has to be exchanged [33]. Based on the presented data for gadolinium a smaller breakthrough volume of only 6400 BV would result in such a scenario.

4.4 Conclusion

To evaluate adsorption of gadolinium chelates first determination of isotherms in bottle point experiments were performed. To this end, tap water was used to include the effect of competitive adsorption, which is of importance for any water matrix to be treated. Isotherm data already revealed that adsorption of the chelates is highly inefficient, as it has been assumed. The poor adsorption may be demonstrated as follows: For a 90% removal of 6.4 nM Gd-DTPA from a drinking water matrix 50 mg L^{-1} Norit SA UF are necessary. Yet, only an addition of 10-20 mg L^{-1} PAC is discussed for advanced wastewater treatment [1, 7] in which the competitive adsorption will take place to an even greater extent than in a drinking water matrix. Hence, an additional treatment step in WWTPs utilizing PAC adsorption will hardly affect gadolinium chelates at effluent concentrations.

Preliminary lab scale experiments assessing breakthrough behavior of the chelates in fixed-bed filters have been performed. The early breakthrough could be calculated using the LDF model. In this case it has been possible to differentiate between a direct competitive adsorption and an additional competitive adsorption in the filter by the DOC of the used drinking water.

Investigations on adsorption of gadolinium in WWTPs activated carbon filtration showed that adsorption is even poorer than assumed. A comparison of results from lab scale filtration and results from filtration in the WWTP show that a 70% breakthrough occurs much quicker in the PSF. The treated BV of the filters in the WWTP are by a factor of ~100 lower for a 70% breakthrough than in the lab scale filters. It has to be considered that adsorption on activated carbon in general is not a suitable process for the removal of metal chelates. But since additional treatment steps for wastewater treatment may include adsorption on activated carbon it is nevertheless necessary to investigate their behavior in such a scenario.

Yet one might take into consideration to use gadolinium as indicator for the quality of the filtration processes in a WWTP. Gadolinium analysis is cheap compared to analysis of most organic trace substances. The LOQ is low and the analysis method is very robust. During water treatment by activated carbon or other adsorption based treatment steps, the gadolinium anomaly could be monitored to indicate breakthrough of organic trace substances in filters. Due to poor adsorption of gadolinium diagnostics breakthrough detection is possible earlier than by monitoring of other commonly used organic substances, like atrazine.

4.5 Supplement

4.5.1 Description of the wastewater treatment plant

- Size: 380000 population equivalents (connected: 185000 population equivalents (ca. 75000 citizens + 110000 population equivalents)
- Dry weather volume: 18000 m³/day
- Maximal volume: 60000 m³/day
- 65% highly poluted industrial waste water
- Treatment steps:
- Bar screening
  - Grit chamber, including grease removal
  - Primary treatment (3000 m³)
  - 1. Biological step (including Bypass, 5000 m³ reactor volume and 5880 m³ settling volume) including intermediary treatment
  - 2. Biological step (9.200 m³ reaktor volume and 12480 m³ settling volume) including intermediary treatment
  - Fixed-bed denitrification as a 3. Biological step (8 chambers each A_f = 37.5 m²)
  - Flocculation-filtration (Biofor®-process, 10 chambers each A_f = 40 m², filter material: Biolit (siliceous diabase))
  - Polishing ponds (42640 m³)

4.5.2 Modeling input parameters

Table S 4.1: Input parameters for modeling the breakthrough of two different filters with both used programs (LDF program and FAST program); NOTE: Isotherm data are given in mg L^{-1} as the program needs input data in this specific unit; $k_F a_v$ and $k_S a_v$ both calculated by the LDF program, the resulting diffusion coefficients were used for FAST program.

Sorbent	Input parameter	Value	Sorbent	Input parameter	Value
Norit 830 EN	$c_{0,\ Gd\text{-}BT\text{-}DO3A}$	0.038 mg L^{-1}	Saratech 1	$c_{0,\ Gd\text{-}BT\text{-}DO3A}$	0.038 mg L^{-1}
	$K_{F\ ,\ Gd\text{-}BT\text{-}DO3A}$	22.2 [g kg^{-1}] / [mg L^{-1}]$^{1/n}$		$K_{F\ ,\ Gd\text{-}BT\text{-}DO3A}$	65.5 [g kg^{-1}] / [mg L^{-1}]$^{1/n}$
	$n_{Gd\text{-}BT\text{-}DO3A}$	0.4		$n_{Gd\text{-}BT\text{-}DO3A}$	0.3
	V_F	10 m h^{-1}		V_F	10 m h^{-1}
	T	15°C		T	15°C
	ε	0.4		ε	0.4
	d_P	1.6 mm		d_P	0.4475 mm
	$m_{adsorbent}$	0.05538 kg		$m_{adsorbent}$	0.04777 kg
	V	0.02 m^3 h^{-1}		V	0.02 m^3 h^{-1}
	p	500 kg m^{-3}		*p*	500 kg m^{-3}
	$c_{0,\ DOC\ 1}$	0.04 mg L^{-1}		Yielded $k_F a_v$	1.93 × 10^{-1} s^{-1}
	$K_{F\ ,\ DOC\ 1}$	5 [g kg^{-1}] / [mg L^{-1}]$^{1/n}$		Yielded $k_S a_v$	3.96 × 10^{-6} s^{-1}
	$c_{0,\ DOC\ 2}$	0.06 mg L^{-1}			
	$K_{F\ ,\ DOC\ 2}$	25 [g kg^{-1}] / [mg L^{-1}]$^{1/n}$			
	$c_{0,\ DOC\ 3}$	0.26 mg L^{-1}			
	$K_{F\ ,\ DOC\ 3}$	60 [g kg^{-1}] / [mg L^{-1}]$^{1/n}$			
	n_{DOC}	0.2			
	Yielded $k_F a_v$	2.71 × 10^{-2} s^{-1}			
	Yielded $k_S a_v$	2.24 71 × 10^{-6} s^{-1}			

4.5.3 Use of the gadolinium anomaly in filter experiments in a wastewater treatment plant

Overall in an adsorption process, the total gadolinium concentration is decreasing but the fraction of geogenic gadolinium is decreasing stronger than the non-geogenic fraction, resulting in an increasing deviation between $[Gd]_{total}$ and the gadolinium anomaly (cf. Figure S 4.1).

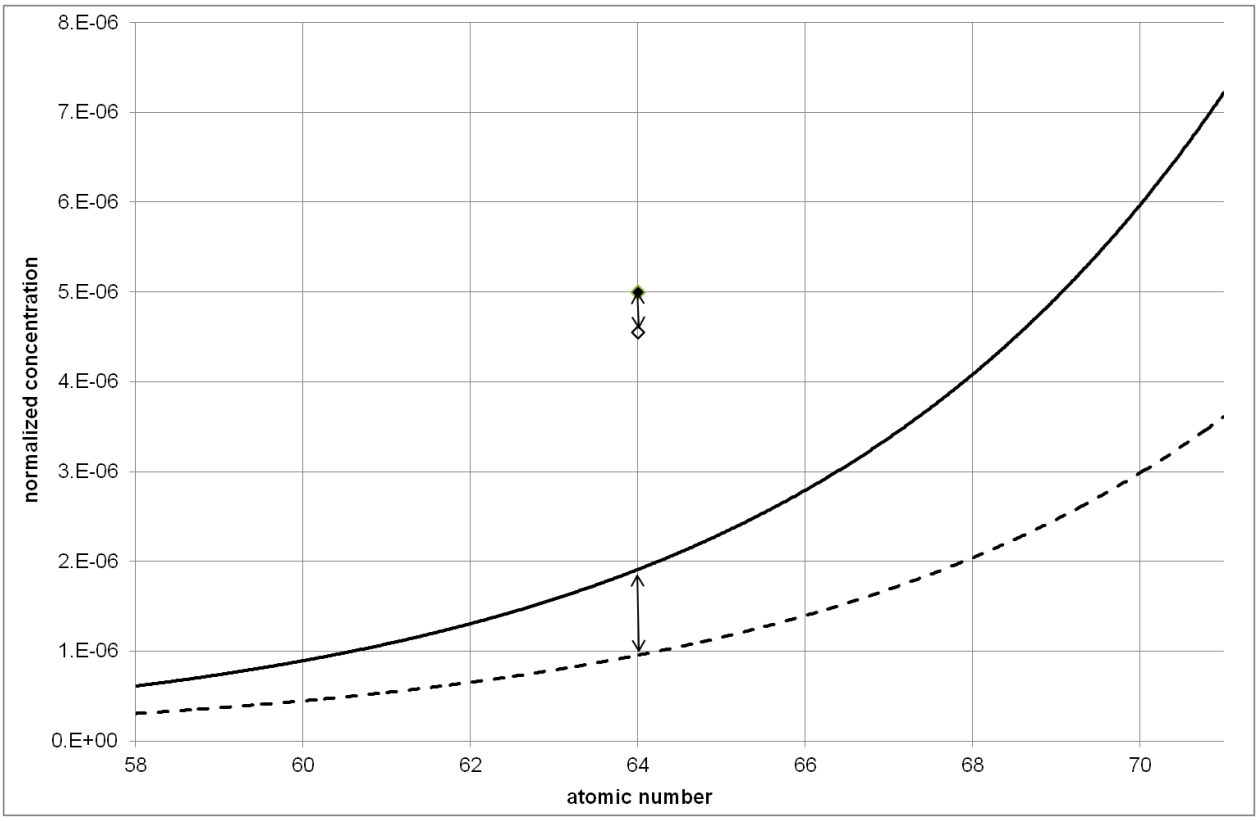

Figure S 4.1: Figure for description of the anomaly increase after a filtration process; black line and black diamond represent the normalized REE concentrations vs. atomic number before a filtration process; dashed line and hollow diamond represent the normalized REE concentration vs. atomic number after a filtration process

For a better understanding of this one has to consider that:

$$Gd_{total} = Gd_{geogenic} + Gd_{non-geogenic} \quad (4.2)$$

More precisely:

$$\lfloor Gd_{total} \rfloor = a \times [Gd] + b \times [Gd] \quad (4.3)$$

In which b > a

In adsorption processes the geogenic fraction is adsorbing better than the non-geogenic fraction. In a filtration process, which is working well, one might represent this as:

$$[Gd_{total}] = (a - d) \times [Gd] + (b - c) \times [Gd] \quad (4.4)$$

In which c > d.

In a filtration process, which is reaching breakthrough, both gadolinium fractions are adsorbing less, until a total breakthrough is reached, described by $[Gd] / [Gd]_0 = 1$.

The gadolinium anomaly is defined as presented above (cf. equation 4.3). Revising this definition by incorporating the filtration process as presented in (cf. eq. 4.4) yields:

$$\text{Gadolinium Anomaly} = \frac{(a - d) \times [Gd] + (b - c) \times [Gd]}{(a - d) \times [Gd]} \quad (4.5)$$

The relation of $[Gd_{total}]_{after\ filtration}$ to $[Gd_{total}]_0$, which is the total gadolinium concentration before filtration is reaching no values > 1. However, the quotient of gadolinium anomaly after the filtration process (gadolinium anomaly) to anomaly before an filtration process (gadolinium $anomaly_0$) might reach values > 1. As in this case not concentrations are related, however, a relation to a reference value ($[Gd_{expected}]$) that may be decreased to a greater extent than the target value ($[Gd_{total}]$). Hence, it is possible, that the anomaly increases at a certain time in comparison to the initial value (gadolinium $anomaly_0$), as the concentration of the geogenic REEs decreases stronger than the concentration of the non-geogenic gadolinium:

$$\frac{\frac{(a - d) \times [Gd] + (b - c) \times [Gd]}{(a - d) \times [Gd]}}{\frac{a \times [Gd] + b \times [Gd]}{a \times [Gd]}} \quad (4.6)$$

Solving equation 4.6 leads to:

$$\frac{1 + \frac{b - d}{a - c}}{1 + \frac{b}{a}} \quad (4.7)$$

Regarding the assumptions made above ($Gd_{anthropogenic} > Gd_{geogenic} \rightarrow b > a$) and adsorption of $Gd_{geogenic}$ > adsorption of $Gd_{anthropogenic} \rightarrow c > d$), the term presented in equation 4.6 is greated than 1.

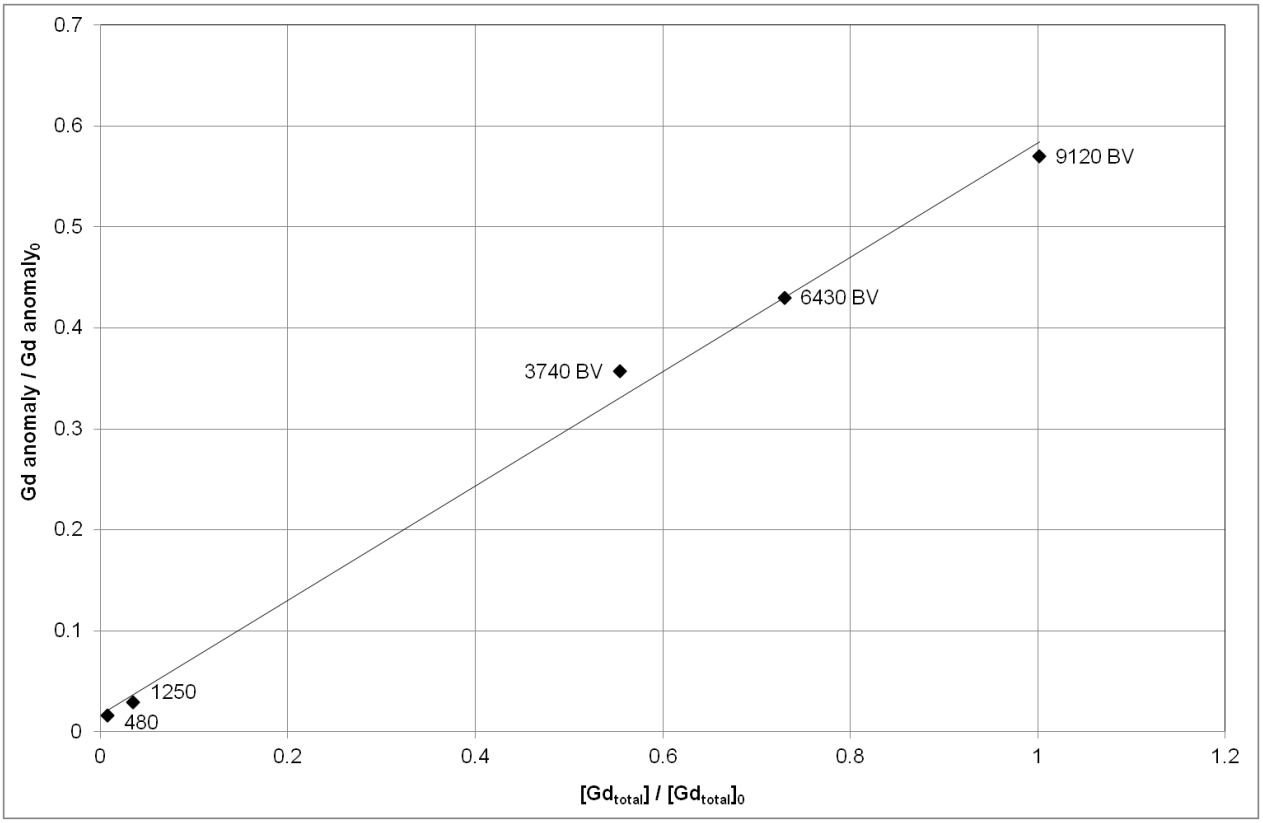

Figure S 4.2: Correlation of $[Gd_{total}] / [Gd_{total}]_0$ to (Gd anomaly) / $(Gd\ anomaly)_0$ in a fixed-bed activated carbon filter in a wastewater treatment plant (details given in 4.2.2.1); the number of treated bed volumes for the given data point is presented in the diagram; linear equation: (Gd anomaly) / $(Gd\ anomaly)_0 = 0.566\ [Gd_{total}] / [Gd_{total}]_0 + 0.0166$ with $r^2 = 0.996$

The quotient of (gadolinium anomaly) / $(gadolinium\ anomaly)_0$ and $[Gd_{total}] / [Gd_{total}]_0$ increases during the course of filtration as $[Gd_{total}] / [Gd_{total}]_0$ will approach 1, whereas (gadolinium anomaly) / $(gadolinium\ anomaly)_0$ will increase less than $[Gd_{total}] / [Gd_{total}]_0$. This is indicated by the slope < 1 (cf. Figure S 4.2).

4.6 References

1. Nowotny, N., B. Epp, C. von Sonntag, and H. Fahlenkamp, Quantification and modeling of the elimination behavior of ecologically problematic wastewater micropollutants by adsorption on powdered and granulated activated carbon. *Environmental Science and Technology*, 2007. 41(6): 2050-2055.

2. Joss, A., H. Siegrist, and T.A. Ternes, Are we about to upgrade wastewater treatment for removing organic micropollutants? *Water Science and Technology*, 2008. 57: 251-255.

3. Ternes, T., *Assessment of technologies for the removal of pharmaceuticals and personal care products in sewage and drinking water facilities to improve the indirect potable water reuse*, in *Poseidon report*. 2005.

4. Benner, J., E. Salhi, T. Ternes, and U. von Gunten, Ozonation of reverse osmosis concentrate: Kinetics and efficiency of beta blocker oxidation. *Water Research*, 2008. 42(12): 3003-3012.

5. Schmidt, C.K. and H.J. Brauch, N,N-dimethylsulfamide as precursor for N-nitrosodimethylamine (NDMA) formation upon ozonation and its fate during drinking water treatment. *Environmental Science and Technology*, 2008. 42(17): 6340-6346.

6. Sein, M.M., M. Zedda, J. Tuerk, T.C. Schmidt, A. Golloch, and C. von Sonntag, Oxidation of diclofenac with ozone in aqueous solution. *Environmental Science and Technology*, 2008. 42(17): 6656-6662.

7. Hollender, J., S.G. Zimmermann, S. Koepke, M. Krauss, C.S. McArdell, C. Ort, H. Singer, U. Von Gunten, and H. Siegrist, Elimination of organic micropollutants in a municipal wastewater treatment plant upgraded with a full-scale post-ozonation followed by sand filtration. *Environmental Science and Technology*, 2009. 43(20): 7862-7869.

8. Hand, D.W., J.C. Crittenden, H. Arora, J.M. Miller, and B.W. Lykins Jr, Designing fixed-bed adsorbers to remove mixtures of organics. *Journal of the American Water Works Association*, 1989. 81(1): 67-77.

9. Worch, E., *Adsorption technology in water treatment: Fundamentals, processes, and modeling*. 2012, Berlin / Boston: De Gruyter.

10. Worch, E., Competitive adsorption of micropollutants and NOM onto activated carbon: Comparison of different model approaches*. Journal of Water Supply: Research and Technology - AQUA*, 2010. 59(5): 285-297.

11. Hobby, R., *Removal of organic pollutants by powdered activated carbon (Entfernung organischer Störstoffe im Spurenbereich mit pulverförmiger Aktivkohle)*.1995, Dissertation at Gerhard-Mercator University Duisburg.

12. Kulaksiz, S. and M. Bau, Anthropogenic gadolinium as a microcontaminant in tap water used as drinking water in urban areas and megacities*. Applied Geochemistry*, 2011. 26(11): 1877-1885.

13. Kümmerer, K. and E. Helmers, Hospital effluents as a source of gadolinium in the aquatic environment*. Environmental Science and Technology*, 2000. 34(4): 573-577.

14. Caravan, P., J.J. Ellison, T.J. McMurry, and R.B. Lauffer, Gadolinium(III) chelates as MRI contrast agents: Structure, dynamics, and applications*. Chemical Reviews*, 1999. 99(9): 2293-2352.

15. Caille, J.M., B. Lemanceau, and B. Bonnemain, Gadolinium as a contrast agent for NMR *American Journal of Neuroradiology*, 1983. 4(5): 1041-1042.

16. Künnemeyer, J., L. Terborg, B. Meermann, C. Brauckmann, I. Möller, A. Scheffer, and U. Karst, Speciation analysis of gadolinium chelates in hospital effluents and wastewater treatment plant sewage by a novel HILIC/ICP-MS method*. Environmental Science and Technology*, 2009. 43(8): 2884-2890.

17. Telgmann, L., C.A. Wehe, M. Birka, J. Künnemeyer, S. Nowak, M. Sperling, and U. Karst, Speciation and isotope dilution analysis of gadolinium-based contrast agents in wastewater*. Environmental Science and Technology*, 2012. 46(21): 11929-11936.

18. Pfundstein, P., C. Martin, W. Schulz, K.M. Ruth, A. Wille, T. Moritz, A. Steinbach, and D. Flottmann, IC-ICP-MS analysis of gadolinium-based MRI contrast agents*. LC-GC Europe*, 2011: 16-18.

19. Bau, M. and P. Dulski, Anthropogenic origin of positive gadolinium anomalies in river waters*. Earth and Planetary Science Letters*, 1996. 143(1-4): 245-255.

20. Rabiet, M., F. Brissaud, J.L. Seidel, S. Pistre, and F. Elbaz-Poulichet, Positive gadolinium anomalies in wastewater treatment plant effluents and aquatic environment in the Herault watershed (South France). *Chemosphere*, 2009. 75(8): 1057-1064.

21. Schwesig, D. and A. Bergmann, Use of anthropogenic gadolinium as a tracer for bank filtrate in drinking water wells. *Water Science and Technology: Water Supply*, 2012. 11(6): 654-658.

22. Haist-Gulde, B., *Zur Adsorption von Spurenverunreinigungen aus Oberflächenwässern*.1991, Dissertation at Technical University Karlsruhe.

23. Neubert, C., R. Länge, and T. Steger-Hartmann, *Gadolinium containing contrast agents for magnetic resonance imaging (MRI) investigations on the environmental fate and effects*, in *Fate of pharmaceuticals in the environment and in water treatment systems*, D.S. Aga, Editor. 2008, CRC Press Taylor & Francis Group: Boca Raton, Fl.

24. Pitter, P. and V. Sykora, Biodegradability of ethylenediamine-based complexing agents and related compounds. *Chemosphere*, 2001. 44(4): 823-826.

25. Sykora, V., P. Pitter, I. Bittnerova, and T. Lederer, Biodegradability of ethylenediamine-based complexing agents. *Water Research*, 2001. 35(8): 2010-2016.

26. *DIN EN 32645: 2008; Chemische Analytik - Nachweis-, Erfassungs- und Bestimmungsgrenze unter Wiederholbedingungen - Begriffe, Verfahren, Auswertung*, G.I.f. Standardization, Editor.

27. Sperlich, A., S. Schimmelpfennig, B. Baumgarten, A. Genz, G. Amy, E. Worch, and M. Jekel, Predicting anion breakthrough in granular ferric hydroxide (GFH) adsorption filters. *Water Research*, 2008. 42(8-9): 2073-2082.

28. Ivancev-Tumbas, I., R. Hobby, B. Kreckel, and R. Gimbel, *Adsorption behavior of carbamazepine and iopromide in bottle isotherm test*, in *Micropo l& Ecohazard 2007, 5th IWA Specialized Conference on Assessment and Control of Micropollutants/Hazardous Substances in water*. 2007: Frankfurt am Main, Germany.

29. Zwiener, C., Occurrence and analysis of pharmaceuticals and their transformation products in drinking water treatment. *Analytical and Bioanalytical Chemistry*, 2007. 387(4): 1159-1162.

30. Benjamin, M.M. and J.O. Leckie, Conceptual model for metal-ligand-surface interactions during adsorption. *Environmental Science and Technology*, 1981. 15(9): 1050-1057.

31. Corapcioglu, M.O. and C.P. Huang, The adsorption of heavy metals onto hydrous activated carbon. *Water Research*, 1987. 21(9): 1031-1044.

32. Huang, C.P. and D.W. Blankenship, The removal of mercury (II) from dilute aqueous solution by activated carbon. *Water Research*, 1984. 18(1): 37-46.

33. Abegglen, C. and H. Siegrist, *Micropollutants in municipal wastewater: Processes for advanced removal in wastewater treatment plants*. 2012: Bern.

5 Reaction of Gadolinium Chelates with Ozone and Hydroxyl Radicals

5.1 Introduction

Ozone and / or hydroxyl radical treatment processes are long known for disinfection and removal of trace substances in drinking water treatment [1-3]. In recent years, these processes have been discussed for the application in wastewater treatment and are in some places already established in full-scale [4]. This is due to frequent detections of trace substances in surface and ground waters [5, 6]. The removal of these substances is often inefficient in conventional wastewater treatment plants (WWTP). According to the European water framework directive the water quality shall reach a “good chemical status” as well as a “good ecological status” [7]. This aim is threatened by the presence of several of these traces substances, especially those with biological activity such as (xeno-)hormones, antibiotics, and other pharmaceuticals. For further elimination of such compounds in an additional treatment step, the application of ozone is one of the preferred methods. Ozone action in wastewater can be divided in two reaction pathways [8, 9]. Mainly it reacts with the wastewater matrix forming hydroxyl radicals to substantial yields[3, 8, 10, 11]. In wastewater the application of ozone generates 13 mol % hydroxyl radicals of the applied ozone dose [10]. In competition to the hydroxyl radical forming reaction, ozone-reactive target compounds are oxidized directly. In many cases, the biological activity of the target compounds is eliminated upon a single ozone attack [3]. Ozone refractory compounds can also be transformed via hydroxyl radicals formed by the matrix. However, again competition between wastewater matrix and target compounds is a limiting factor. The hydroxyl radical rate constants are strongly influencing the efficiency of target compound oxidation [3, 11]. To understand the oxidation of target compounds in a wastewater matrix it is necessary to investigate both the reaction via ozone and hydroxyl radicals separately.

The reactions of chelates with ozone and hydroxyl radicals are rarely studied [12]. There are few studies on the reaction of metal EDTA complexes [13-16] and on metal DTPA complexes [17, 18], but to the authors’ knowledge, no other chelates are covered in such studies. Here, we focus on gadolinium chelates (cf. Figure 5.1), used as contrast agents in magnetic resonance imaging. They have a very high complex

stability, and are excreted without metabolization [19], hence reaching WWTPs without any modification. Conventional wastewater treatment does not remove them substantially [20]. They remain intact, and no free Gd(III) is released.

This may be different in oxidative (waste)water treatment processes which are potentially able to destroy gadolinium chelates and Gd(III) ions, which are toxic in contrast to the chelated form ((LD_{50} in mice for $GdCl_3$ = 0.1 mmmol kg^{-1} and for Gd-DTPA-BMA = 12 mmmol kg^{-1}) [21], may be liberated. Hence, not only reactivity of the chelates has been analyzed in this work, but also toxicity of reaction products has been studied. Similar toxicity studies were performed with triclosan containing wastewater before and after oxidative wastewater treatment [22].

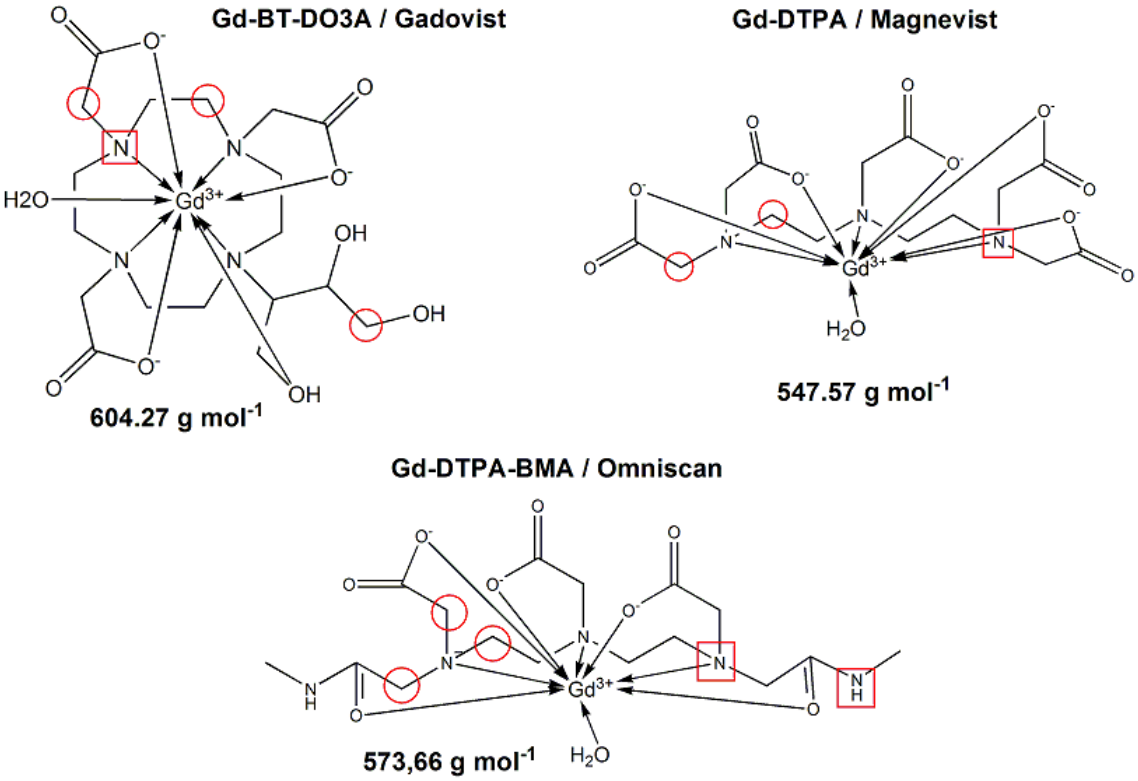

Figure 5.1: Molecular structures of tested gadolinium chelates including trade names and molar weights, marked as circles: examples for the reactive center for the reaction with hydroxyl radicals, marked as square: examples for the reactive center for the reaction with ozone

5.2 **Experimental**

5.2.1 Reagents

For the generation of ozone an oxygen-fed ozonator (BMT 802X, BMT Messtechnik, Berlin) was used. Ozone was bubbled through 0.5 L ultrapure water (Elga: Purelab ultra) for 30-60 min. The ozone concentration in this solution was determined spectrophotometrically at 260 nm ($\varepsilon_{260\,nm}$ = 3300 M^{-1} cm^{-1}). Hydrogen peroxide (Sigma Aldrich, p.a.) stock solution of 5 mM was prepared for the generation of hydroxyl radicals by the peroxone process.

The gadolinium chelate stock solutions of 10 mM were prepared in ultrapure water from the medical solutions (Gd-BT-DO3A as Gadovist from Bayer-Schering and Gd-DTPA-BMA as Omniscan from GE Healthcare), with exception of Gd-DTPA which was purchased from Sigma-Aldrich as diethylenetriaminepentaacetic acid gadolinium(III) dihydrogen salt hydrate. The stock solutions were prepared in PFA- or PP-vessels to avoid effects on the chelates by contact with glass. Such effects of chelates are suggested to be due to sorption [20] or transmetalation. [23].

The buffer solution was prepared from dipotassium hydrogen phosphate and potassium dihydrogen phosphate (both purchased from Sigma Aldrich, p.a.) in Elga water to yield a concentration of 100 mM and a pH of 7 ± 0.5. A stock solution of 400 mM *tert*-butanol (*t*BuOH) (Sigma Aldrich p.a.) prepared in ultrapure water was diluted to the specific concentration necessary for the use as radical scavenger (20 mM in the reaction solution) or as competitor (1 µM in the reaction solution).

The *para*-chlorobenzoic acid (*p*CBA) and *para*-nitrobenzoic acid (*p*NBA) (both purchased from Sigma Aldrich, p.a.) stock solutions (4 mM) were prepared in ultrapure water alkalinized with sodium hydroxide (Sigma Aldrich, p.a.) to yield pH 7 in the reaction solutions. At this pH *p*CBA and *p*NBA is present in its dissociated form (pKa = 3.99 [24] and 4.03 [25], respectively. This has been considered for calculation of the rate constants.

5.2.2 Rate constants

Rate constants of the chelates with ozone and hydroxyl radicals have been determined. Rate constants for the reaction with ozone have been determined under pseudo-first-order conditions. Ozone decrease was followed by the indigo method [26]. As radical scavenger *t*BuOH was used and the reaction was buffered with phosphate (100 mM) at pH = 7. Ozone rate constants were calculated by plotting the reaction time against the natural logarithm of the ratio of the residual ozone concentration vs. the initial ozone concentration.

The hydroxyl radical rate constants were determined by pulse radiolysis experiments, which is the ultimate reference method for the determination of hydroxyl radical rate constants. Very reliable values, within an error margin of < 10%, are obtained for well soluble compounds that form intermediates with high molar absorption coefficients in a convenient wavelength region (250 – 600 nm). All three gadolinium chelates show transient spectra in the region of interest (cf. Figure S 5.1).

Pulse radiolysis experiments were carried out by using 5 ns electron pulses from a 10 MeV linear accelerator (ELEKTRONIKA, Toriy Corp., Moscow) of the Leibniz-Intitut für Oberflächenmodifizierung (IOM), Leipzig. All solutions were bubbled for 10 min prior to the measurement with N_2O. The dose per pulse (~18 Gy) was determined using the thiocyanate dosimeter system [27]. The optical detection system consisted of a pulsed 1000 W xenon lamp, Suprasil cell (light path 1 cm), high-intensity grating monochromator (Acton Research Corp., SP275), R 928 photomultiplier (Hamamatsu) and a fast transient recorder (Tektronix, TD5034B). Four signals were averaged for each kinetic trace at a defined wavelength. Linear accelerator operation and data acquisition were computer controlled.

In brief, the free radicals $^{\bullet}OH$, $H^{\bullet}$ and solvated electrons (e_{aq}^{-}) are generated in a short electron beam pulse (cf. reaction 5.1) The radiation-chemical yields of the primary radicals are $G(^{\bullet}OH) \approx G(e_{aq}^{-}) = 2.8 \times 10^{-7}$ mol J^{-1} and $G(H^{\bullet}) = 0.6 \times 10^{-7}$ mol J^{-1} [28]. The hydrated electrons are readily converted into further hydroxyl radicals (cf. reaction 5.2) by saturating the solution with N_2O ($k_2 = 9.1 \times 10^9$ M^{-1} s^{-1} [29]), thus $G(^{\bullet}OH)$ becomes ~ 5.6×10^{-7} mol J^{-1}.

$$H_2O + \text{ionizing radiation} \rightarrow {}^{\bullet}OH, e_{aq}^{-}, H^{\bullet}, H^{+}, H_2O_2, H_2 \qquad (5.1)$$

$$e_{aq}^{-} + N_2O + H_2O \rightarrow {}^{\bullet}OH + N_2 + OH^{-} \qquad (5.2)$$

$$^{\bullet}OH + \text{Gd chelates} \rightarrow \text{products absorbing at ~250 - 400 nm} \qquad (5.3)$$

$$^{\bullet}OH + SCN^{-} \xrightarrow{SCN^{-}} OH^{-} + SCN_2^{\bullet -} \quad \text{(absorbing at 475 nm)} \qquad (5.4)$$

The gadolinium chelates react with hydroxyl radicals (cf. reaction 5.3), forming a well observable transient species (cf. Figure S 5.1). $H^{\bullet}$ atoms may also react with the compounds. However, in N_2O-saturated solutions their concentration is only about 10% of the hydroxyl radical concentration (see above) and their reaction is usually 1 to 3 orders of magnitude slower compared to hydroxyl radical reactions, thus a contribution to the observed spectra and kinetics can be neglected.

For further confirmation of the measured rate constants, competition with a good hydroxyl radical scavenger with well known rate constant and spectrum was applied. In presence of gadolinium chelate and the competitor SCN^{-} ($k_{\bullet OH} = 1.1 \times 10^{10}$ M^{-1} s^{-1} [29], both compounds react with $^{\bullet}OH$ (cf. reactions 5.3 and 5.4). Further experimental details are provided in chapter 5.5.1.

Pulse radiolysis is due to availability of pulse generators not possible in most cases. Hence, another method for the determination of hydroxyl radical rate constants has been tested. For this, competition kinetics were applied using *p*CBA ($k_{\bullet OH} = 5.5 \times 10^9$ $M^{-1}s^{-1}$ [4]) (monitoring the decrease) and *t*BuOH (monitoring product formation) as competitors. Hydroxyl radicals were in this case generated by the peroxone process (~200 µM O_3 / 100 µM H_2O_2). This process has been chosen to avoid interferences from transmetalation of gadolinium by other metals, as in the Fenton-Process Fe(II) is used and in Fenton like processes other metals like Cu(II) may be used for the generation of hydroxyl radicals. UV-based processes for the

generation of hydroxyl radicals have to be performed in glass, which should be avoided when working with (gadolinium) chelates [20, 23]. The pH was set to 7 by addition of NaOH (purchased from Sigma Aldrich, p.a.) to the *p*CBA stock solution. The determination of the formed product (formaldehyde from *t*BuOH) as well as the determination of the decrease of the competitor (*p*CBA) was performed by HPLC-UV (Agilent). The ratio of gadolinium vs. competitor concentration ranged from 1:1 to 1:1000, depending on the metal chelate and the competitor used. All samples were prepared in PFA-bottles, to avoid reaction of ozone with PP and to avoid any effects due to glass contact [20, 23].

To prove the concept of the competition method applied for the determination of hydroxyl radical rate constants of gadolinium chelates the rate constant of *p*NBA was determined in the same way. *p*NBA was choosen as its rate constant is also known ($k_{\bullet OH} = 2.6 \times 10^9\ M^{-1}s^{-1}$ [29]) and in the same range as the ones of the chelates. The degradation of *p*CBA in the presence of different ratios of *p*NBA was determined by HPLC-UV.

The competition kinetics plot for the determination of the hydroxyl radical rate constants using *p*CBA as reference substance was modified. Instead of plotting ([*p*CBA $_{\text{reaction product; without Gd chelate addition}}$] / [*p*CBA $_{\text{reaction product; with addition of Gd chelate}}$]) - 1 on the y-axis against the relation of gadolinium chelate to reference substance (*p*CBA) on the x-axis as it is the usual for such competition plots [30], ([*p*CBA $_{\text{initial}}$] - [*p*CBA $_{\text{without addition of Gd chelate}}$]) / ([*p*CBA $_{\text{initial}}$] – [*p*CBA $_{\text{with addition of Gd chelate}}$]) - 1 was used for the y- axis, to determine $k_{\text{OH, Gd chelate}}$.

Determinations of rate constants with *t*BuOH, another standard reference compound, where performed to verify results. For this method, another modification was necessary since in the reaction of gadolinium chelates with hydroxyl radicals, formaldehyde is formed as well as [unpublished results] in the reaction of *t*BuOH with hydroxyl radicals. Hence, a plot of another reaction product (2-hydroxy-2-methylpropanal) of *t*BuOH was chosen for the competition plot. It has to be noted, that peak areas were used instead of concentrations as there is no commercially available standard of 2-hydroxy-2-methylpropanal.

5.2.3 Toxicity tests

Toxicity tests were performed for mixtures of all reaction products of each chelate. The chelates (0.1 mM) were treated with either ozone only (0.1 mM) or ozone (0.1 mM) and H_2O_2 (0.05 mM). Excess H_2O_2 was removed by addition of catalase from bovine liver, Sigma Aldrich (0.01 mg L^{-1} ~ 20-50 units).

For cytotoxicity tests of reaction products from the reaction with $^{\bullet}OH$, a well established mammalian cell line (Chinese hamster ovary (CHO-9)) was used. These cells were cultured in Ham's F-12 medium (c.c.pro GmbH) supplemented with 10% fetal calf serum (FCS), 0.5% L-glutamine, and 0.5% gentamycin at 37°C under 5% CO_2 and 95% humidity conditions. For cytotoxicity and estrogenity test (for experimental and results of estrogenity tests cf. 5.5.2) of reaction products from the reaction with ozone another mammalian cell line T47D cells (human breast carcinoma cells) were used. T47D cells were cultured in Dulbecco's Modified Eagle's Medium (DMEM) with phenol red supplemented with 41 mL FCS, 5 mL non-essential amino acids, and 3 mL gentamycin were used. Genotoxicity tests were performed with CHO-9 cells.

For cytotoxicity tests, the inner wells of a 96 well plate were filled with 200 µL medium containing 10^4 CHO-9 or T47D cells per well. Outer wells were filled with 200 µL PBS (Phosphate Buffered Saline) and afterwards the plates were incubated at 37°C for 24 h. For exposure, the medium was removed and 180 µL fresh medium and 20 µL sample were added to the cells which were further incubated at 37°C for another 24 h. After exposure, the medium was removed and 100 µL fresh medium as well as 10 µL MTT solution (0.5 mg 3-(4-dimethylthiazol-2-yl)-2,5-diphenyl-tetrazoliumbromid dissolved in 1 mL PBS) were added. Cells were again incubated at 37°C for 2 h. Then the supernatant was removed from the wells and 100 µL lysis solution (99.4 mL DMSO (dimethylsulfoxide), 0.6 mL acetic acid (100%) and 10 g SDS (Sodium dodecyl sulfate)) were added per well followed by 5 min incubation at room temperature and 5 min shaking. Afterwards absorbance was measured at 595 nm with a TECAN GENios platereader (TECAN; Crailsheim, Germany). Triton-X 100® in a ration of 1:10 into medium was used as a positive control.

For genotoxicity testing, 5×10^5 CHO-9 cells per 10 mL were seeded into 75 cm^2 cell culture flasks and incubated at 37°C over night. Then cells were exposed to the negative control (1 mL sterile water, 9 mL medium, 10 µL Cytochylasin B), positive control (20 µL Mitomycin C, 9.98 mL medium, 10 µL Cytochylasin B) and samples (1 mL sample, 9 mL medium, 10 µL Cytochylasin B) for 24 h at 37°C, 5% CO_2 and 95% humidity. Afterwards the medium was removed and 10 mL new medium containing 10 µL Cytochylasin B was added for another 20 h before cells were washed with PBS, trypsinated and 8×10^4 cells were seeded on microscope slides covered with 4 mL of medium. After the cells attached to the microscope slide, the medium was removed and 5 mL of 0.075 M KCl solution were added for 5 min. Microscope slides were afterwards transferred to cooled methanol (-20°C) and stored at -20°C over night. For analysis, the DNA was stained with 2-(4-carbamimidoylphenyl)-1H-indol-6-carboximidamid (DAPI). The Metafer 4 software (MetaSystems; Altussheim, Germany) was used for the detection of micronuclei. Three individual tests were performed for each sample.

5.3 Results and discussion:

The result of the determination $k_{Ozone,\ Gd\text{-}chelate}$ is shown in Table 5.1 (detailed experimental results shown for Gd-BT-DO3A in Figure 5.2). The reaction of all three chelates is rather slow (< 50 M^{-1} s^{-1} cf. Table 5.1). A degradation via this pathway in wastewater treatment is thus of minor importance. A comparison of the results with the complex stability (cf. Table 5.1) shows that with decreasing stability of the chelates the rate constant for the reaction of the chelates with ozone increases. Hence, the more stable the gadolinium chelate, the slower the reaction with ozone. This is due to the nature of the complexes: The gadolinium ion binds to the free electrons in the carboxyl- and amino-groups of the ligand. Accordingly electrons are withdrawn from these groups. In a reaction with ozone, the amino groups are usually attacked due to their high electron density. Hence, the more stable the chelate, the more of the electron density is withdrawn from the amino groups and the less probable is an ozone attack.

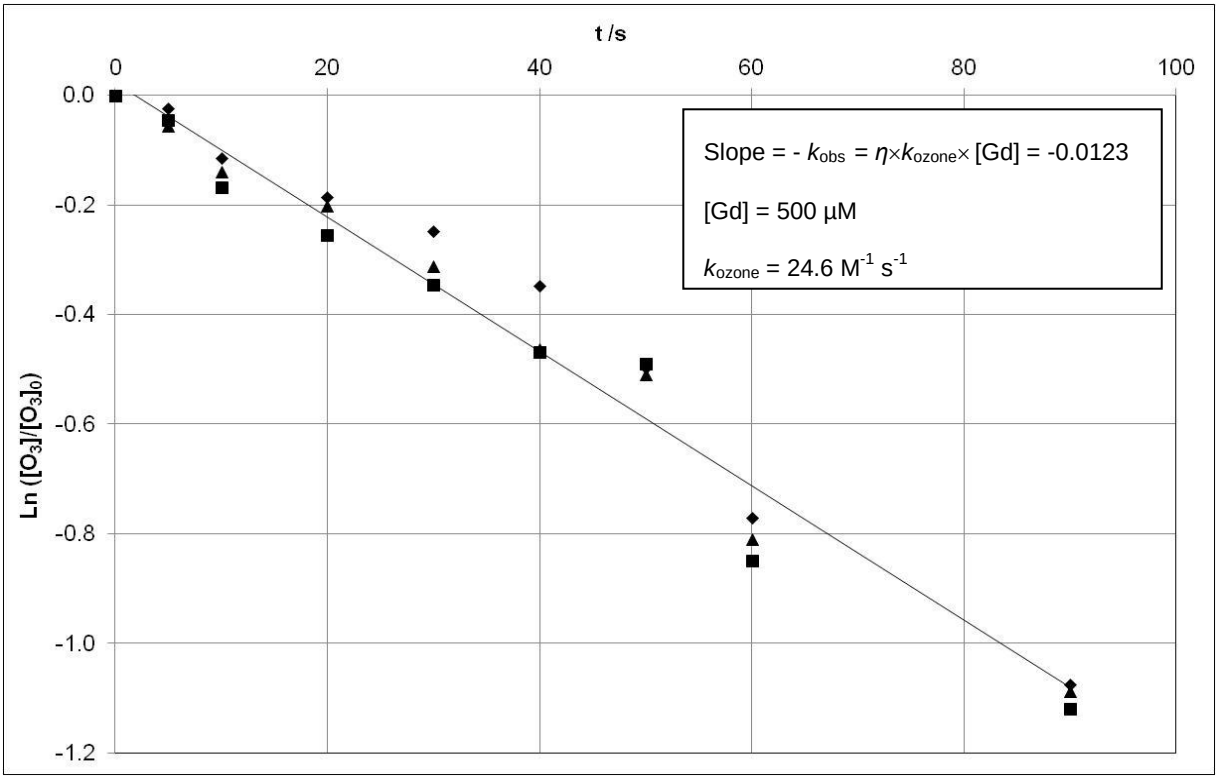

Figure 5.2: Results of the determination of the rate constant for the reaction of Gd-BT-DO3A (Gadovist) with ozone in a triplicate experiment (k_{obs} = observed rate constant, η = stoichiometric coefficient for gadolinium in the reaction, k_{Ozone} = rate constant)

Table 5.1: Complex stability constants and rate constants (in M^{-1} s^{-1}) for different coordinated ligands with hydroxyl radicals and ozone

Central ion		Ligand								
		NTA	EDTA	DTPA		BT-DO3A		DTPA-BMA		
Fe(III)	*K*	15.9 [31]	25.0 [31]	28.0 [31]						
	$k_{\bullet OH}$	1.6×10^8 [1]	5×10^8 [1]	1.5×10^9 [17]						
	k_{O_3}		3.3×10^2 [16]	<10 [17]						
Gd(III)	*K*	11.5 [31]	17.4 [31]	22.5 [31]		21.8 [32]		16.9 [33]		
	$k_{\bullet OH}$			**Pulse Radiolysis (method 1):**	**$2.6 \pm 0.2 \times 10^9$**	**Pulse Radiolysis (method 1):**	**$4.3 \pm 0.2 \times 10^9$**	**Pulse Radiolysis (method 1):**	**$1.9 \pm 0.7 \times 10^9$**	
				Peroxone process; competition with pCBA (method 3)	*$1.7 \pm 4.1 \times 10^8$*	*Peroxone process; competition with pCBA (method 3)*	*$8.5 \pm 1.2 \times 10^8$*	*Peroxone process; competition with pCBA (method 3)*	*$7.5 \pm 2.9 \times 10^8$*	
	k_{O_3}			**4.8 ± *0.88***		**24 ± *1.5***		**46 ± *2.5***		
Free ligand	$k_{\bullet OH}$	2.5×10^9 [1]	4×10^8 [1]	3.9×10^9 [34]						
	k_{O_3}	9.8×10^5 [1]	3.2×10^6 [1]							

The rate constant for the reaction of the chelates with hydroxyl radicals was determined by four different methods:

1. Generation of hydroxyl radicals by pulse radiolysis and determination of the rate constant by direct measurement of the degradation of the chelates (monitoring absorbance of transient products from the reaction of gadolinium chelates)
2. Generation of hydroxyl radicals by pulse radiolysis and determination of the rate constant by competition kinetics using SCN^- as competitor (monitoring the decrease of $SCN_2^{\bullet-}$ at 475 nm)
3. Generation of hydroxyl radicals by the peroxone process and determination of the rate constant by competition kinetics with *p*CBA as reference substance
4. Generation of hydroxyl radicals by the peroxone process and determination of the rate constant by competition kinetics with *t*BuOH as reference substance

The results for the rate constant determination of Gd-BT-DO3A with hydroxyl radicals using the third method with *p*CBA as reference compound are shown in Figure 5.4. Results for the same compound using method 1 are shown in Figure 5.3. Furthermore, Figure 5.3 shows the absorption spectra and the time dependence of the absorbance at 270 nm for different molar gadolinium concentrations in case of Gd-DTPA. From a plot of the observed decay rate against the molar Magnevist concentration (cf. Figure 5.3) a rate constant of $2.6 \pm 0.2 \times 10^9\ M^{-1}\ s^{-1}$ can be derived for the reaction with hydroxyl radicals. In a similar manner, rate constants of $1.9 \pm 0.7 \times 10^9$ and $4.3 \pm 0.2 \times 10^9\ M^{-1}\ s^{-1}$ were derived for Gd-DTPA-BMA and Gd-BT-DO3A, respectively (for detailed calculations cf. chapter 5.5.1).

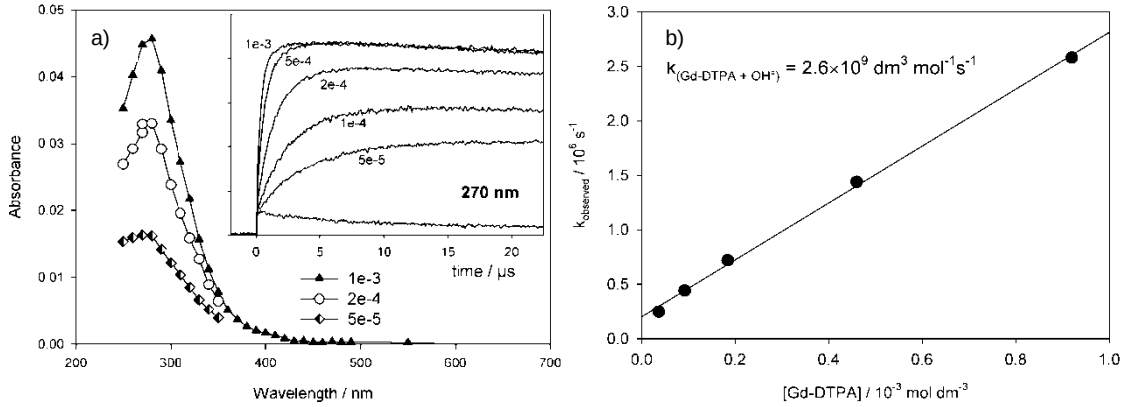

Figure 5.3: a) Transient absorption spectra observed after electron irradiation of N_2O-saturated aqueous solutions of Gd-DTPA (Magnevist); concentration given in M. Inset: time dependence of the absorbance at 270 nm, for 5 different concentration levels of Gd-DTPA; b) Plot of k_{obs} against Magnevist concentration. The slope yields a bimolecular rate constant of $2.6 \pm 0.2 \times 10^9$ M^{-1} s^{-1} for the reaction hydroxyl radicals with Gd-DTPA (for a discussion of competition kinetics cf. 5.5.1)

From competition kinetics in pulse radiolysis experiments, slope of the plot of $(A_0/A)_{475nm} - 1$ vs. [Gd]/[SCN^-] and the given rate constant of $^\bullet$OH with SCN^- the rate constant of Gd-DTPA with hydroxyl radicals,

$k_{\bullet OH + Gd\text{-}DTPA_{comp}} = (2.4 \pm 0.5) \times 10^9$ M^{-1} s^{-1} is obtained in good agreement with the direct determination. In similar manner, rate constants of $3.1 \pm 0.5 \times 10^9$ and $4 \pm 0.5 \times 10^9$ M^{-1} s^{-1} were derived for Omniscan and Gadovist, respectively (for more details cf. chapter 5.5.1).

In Figure 5.4 results for the rate constant determination of Gd-BT-DO3A with hydroxyl radicals in the peroxone process using *p*CBA as reference compound are presented. Rate constants of the other gadolinium chelates are presented in Table 5.1. For Gd-DTPA further experiments were carried out using *t*BuOH as reference compound in the same processes. The determined rate constants using *t*BuOH ($k_{\bullet OH + Gd\text{-}DTPA} = 3.55 \pm 1.75 \times 10^6$ M^{-1} s^{-1}) differs greatly from the one determined by using *p*CBA as reference compound and determinations in pulse radiolysis experiments.

Method 3 and 4 are very prone to errors, among others these are:

- Variable exposure to hydroxyl radicals due to variation of the concentration of the ozone stock solution and dosage issues
- Complex formation of (transformation products of) reference compounds with gadolinium
- Further reaction of transformation products of reference compound and / or gadolinium chelates with hydroxyl radicals

The determined rate constants using the peroxone process differ by a factor of ~5 for Gd-DTPA and Gd-BT-DO3A from the ones obtained from pulse radiolysis studies for these chelates (cf. Table 5.1). Only for Gd-DTPA-BMA $k_{\bullet OH}$ is determined within the margin of error equally in all three methods. The correlation of the competition plot, as well as the deviation is rather low (cf. Figure 5.4). The residual standard deviation (RSD) for the determination of $k_{\bullet OH}$ for Gd-BT-DO3A and Gd-DTPA is 0.137, whereas for the determination of $k_{\bullet OH + Gd\text{-}DTPA\text{-}BMA}$ RSD is even higher (0.517). This is due to inconstant exposure to hydroxyl radicals. Variability of the ozone concentration (variation in concentration of the stock solution due to outgasing / temperature or dosage errors) in the sample vessels lead to inconstant yields of hydroxyl radicals and hence, in higher scattering of the measuring points.

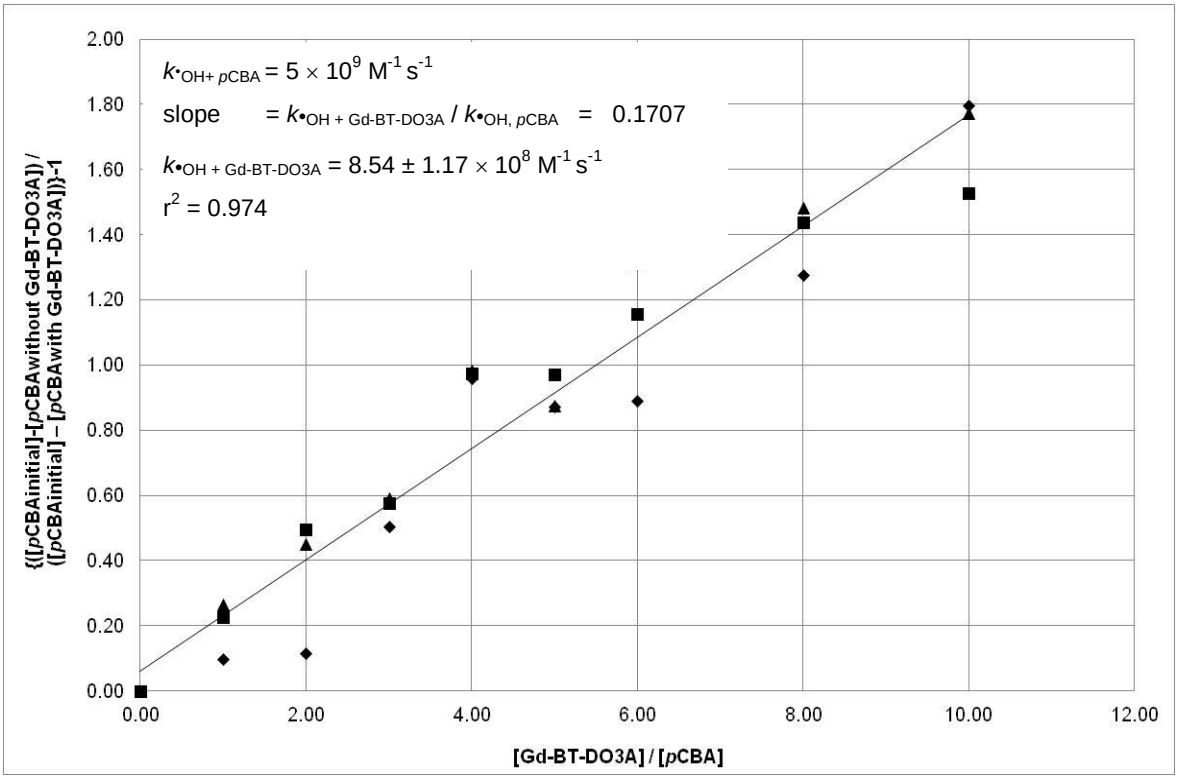

Figure 5.4: Results of the determination of the rate constant for the reaction of Gadovist with hydroxyl radicals (generated by peroxone process) by the use of *p*CBA as reference compound in a triplicate experiment; only the concentration of *p*CBA was determined and (([$pCBA_{initial}$]-[$pCBA_{without\ addition\ of\ Gd\ chelate}$]) / ([$pCBA_{initial}$] – [$pCBA_{with\ addition\ of\ Gd\ chelate}$])) -1 was plotted instead of using ([$pCBA_{reaction\ product;\ without\ Gd\ chelate\ addition}$] / [$pCBA_{\ reaction\ product;\ with\ addition\ of\ Gd\ chelate}$]) -1 on the y-axis against the relation of gadolinium chelate to reference substance (*p*CBA) on the x-axis

In general, pulse radiolysis is the method of choice for determination of rate constants and both methods using pulse radiolysis yield the same rate constants. Therefore, it has been assumed that the results produced by method 1 and 2 (pulse radiolysis) are more reliable than those of methods 3 and 4 (peroxone based competition). To exclude that reaction products and / or *p*CBA form complexes with gadolinium which might lead to an underestimation of *p*CBA, experiments have been performed in which gadolinium chelate was added after the reaction of *p*CBA with hydroxyl radicals (equal *p*CBA concentration with and without addition of gadolinium chelate). These experiments have shown that no such transmetalation reactions have occurred, as the decrease of the *p*CBA concentration was the same with and without addition of gadolinium chelates (cf. Figure S 5.5).

Owing to the deviation of results from pulse radiolysis and peroxone use, the concept to determine the rate constant of gadolinium by only monitoring the decrease of a reference compound was tested with a reference compound with a known rate constant. In this case the rate constant of *p*NBA was determined (cf. Figure 5.5).

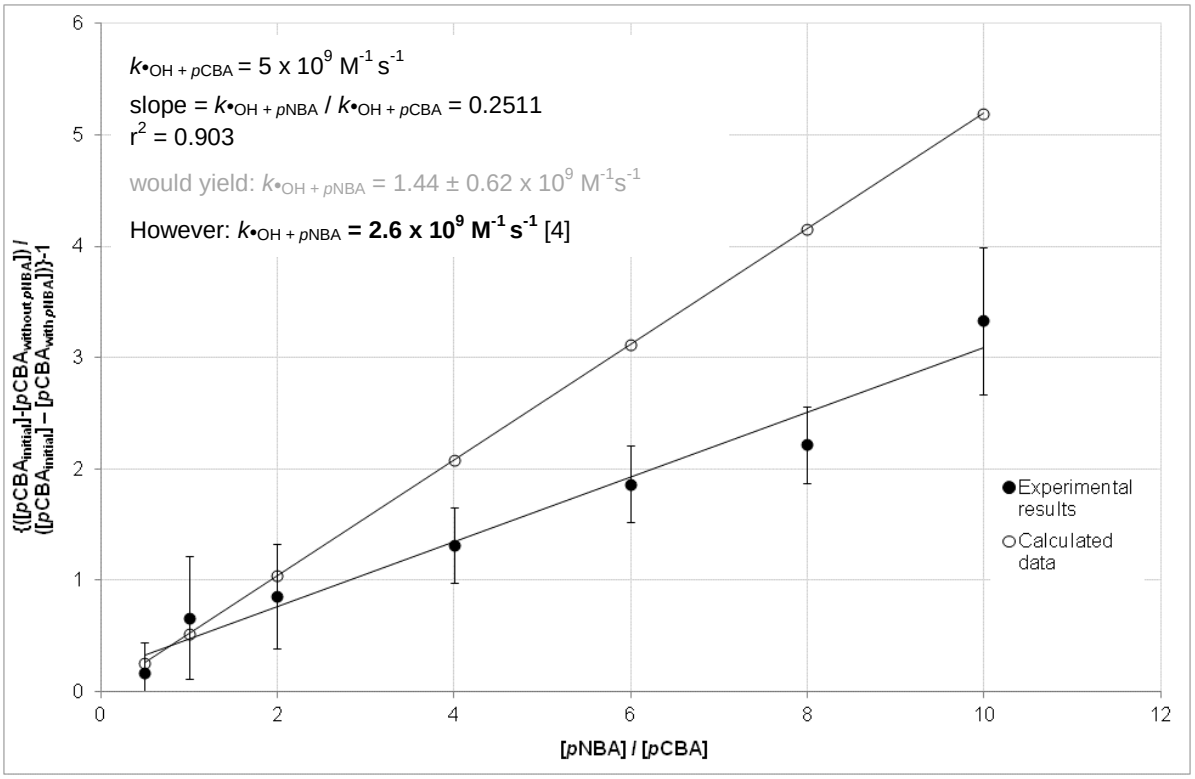

Figure 5.5: Test of the concept for the determination of the rate constants in the peroxone process: Reaction of *p*NBA with hydroxyl radicals (generated by peroxone process) by the use of *p*CBA as reference compound; only the concentration of *p*CBA was determined and {([*p*CBA$_{initial}$]-[*p*CBA$_{without\ addition\ of\ pNBA}$]) / ([*p*CBA$_{initial}$] – [*p*CBA$_{with\ addition\ of\ pNBA}$])}-1 was plotted instead of using ([*p*CBA$_{reaction\ product;\ without\ pNBA\ addition}$] / [*p*CBA $_{reaction\ product;\ with\ addition\ of\ pNBA}$])-1 on the y-axis against the relation of *p*NBA to reference substance (*p*CBA) on the x-axis

As it is clearly shown, a determination of the rate constant applying this method leads to an underestimation of the rate constant. Usually, such competition plots are based on the determination of two reaction products [31]. In this case, the decrease of the reference compound was measured and used for the calculation of the rate constant. An underestimation of the rate constant is due to the assumption that more reference compound (in this case *p*CBA) has reacted with hydroxyl radicals than it truly has. If the reaction is via stable intermediates and hence a complete reaction (, which should be observable for such competition kinetics) is not detectable by decreasing concentration of the reference compound (in this case *p*CBA), the reaction of the reference compound (*p*CBA) with hydroxyl radicals is overestimated. Thus rate constants are underestimated. This known error is typically not higher than a factor of two or three which is acceptable for most applications [3].

Concerning the rate constants for the reaction with hydroxyl radicals, a correlation with complex stability, as it was found for the reaction with ozone, was not observed. Yet one has to consider that the reaction pathway of hydroxyl radicals is different to the one of ozone. Hydroxyl radicals react usually by either H-abstraction or electron transfer. It is proposed that the reaction of the chelates occurs via H-abstraction, analog to the reaction of EDTA with hydroxyl radicals [16]. This is supported by increasing rate constants of Gd-DTPA-BMA < Gd-DTPA < Gd-BT-DO3A. Usually one might have expected Gd-DTPA to react slower than Gd-DTPA-BMA, as the +I effect of the two keto-groups in Gd-DTPA-BMA should increase electron density at the neighboring carbon atoms, making it more prone to attacks. However, the +I effect effect is hindered due to the binding of gadolinium to the keto-groups. Hence, electron density at the reactive center is lower than in the basic structure of Gd-DTPA. For Gd-DTPA, which is charged -2, $k_{\bullet OH}$ is higher ($2.6 \pm 0.2 \times 10^9\ M^{-1}\ s^{-1}$) due to the high electron density.

Interestingly, the reactivity of the chelates can be linked to complex stability in another way. For DTPA, rate constants and stability constants are available for four different metal chelates. The plot of rate constants for the reaction with hydroxyl radicals vs. the complex stability is shown in Figure 5.6.

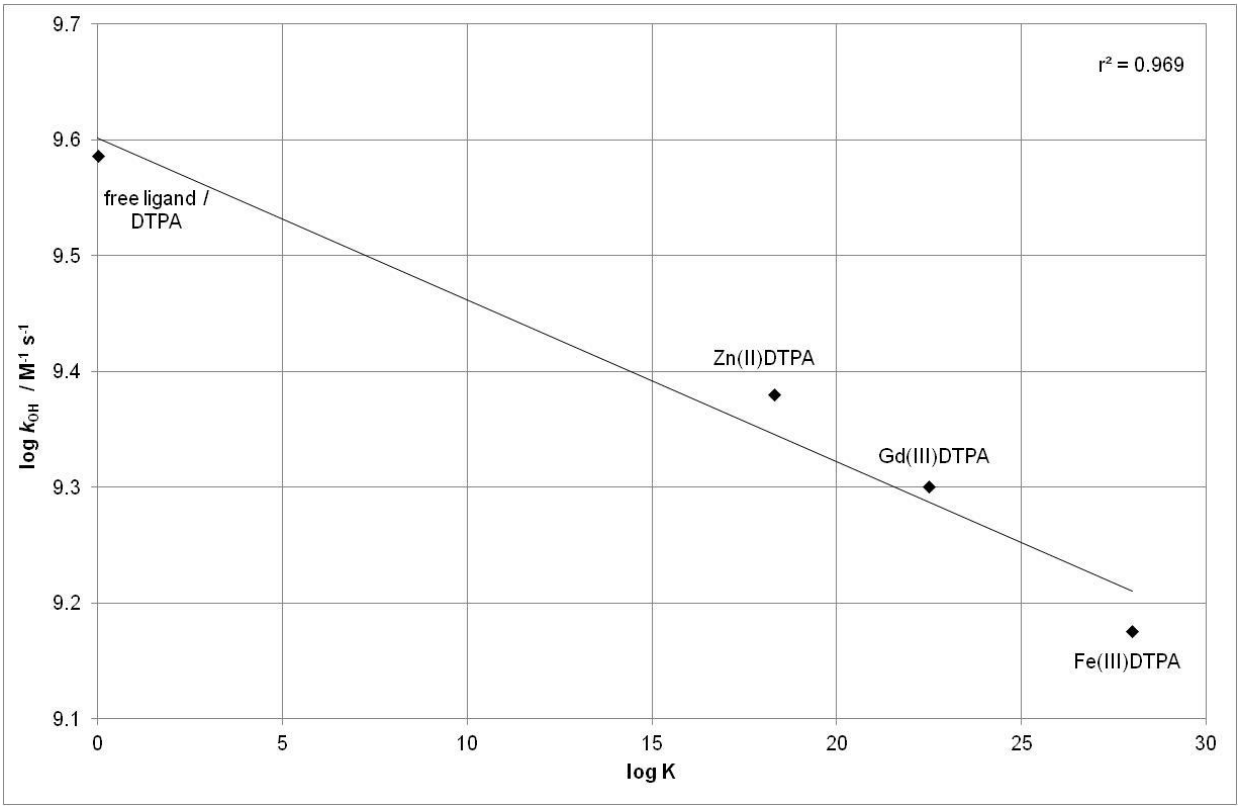

Figure 5.6: Correlation of hydroxyl radical rate constant at pH = 7 and stability constant for different metal DTPA complexes (DTPA speciation: DTPA-H_2^{3-})

This plot (cf. Figure 5.6) endorses the statements made above. Lower electron density at the reactive centers due to complexation with the metals will lead to a decreased rate constant. A correlation of *k* and complex stability was not notable by comparing the different gadolinium ligand systems, as the ligands vary strongly in donating groups.

The highest of the three determined rate constants is the one of Gd-BT-DO3A which can be explained by the presence of the glycol group. This functional group has a rate constant of 1.4×10^9 M^{-1} s^{-1} [35] which is an explanation for the high rate constant of $4.3 \pm 0.2 \times 10^9$ M^{-1} s^{-1} for the chelate.

Due to the great difference in rate constants, it is assumed, that the fraction of the Gd chelates which react with •OH is higher than the fraction, which reacts with ozone. Yet, in a wastewater matrix with 10 mg L^{-1} DOC only 0.01% of the •OH generated by ozone reactions will react with Gd-BT-DO3A. Rate constants and concentrations for this calculation were adapted from Pocostales et al. [11] and Nöthe et. al [10]. However, even though only this small percentage of the generated •OH is available for reaction with the Gd chelates these will be degraded by •OH to a large extent.

Using ozone and •OH exposure data from a wastewater treatment plant, with a DOC of 8 mg L^{-1} and a specific ozone dosage of 0.9 mg L^{-1} (mg L^{-1} DOC)$^{-1}$, the chelates Gd-BT-DO3A, Gd-DTPA and Gd-DTPA-BMA will be reduced within 3 min to 6, 15 and 22%, respectively. This high reduction rates are to a major extent due to the reactions with •OH. In such a wastewater matrix with 0.7 µg L^{-1} Gd_{total} (highest measured concentration in a monitoring campaign of European WWTPs (cf. chapter 3), potentially 0.66 µg L^{-1} of gadolinium (assumed that all of Gd_{total} is present as Gd-BT-DO3A) may be released from the chelate after such a treatment.

The results of the toxicity experiments are displayed in Figure 5.7 - Figure 5.8. The products of the reaction with ozone show no significant cyto- and genotoxic effect in the applied test systems for all three tested chelates.

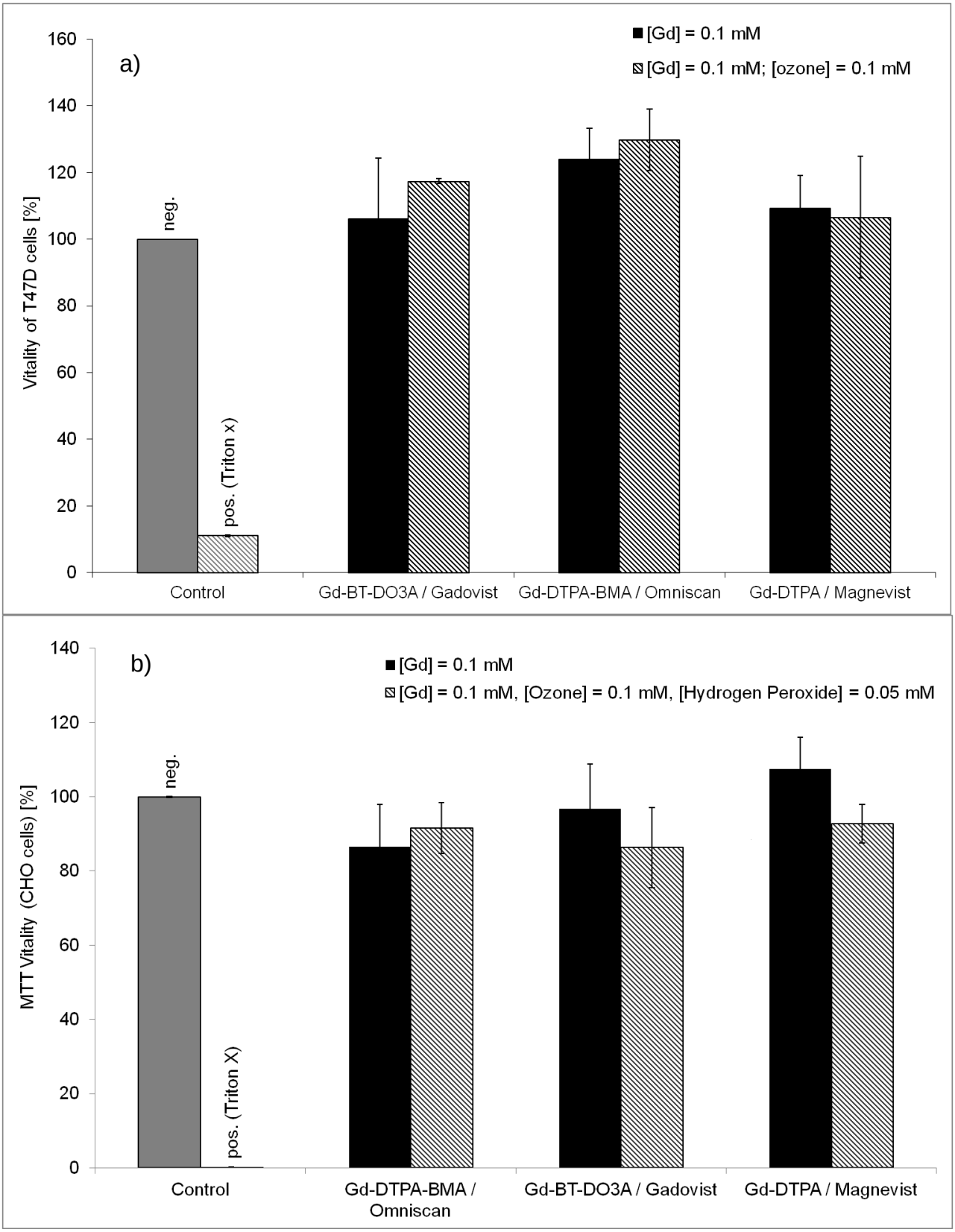

Figure 5.7: a) Results of cytotoxicity test (for detailed test method cf. 5.2.3) for all tested chelates ([Gd] = 0.1 mM) before and (black) after reaction with ozone (hatched) ([ozone] = 0.1 mM); b) Results of the cytotoxicity test for two experiments with each 0.1 mM Gd, 0.1 mM ozone and 0.05 mM H_2O_2 (for detailed test method cf. 5.2.3**)** for reaction products of all three tested diagnostics with hydroxyl radicals

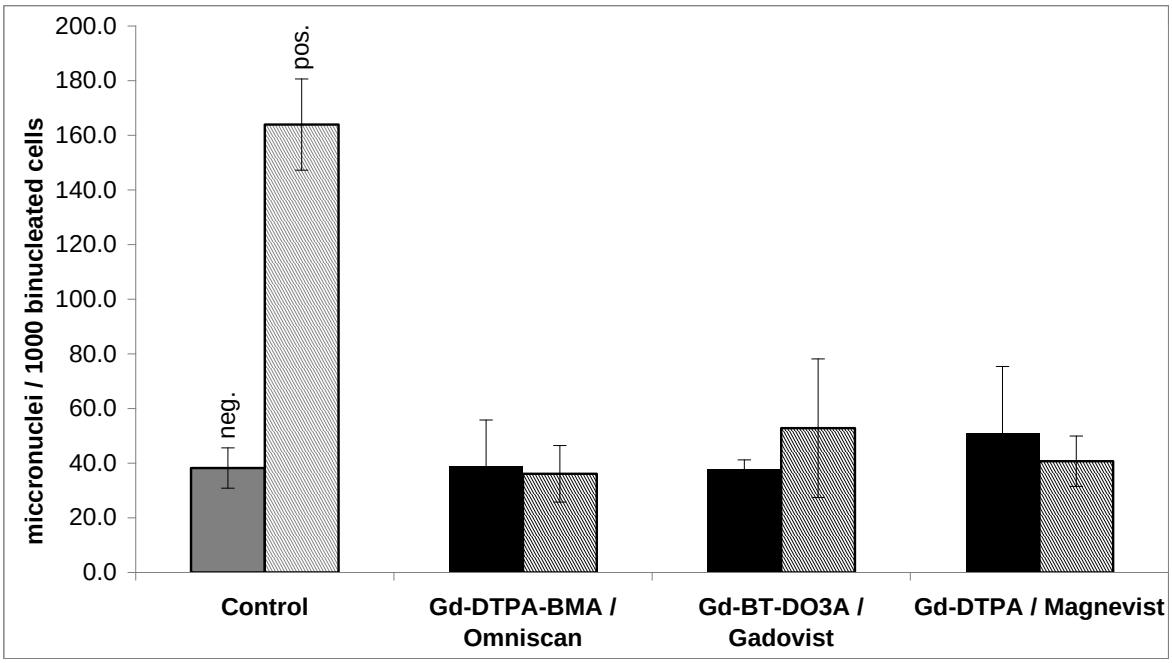

Figure 5.8: Results of the genotoxicity test for two experiments with each 0.1 mM Gd, 0.1 mM ozone and 0.05 mM H_2O_2 (detailed test method in 2.3) for reaction products of all three tested diagnostics with hydroxyl radicals

For the reaction with hydroxyl radicals (cf. Figure 5.7 and Figure 5.8) also no toxic effects were observable. Neither cytotoxic nor genotoxic effects were detected for all tested chelates before and after treatment compared to negative controls.

The mixtures of all reaction products, which are generated in the oxidation reactions with either hydroxyl radicals or ozone, have been tested and not a single, separated transformation product. Hence, it is concluded that none of the reaction products causes any cyto- and genotoxic effects in the tested concentration. The concentration used for the toxicity tests was set very high in comparison to any concentration expected in a real wastewater matrix ($< 6 \times 10^{-9}$ M Gd, as gadolinium chelates and / or Gd(III) (cf. chapter 3), to ensure that even minor effects of reaction products would be detectable in the toxicity tests. Since no effects have been detected in the applied tests, no further and / or more specific tests have been performed.

5.4 Conclusion

It is concluded that degradation of gadolinium chelates via ozone is very slow and rather ineffective for their removal. However, degradation via hydroxyl radicals is very fast - almost diffusion controlled. This degradation pathway has only been investigated for other, smaller chelates before [12].

Yet it has to be emphasized that degradation of these chelates is not desirable, in contrast to many organic trace substances. The chelates are very stable and degradation of these chelates might in principle lead to a release of the toxic non-complexed Gd(III) ion, although such an effect of free gadolinium was not detectable in the applied toxicity tests.

Furthermore, one has to consider that also the reaction products of the chelates may serve as ligands capable of binding the gadolinium ions. Yet it is unknown which new chelates are formed and how stable these are. Transformation products like IDA, which arises from ozonation of Fe-EDTA [16], forms less stable chelates with gadolinium (log K([Gd-EDTA]/[Gd][EDTA] = 17.4 [31] and
log K([Gd-IDA]/[Gd][IDA] = 6.7 [31]). Hence, transmetalation may be facilitated. Transmetalation reactions may occur in flocculation processes for water treatment, but are rather unlikely in the environment. These reactions may lead to an incorporation of iron used in the flocculation process into the complex and a release of gadolinium due to a shift in the equilibrium (increased concentration of e.g. Fe(III)). For aluminum, which is also used as flocculant, the complex stability constants with the ligands in the diagnostics are smaller than the ones of gadolinium.

It is proposed, that further research on newly formed metal-ligand-systems, especially on their stability, in hydroxyl radical based oxidation processes is needed. The bioavailability of metals might change due to newly formed complexes during oxidation steps in wastewater treatment. Furthermore, metal transport in the environment might be influenced.

5.5 Supplement

5.5.1 Details for determination of rate constants

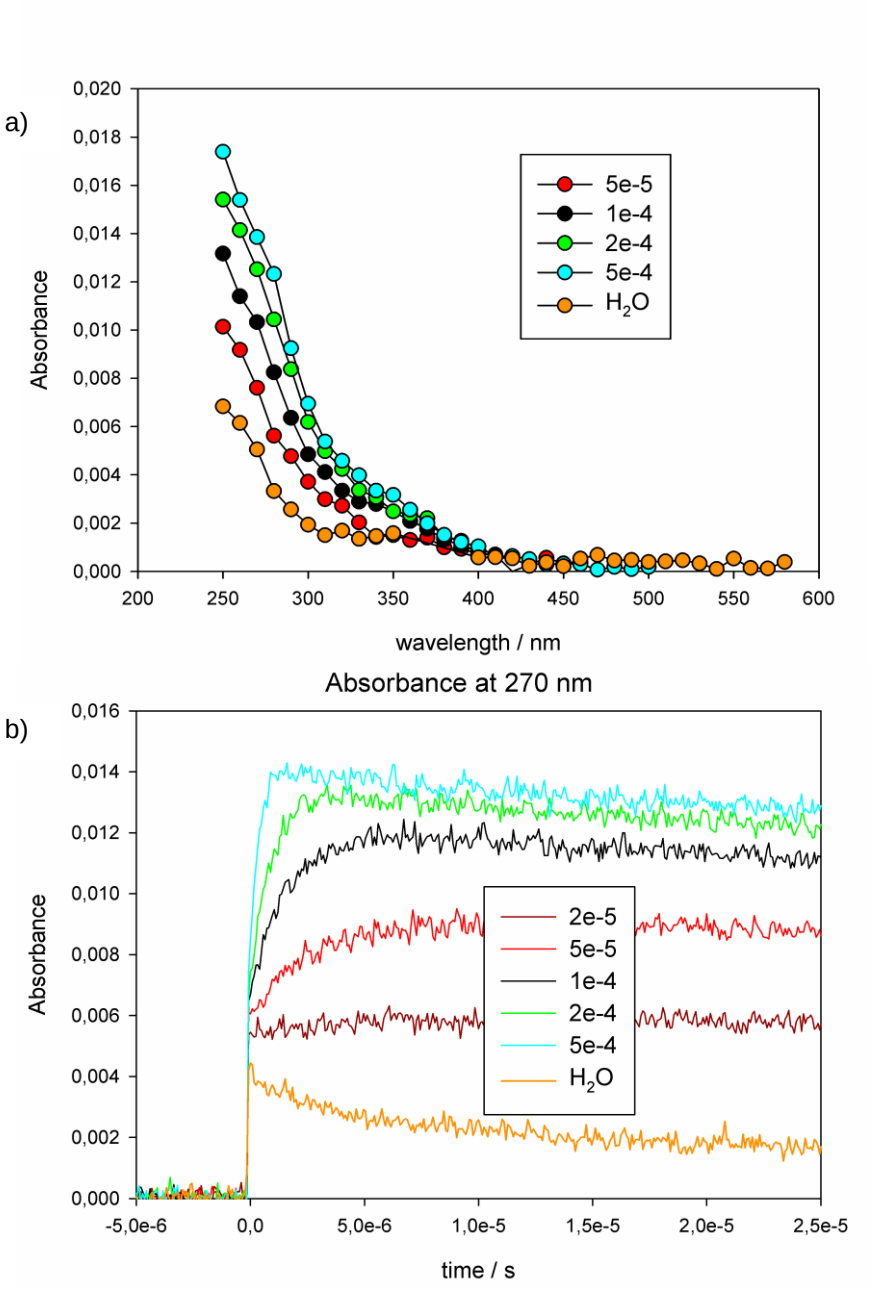

Figure S 5.1: a) Transient absorption spectra observed after electron irradiation of N_2O-saturated aqueous solutions of Gd-BT-DO3A, concentration is given in M; b) time dependence of the absorbance at 270 nm, for 5 different concentration levels of Gd-BT-DO3A.

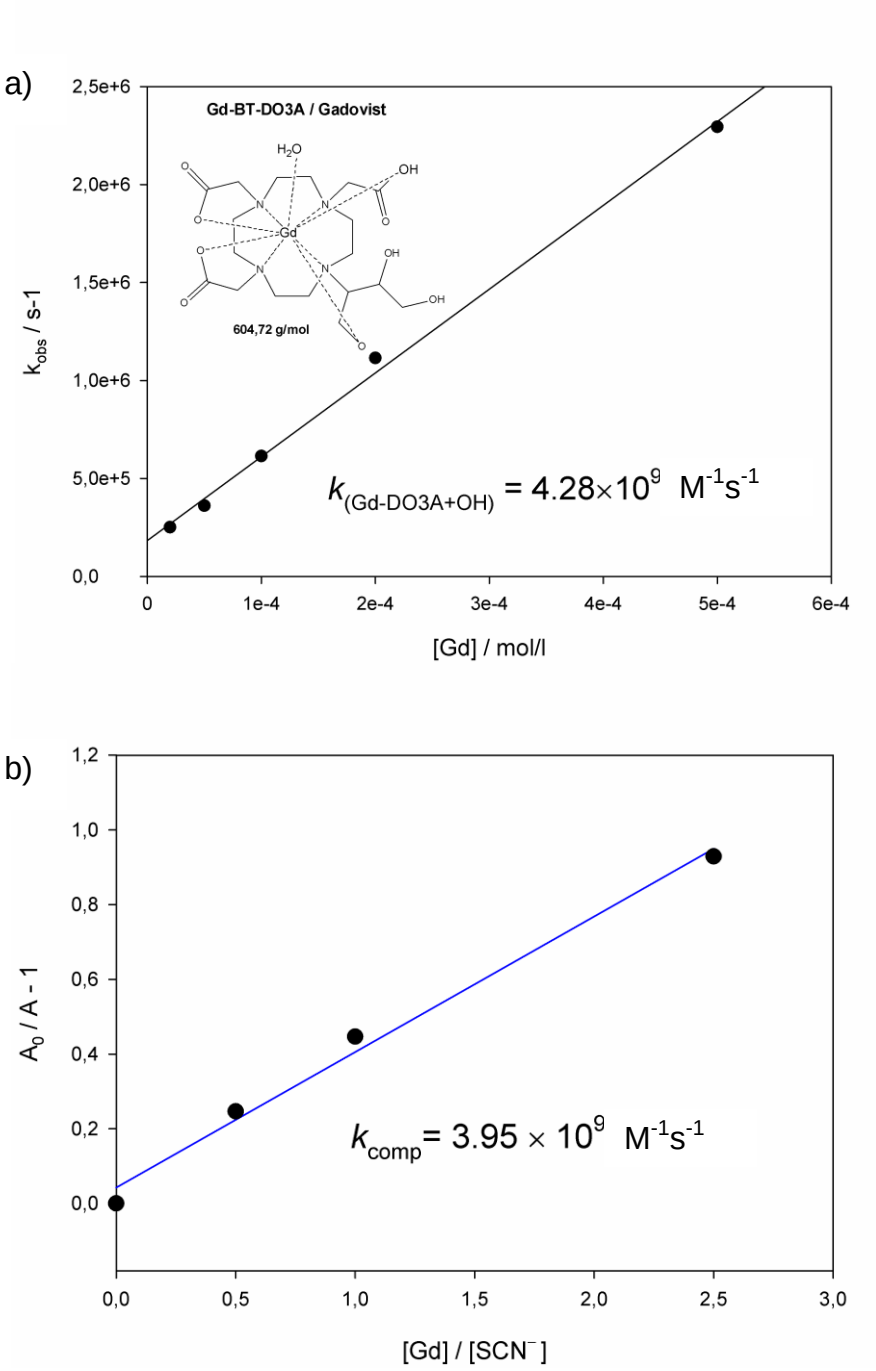

Figure S 5.2: a) Plot of k_{obs} against Gadovist concentration; the slope yields a bimolecular rate constant of $4.3 \pm 0.2 \times 10^{9} M^{-1} s^{-1}$ for the reaction of hydroxyl radicals with Gd-BT-DO3A; b) Competition kinetics, the plot of $(A_0/A)_{475nm} - 1$ vs. [Gd]/[SCN^{-}] and the known rate constant of $k_{\bullet OH + SCN^{-}} = 1.1 \times 10^{10} M^{-1} s^{-1}$ [29] yields a bimolecular rate constant of $4 \pm 0.4 \times 10^{9} M^{-1} s^{-1}$ for the reaction of hydroxyl radicals with Gd-BT-DO3A

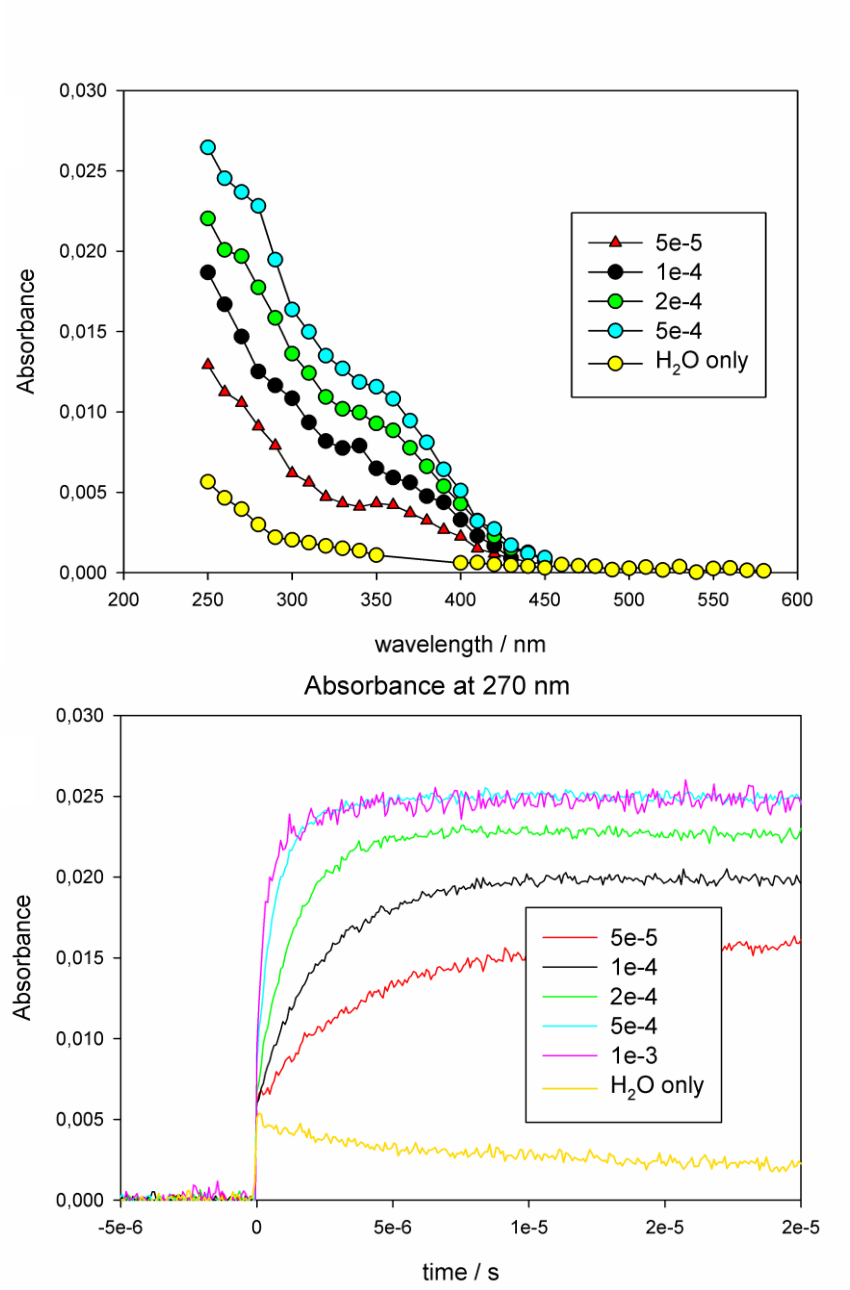

Figure S 5.3: a) Transient absorption spectra observed after electron irradiation of N_2O-saturated aqueous solutions of Gd-DTPA-BMA (Omniscan), concentration given in M; b) Time dependence of the absorbance at 270 nm, for 5 different concentration levels of Gd-DTPA-BMA

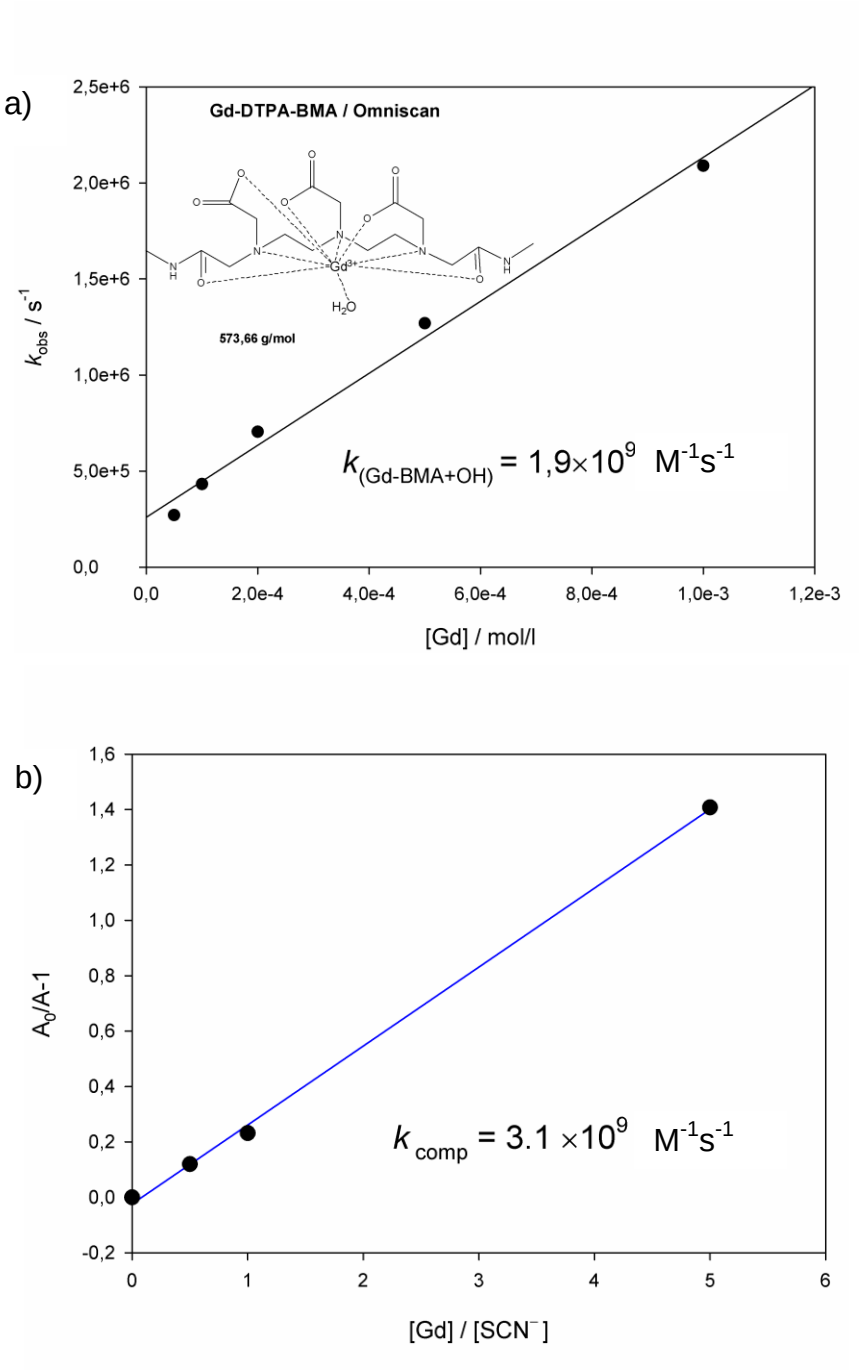

Figure S 5.4: a) Plot of k_{obs} against Omniscan concentration; the slope yields a bimolecular rate constant of $1.9 \pm 0.7 \times 10^9$ M^{-1} s^{-1} for the reaction of hydroxyl radicals with Gd-DTPA-BMA. b) Competition kinetics; plot of $(A_0/A)_{475nm} - 1$ vs. [Gd]/[SCN^-] and the known rate constant of $k_{\bullet OH + SCN^-} = 1.1 \times 10^{10}$ M^{-1} s^{-1} [29] yields a bimolecular rate constant of $3 \pm 0.5 \times 10^9$ M^{-1} s^{-1} for the reaction of hydroxyl radicals with Gd-DTPA-BMA. The small discrepancy of the competition value in comparison with the direct determination is still within margin of error

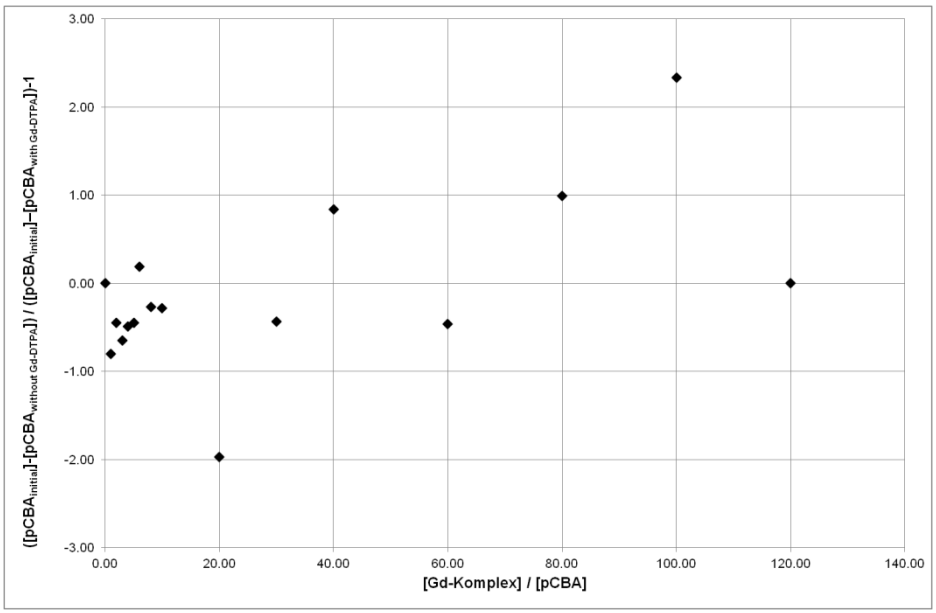

Figure S 5.5: Results of the experiment to verify if *p*CBA transformation products form complexes with gadolinium, to exclude that reaction products and / or *p*CBA form complexes with gadolinium, which might lead to an underestimation of *p*CBA, experiments have been performed, in which gadolinium chelate was added after the reaction of *p*CBA with $^{\bullet}$OH (equal *p*CBA concentration with and without addition of gadolinium chelate). For this, Gd-DTPA was added after the addition of ozone, which initiates hydroxyl radical formation in the peroxone process. Hence, if pCBA was underestimated due to such complexation reactions, a decrease should be observable with increasing chelate addition

5.5.2 Estrogenity tests

Eventhough an estrogen disrupting effect of oxidation reaction products is rather unlikely due to the structure of the parent compound, also estrogenic activity has been evaluate by applying a cell assay. The estrogenicity was investigated by using the ER Calux test (BioDetections Systems; Amsterdam, NL). For this, 1×10^4 T47D cells in 100 µL DMEM medium without phenol red were seeded into each inner well of a 96-well plate. The outer wells were filled with 200 µL PBS. After seeding, cells were incubated for 24 h at 37°C and 5% CO_2. Then the medium was changed and cells were incubated for further 24 h. To expose cells to the 17β-estradiol standard series, medium and water were mixed at a ratio of 1:10. The final concentration of the standards in the wells was between 0 and 30 pM 17β-estradiol. The exposure medium for the gadolinium samples contained 1% DMSO and the exposure of the samples was then done at a ratio of 1:10 (90 µL medium containing 1% DMSO and 10 µL sample). After exposure the cells were incubated at 37°C and 5% CO_2 for further 24 h. Each standard as well as the gadolinium sample were tested in triplicate. After 24 h of exposure of the T47D cells to the 17β-estradiol standards and the gadolinium samples the medium was removed, 50 µL lysis solution were added into each well and the plate was incubated at room temperature for 15 min. Then 30 µL supernatant were transferred into a white 96-well plate and after the addition of 30 µL GlowMix containing luciferin the luminescence was measured.

Results of the ER Calux are presented in Figure S 5.6. The assumption, that no estrogen disrupting effect should be detectable could be verified by the outcome of the test. The test results of the oxidized samples do not differ from the ones of a negative control.

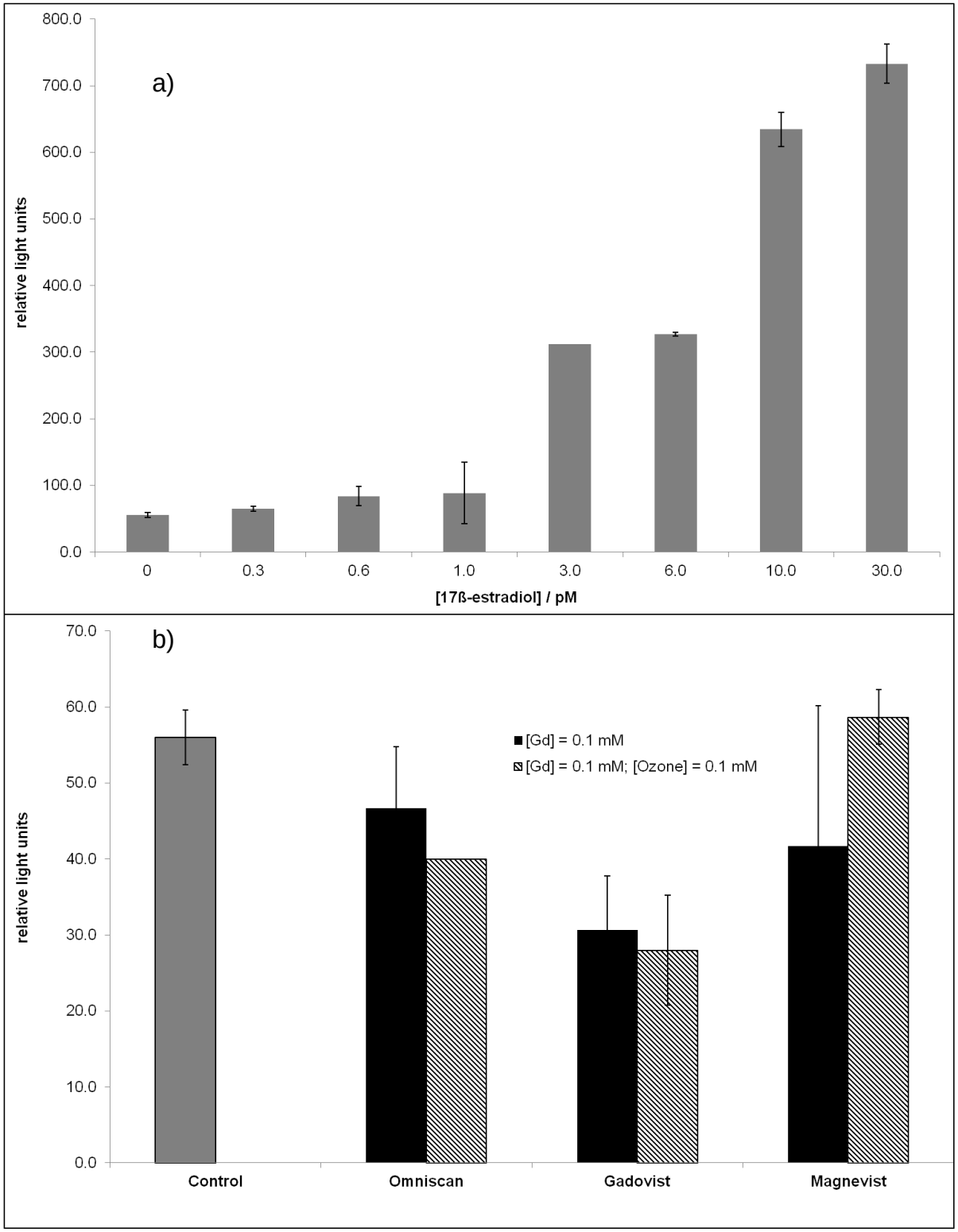

Figure S 5.6: Results of estrogenicity test (detailed test method in 2.3) for all tested chelates; a) positive controls; b) negative control and samples ([Gd] = 0.1 mM) before and (black) after reaction with ozone (hatched) ([O_3] = 0.1 mM)

5.6 Literature

1. Von Gunten, U., Ozonation of drinking water: Part I. Oxidation kinetics and product formation. *Water Research*, 2003. **37**(7): 1443-1467.

2. Von Gunten, U., Ozonation of drinking water: Part II. Disinfection and by-product formation in presence of bromide, iodide or chlorine. *Water Research*, 2003. **37**(7): 1469-1487.

3. von Sonntag, C. and U. von Gunten, *Chemistry of ozone in water and wastewater treatment: From basic principles to applications*. 2012, London / New York: IWA.

4. Hollender, J., S.G. Zimmermann, S. Koepke, M. Krauss, C.S. McArdell, C. Ort, H. Singer, U. Von Gunten, and H. Siegrist, Elimination of organic micropollutants in a municipal wastewater treatment plant upgraded with a full-scale post-ozonation followed by sand filtration. *Environmental Science and Technology*, 2009. **43**(20): 7862-7869.

5. Nowotny, N., B. Epp, C. von Sonntag, and H. Fahlenkamp, Quantification and modeling of the elimination behavior of ecologically problematic wastewater micropollutants by adsorption on powdered and granulated activated carbon. *Environmental Science and Technology*, 2007. **41**(6): 2050-2055.

6. Lewandowski, J., A. Putschew, D. Schwesig, C. Neumann, and M. Radke, Fate of organic micropollutants in the hyporheic zone of a eutrophic lowland stream: Results of a preliminary field study. *Science of the Total Environment*, 2011. **409**(10): 1824-1835.

7. *Directive 2000/60/EC of the European Parliament and of the Council of 23 October 2000 establishing a framework for community action in the field of water policy*. 2000.

8. Buffle, M.O., J. Schumacher, S. Meylan, M. Jekel, and U. Von Gunten, Ozonation and advanced oxidation of wastewater: Effect of O_3 dose, pH, DOM and $HO^{\bullet}$-scavengers on ozone decomposition and $HO^{\bullet}$ generation. *Ozone: Science and Engineering*, 2006. **28**(4): 247-259.

9. Huber, M.M., T.A. Ternes, and U. von Gunten, Removal of estrogenic activity and formation of oxidation products during ozonation of 17alpha-ethinylestradiol. *Environmental Science and Technology*, 2004. **38**(19): 5177-5186.

10. Nöthe, T., H. Fahlenkamp, and C. von Sonntag, Ozonation of wastewater: Rate of ozone consumption and hydroxyl radical yield. *Environmental Science and Technology*, 2009. **43**(15): 5990-5995.

11. Pocostales, J.P., M.M. Sein, W. Knolle, C. von Sonntag, and T.C. Schmidt, Degradation of ozone-refractory organic phosphates in wastewater by ozone and ozone/hydrogen peroxide (peroxone): The role of ozone consumption by dissolved organic matter. *Environmental Science and Technology*, 2010. **44**(21): 8248-8253.

12. Sillanpää, M.E.T., T.A. Kurniawan, and W.H. Lo, Degradation of chelating agents in aqueous solution using advanced oxidation process (AOP). *Chemosphere*, 2011. **83**(11): 1443-1460.

13. Höbel, B. and C. von Sonntag, OH-Radical induced degradation of ethylenediaminetetraacetic acid (EDTA) in aqueous solution: A pulse radiolysis study. *Journal of the Chemical Society. Perkin Transactions 2*, 1998(3): 509-513.

14. Korhonen, M.S., S.E. Metsärinne, and T.A. Tuhkanen, Removal of ethylenediaminetetraacetic acid (EDTA) from pulp mill effluents by ozonation. *Ozone: Science and Engineering*, 2000. **22**(3): 279-286.

15. Lati, J. and D. Meyerstein, Oxidation of first-row bivalent transition-metal complexes containing ethylenediaminetetra-acetate and nitrilotriacetate ligands by free radicals: A pulse-radiolysis study. *Journal of the Chemical Society, Dalton Transactions*, 1978(9): 1105-1118.

16. Munoz, F. and C. von Sonntag, The reactions of ozone with tertiary amines including the complexing agents nitrilotriacetic acid (NTA) and ethylenediaminetetraacetic acid (EDTA) in aqueous solution. *Journal of the Chemical Society. Perkin Transactions 2*, 2000(10): 2029-2033.

17. Stemmler, K., G. Glod, and U. Von Gunten, Oxidation of metal-diethylenetriamine-pentaacetate (DTPA) - Complexes during drinking water ozonation. *Water Research*, 2001. **35**(8): 1877-1886.

18. Ternes, T.A., K. Stolte, and K. Haberer, Degradation of DTPA by UV/H_2O_2 during drinking water treatment. *Vom Wasser* 1997. **88**: 243-256.

19. Caravan, P., J.J. Ellison, T.J. McMurry, and R.B. Lauffer, Gadolinium(III) chelates as MRI contrast agents: Structure, dynamics, and applications. *Chemical Reviews*, 1999. **99**(9): 2293-2352.

20. Künnemeyer, J., L. Terborg, B. Meermann, C. Brauckmann, I. Möller, A. Scheffer, and U. Karst, Speciation analysis of gadolinium chelates in hospital effluents and wastewater treatment plant sewage by a novel HILIC/ICP-MS method. *Environmental Science and Technology*, 2009. **43**(8): 2884-2890.

21. Chang, C.A., Magnetic resonance imaging contrast agents. Design and physicochemical properties of gadodiamide. *Investigative Radiology*, 1993. **28** (Suppl 1): S21-27.

22. Chen, X., J. Richard, Y. Liu, E. Dopp, J. Tuerk, and K. Bester, Ozonation products of triclosan in advanced wastewater treatment. *Water Research*, 2012. **46**(7): 2247-2256.

23. Ulanski, P., E. Bothe, K. Hildenbrand, J.M. Rosiak, and C. von Sonntag, Hydroxyl-radical-induced reactions of poly(acrylic acid); a pulse radiolysis, EPR and product study. Part I. Deoxygenated aqueous solutions. *Journal of the Chemical Society, Perkin Transactions 2*, 1996(1): 13-22.

24. Dean, J.A., ed. *Lange's handbook of chemistry* 13. ed. 1985, McGraw-Hill Book Co.: New York.

25. Patty, F., ed. *Industrial hygiene and toxicology: Volume II: Toxicology*. 2nd. ed. 1963, Interscience Publishers: New York.

26. Hoigné, J., Bader, H., Determination of ozone and chlorine dioxide in water by the indigo carmine method. *Vom Wasser*, 1980. **55**: 261-279.

27. Buxton, G.V. and C.R. Stuart, Re-evaluation of the thiocyanate dosimeter for pulse radiolysis. *Journal of the Chemical Society, Faraday Transactions*, 1995. **91**(2): 279-281.

28. Von Sonntag, C., *The chemical basis of radiation biology*. 1987, London: Taylor & Francis.

29. Buxton, G.V., C.L. Greenstock, W.P. Helman, and A.B. Ross, Critical review of rate constants for reactions of hydrated electrons, hydrogen atoms and hydroxyl radicals in aqueous solution. *Journal of Physical and Chemical Reference Data*, 1988. **17**(2): 513-886.

30. Munoz, F. and C. von Sonntag, Determination of fast ozone reactions in aqueous solution by competition kinetics. *Journal of the Chemical Society, Perkin Transactions 2*, 2000(4): 661-664.

31. Smith, R.M. and A.E. Martell, Critical stability constants, enthalpies and entropies for the formation of metal complexes of aminopolycarboxylic acids and carboxylic acids. *Science of the Total Environment*, 1987. **64**(1-2): 125-147.

32. Frenzel, T., P. Lengsfeld, H. Schirmer, J. Huetter, and H.-J. Weinmann, Stability of gadolinium-based magnetic resonance imaging contrast agents in human serum at 37 °C. *Investigative Radiology*, 2008. **43**(12): 817-828.

33. Khurana, A., V.M. Runge, M. Narayanan, J.F. Greene Jr, and A.E. Nickel, Nephrogenic systemic fibrosis: A review of 6 cases temporally related to gadodiamide injection (Omniscan). *Investigative Radiology*, 2007. **42**(2): 139-145.

34. Mori, Y., R. Watanabe, S. Sakamoto, N. Endo, S. Nakano, K. Kanaori, H. Takashima, M. Ohkawa, and K. Tajima, Flow-injection EPR investigation on OH radical scavenging activity of Gd(III) containing MRI contrast media. *Journal of Medicine*, 2004. **35**(1-6): 49-61.

35. Adams, G.E., J.W. Boag, J. Currant, and B.D. Michael, *Absolute rate constants for the reaction of the hydroxyl radical with organic compounds*, in *Pulse radiolysis*, M. Ebert, et al., Editors. 1965, Academic Press: New York.

6 Concluding Remarks and Future Perspectives

In the studies presented in this work it was demonstrated that gadolinium, in detail chelated gadolinium, has become a relevant substance in the water cycle. Monitoring campaigns in wastewater and drinking water have been performed. An average concentration of 118 ng L^{-1} gadolinium has been determined in a European monitoring campaign of wastewater treatment plant effluents, with a corresponding average anomaly of 69, which represents an anthropogenic gadolinium concentration of 116 ng L^{-1}. By this European monitoring campaign it could be shown that anthropogenic gadolinium, which is assumed to be gadolinium in chelated from [1], is present in concentrations relevant for wastewater treatment. The results from a drinking water campaign in the Ruhr area, which is a densely populated region in western Germany with a high re-use rate of water, have shown that also in this water matrix the anomaly is detectable. The average gadolinium concentrations in this area were by a factor of 5 lower than the average concentrations in the investigated wastewater samples. Hence, gadolinium chelates are also found in drinking water and are as well affected by drinking water treatment processes. The determined concentrations are by orders of magnitude lower than acute toxic effect concentrations and ecotoxicological endpoints (e.g. EC_{50} for Gd-DTPA is 0.18 mmol L^{-1} [2], which is 1.1 µg L^{-1} gadolinium). It is not known in which speciation gadolinium is present in the investigated samples, as only total element concentration has been determined. However, this speciation is of great importance when evaluating toxicological relevance. The Gd(III) ion is by orders of magnitude more toxic than the chelated form and the same applies for the ligands. Long term studies on toxicity of both Gd(III) and its chelated form are missing. In drinking water even lowest level concentrations of such micropollutants could be of concern, especially if it cannot be ruled out that applied treatment steps, such as flocculation, may change speciation of gadolinium into a more toxic form.

To gain insight on water treatment processes which may change the speciation oxidation reactions of gadolinium chelates were investigated for both ozone and hydroxyl radicals. In drinking water ozonation, the reaction pathway via ozone is dominant because radical scavengers, such as bicarbonate, are present in high

concentration. Rate constants have been determined for three chemically different types of representative gadolinium chelates. For all three chelates, the rate constants were < 50 $M^{-1}s^{-1}$. Hence, the chelates are considered to be ozone refractory. This is mainly due to the electron withdrawing effect of gadolinium. Electrons of functional groups which are usually prone to electrophilic attack of ozone (e.g. amines) are incorporated in the binding of gadolinium and in consequence they are not available for such an attack. From determination of rate constants for ozone reactions it has been concluded that a reaction of these chelates via the ozone reaction pathway is rather unlikely and gadolinium chelates will stay intact during wastewater and drinking water treatment. For determination of reaction rate constants with hydroxyl radicals, several different methods were applied, and yielded comparable results. The rate constants for the representative gadolinium chelates have shown that the reactions are almost diffusion controlled (> 10^9 M^{-1} s^{-1}). These high rate constants make a reaction feasible even in highly competitive matrices. It is concluded that in wastewater treatment a reaction of gadolinium chelates with hydroxyl radicals will occur. Taking a typical wastewater matrix into account, oxidation of 0.7 µg L^{-1} Gd, (, which was the highest measured gadolinium concentration in the European monitoring campaign) would yield 0.66 µg L^{-1} reacted chelate (assumed that all gadolinium is present as Gd-BT-DO3A, which had the highest measured rate constant). However, also low concentration levels might be of concern. Therefore, information on gadolinium speciation and long-term studies on toxicity are needed.

The evaluation of adsorption processes for removal of gadolinium chelates from water has shown that adsorption strength of the investigated chelates is rather low. The chelates have K_F values for adsorption on activated carbon similar to iopamidole, an X-ray contrast agent which is insufficiently removable by activated carbon [3]. Furthermore, synthetic activated polymers have been tested as adsorbent. Applying these, better adsorption could be achieved. However, one has to consider the high costs for such materials. Additional to the determination of bottle point isotherms, filtration experiments in drinking water matrix have been performed to evaluate the behavior of the chelates in filters. Again adsorption was rather poor and breakthrough of the chelates occurred early. The breakthrough behavior could be explained by

application of the Linear Driving Force model (LDF). A filter competition effect, different to the direct competition effect could be shown by using the LDF model. The direct competition effect is included in adsorption isotherm data, determined by bottle point isotherms in drinking water. The additional filter competition effect is due to competition of each fraction of the water matrix (from very well adsorbable to very poorly adsorbable) for each filter layer which is proceeding over the whole operation period with constant gadolinium and matrix feed. Furthermore, to support the results from lab scale experiments, samples were taken in a WWTP equipped with an activated carbon filter. The results of these first investigations indicated that the adsorption is as poor as expected. The breakthrough occurs even earlier than in a worst case scenario prediction for treatment of hospital wastewater. From data of lab scale experiments, as well as from the investigations at the WWTP, it is concluded that a removal of gadolinium chelates via adsorption on activated carbon in wastewater, as well as in drinking water, is negligible. Due to the poor adsorbability of gadolinium chelates, it is possible to use it as indicator compound for determination of filter breakthrough. This would allow even earlier breakthrough detection than by monitoring organic substances like atrazine.

For future research it is necessary to have a reliable speciation method for quantification of lowest gadolinium concentrations. The speciation of gadolinium in the environment has not been performed up to date [4]. Only a pseudo-speciation by the gadolinium anomaly is performed. However, a sensitive speciation method is needed to fully understand environmental behavior of gadolinium. Research on oxidation of the chelates during water treatment pointed out the relevance of such speciation methods. It has been possible to determine kinetics of oxidation reactions, both via ozone and hydroxyl radicals. By the applied cytotoxicity and genotoxiciy and estrogenity tests, no toxic transformations products were determined. Yet it has to be considered, that the chosen tests are not a full toxicological assessment, but rather a screening. Reaction products other than formaldehyde during the reaction with hydroxyl radicals were not identified. It is expected that similar or even the same reaction products are formed as in the reaction of structural related chelates, like Fe-EDTA or Fe-DTPA, with hydroxyl radicals. These reaction products are, among others, formaldehyde and iminodiacetic acid [5]. However, speciation of the central

ion after such oxidation reactions has not been performed. It is most likely that the ion forms new chelates with ligands formed during oxidation. These newly formed chelates may have lower stability constants than the original chelates which benefits transmetalation. This effect might even be stronger in a wastewater matrix. It is pointed out that this may be of interest for all other chelates present in a wastewater matrix as well, consequently changing metal transport as well as bioavailability. Research, considering these effects is strongly recommended.

6.1 References

1. Bau, M. and P. Dulski, Anthropogenic origin of positive gadolinium anomalies in river waters*. Earth and Planetary Science Letters*, 1996. **143**(1-4): 245-255.
2. Neubert, C., R. Länge, and T. Steger-Hartmann, *Gadolinium containing contrast agents for magnetic resonance imaging (MRI) investigations on the environmental fate and effects*, in *Fate of pharmaceuticals in the environment and in water treatment systems*, D.S. Aga, Editor. 2008, CRC Press Taylor & Francis Group: Boca Raton, Fl.
3. Ternes, T., *Assessment of technologies for the removal of pharmaceuticals and personal care products in sewage and drinking water facilities to improve the indirect potable water reuse*, in *Poseidon report*. 2005.
4. Lawrence, M.G., Detection of anthropogenic gadolinium in the Brisbane River plume in Moreton Bay, Queensland, Australia*. Marine Pollution Bulletin*, 2010. **60**(7): 1113-1116.
5. Munoz, F. and C. von Sonntag, The reactions of ozone with tertiary amines including the complexing agents nitrilotriacetic acid (NTA) and ethylenediaminetetraacetic acid (EDTA) in aqueous solution*. Journal of the Chemical Society. Perkin Transactions 2*, 2000(10): 2029-2033.

7 Appendix

7.1 Abbreviations

Symbol / Abbreviation	Quantity name or names
3D	Three-dimensional
A	Absorbance
AAS	Atomic absorption spectroscopy
AC	Activated carbon
ACN	Acetonitrile
BET	Brunauer, Emmett, and Teller isotherm
Bo	Bochum
Bot	Bottrop
BV	Bed volumes
C	Competitor
c_0	Initial concentration
CAT	Computed axial tomography
CE	Capillary electrophoresis
CHO	Chinese hamster ovary
CT	Computer tomography
D	Düsseldorf
DALE	Disability-adjusted life expectancy
DALY	Disability-adjusted life year
DAPI	2-(4-carbamimidoylphenyl)-1H-indol-6-carboximidamid
d_i	Inner diameter
D_L	Diffusion coefficient

Symbol / Abbreviation	Quantity name or names
DMEM	Dulbecco's modified eagle's medium
DMSO	Dimethylsulfoxide
DNA	Deoxyribonucleic acid
Do	Dortmund
DOC	Dissolved organic carbon
DOTA	1,4,7,10-tetraazacyclododecane-1,4,7,10-tetraacetic acid
d_P	Particle diameter
DTPA	Diethylene triamine pentaacetic acid
Du	Duisburg
E	Essen
ε	Bed porosity
ε	Molar absorption coefficient
EC_{50}	Half maximal effective concentration
E2	17β estradiol
EE2	17α Ethinylestradiol
EDTA	Ethylenediaminetetraacetic acid
ESI	Electrosray ionization
Eq	Equation
FCS	Fetal calf serum
GAC	Granulated activated carbon
GC	Gaschromatography
Gd-BOPTA	Gadolinium(III) 2-[2-[2-[bis(carboxylatomethyl)amino]ethyl-(carboxylatomethyl)amino] ethyl-(carboxylatomethyl)amino]-3-phenylmethoxypropanoate;hydron
Gd-BT-DO3A	Gadolinium(III) 2,2',2''-(10-((2R,3S)-1,3,4-trihydroxybutan-2-yl)-1,4,7,10-tetraazacyclododecane-1,4,7-triyl)triacetate

Symbol / Abbreviation	Quantity name or names
Gd-DTPA-BMA	Gadolinium (III) 5,8-bis(carboxylatomethyl)-2-[2-(methylamino)-2-oxoethyl]-10-oxo-2,5,8,11-tetraazadodecane-1-carboxylate hydrate
Gd-DTPA-BMEA	Gadolinium(III) 2-[bis[2-[carboxylatomethyl-[2-(2-methoxyethylamino)-2-oxoethyl]amino] ethyl]amino]acetate
Gd-EOB-DTPA	Disodium;2-[[(2S)-2-[bis(carboxymethyl)amino]-3-(4-ethoxyphenyl)propyl]-[2-[bis(carboxymethyl)amino]ethyl]amino]acetic acid gadolinium
Gd-HP-DO3A	Gadolinium(III) 2-[4,7-bis(carboxylatomethyl)-10-(2-hydroxypropyl)-1,4,7,10-tetrazacyclododec-1-yl]acetate
Gd-MS-325	Trisodium 2-[[(2R)-2-[bis(2-oxido-2-oxoethyl)amino]-3-[(4,4-diphenylcyclohexyl)oxy-oxidophosphoryl]oxypropyl]-[2-[bis(2-oxido-2-oxoethyl)amino]ethyl]amino]acetate gadolinium(III) hydrate
Ge	Gelsenkirchen
Her	Herne
HPLC	High performance liquid chromatography
HILIC	Hydrophobic interaction liquid chromatography
HPLC	High-performance liquid chromatography
HSDM	Homogeneous surface diffusion model
IAST	Ideal adsorbed solution theory
IC	Ion chromatography
ICP	Inductive coupled plasma
k	Reaction rate constant
K_F	Freundlich coefficient
k_f	Liquid-phase mass transfer coefficient
LD_{50}	Median lethal dose
LDF	Linear driving force
LOD	Limit of detection

Symbol / Abbreviation	Quantity name or names
LOQ	Limit of quantification
LSF	Large scale filter
m	Mass
MBR	Membrane bioreactor
MEKC	Micellar electrokinetic chromatography
Mh	Mülheim
MRI	Magnetic resonance imaging
MS	Mass spectrometry
MTT	3-(4-dimethylthiazol-2-yl)-2,5-diphenyltetrazoliumbromid
MUQ	Mud from Queensland
MW	Molecular weight
n	Freundlich exponent
η	Stoichiometric number
NASC	North American shale composite
NMR	Nuclear magnetic resonance
NOEC	No observed effect concentration
NTA	Nitrilotriacetic acid
Ob	Oberhausen
OECD	Organisation for economic co-operation and development
OES	Optical emission spectrometry
Ox	Oxidant
obs	Observed
P	Probe compound
P	Particle density
p.a.	Pro analysis

Symbol / Abbreviation	Quantity name or names
PAC	Powdered activated carbon
PAAS	Achaean Australian shell
$P_{butanol/water}$	Partitioning coefficient between butanol and water
PBS	Phosphate buffered saline
***p*CBA**	*para*-Chlorobenzoic acid
PET	Positron emission tomography
pK_a	Acid dissociation constant
***p*NBA**	*para*-Nitrobenzoic acid
PFA	Perfluoroalkoxy
PP	Polypropylene
PSF	Pilot scale filter
PVC	Polyvinyl chloride
QSAR	Quantitative structure activity relationship
R	Electrical resistence
r	Relaxivity
REE	Rare earth element
REACH	Registration, Evaluation, Authorization and Restriction of Chemicals
RSD	Residual standard deviation
SDS	Sodium dodecyl sulfate
SEC	Size-exclusion chromatography
SMILES	Simplified molecular input line entry system
SPE	Solid phase extraction
T	Temperature
t	Time
T_1	Spin-lattice relaxation time

Symbol / Abbreviation	Quantity name or names
T_2	Spin spin relaxation time
$1/T_1$	Longitudinal relaxation rates
$1/T_2$	Transverse relaxation rates
***t*BuOH**	*tertiary*-Butanol
T_{obs}	Observed solvent relaxation rate
TXRF	Total reflection X-ray fluorescence
US EPA	Environmental protection agency of the United States of America
UV	Ultra violet light
V	Volume
$\dot{V}$	Flow
v_f	Filter velocity
VIS	Visible light
WHO	World Health Organization
WWTP	Wastewater treatment plant

7.2 List of publications

Publications in peer-reviewed journals

Cyris M, Knolle W, Richard J, Dopp E, von Sonntag C, Schmidt T C(2013): Oxidation of gadolinium-based Diagnostics. Submitted to Environmental Science and Technology

Gabriel F L P, Cyris M, Giger W, Kohler H P E (2007): ipso-substitution: A general biochemical and biodegradation mechanism to cleave alpha-quaternary alkylphenols and bisphenol A. Chemistry and Biodiversity, 4(9), 2123-2137.

Gabriel F L P, Cyris M, Jonkers N, Giger W, Guenther K, Kohler H P E (2007): Elucidation of the ipso-substitution mechanism for side-chain cleavage of alpha-quaternary 4-nonylphenols and 4-*t*-butoxyphenol in Sphingobium xenophagum Bayram. Applied and Environmental Microbiology, 73(10), 3320-3326.

Posters

Cyris M, Brecht D, Rübel A, Schwesig D, Von Sonntag C, Schmidt T C (2012): Fate of gadolinium-based contrast agents in advanced wastewater treatment. 3rd International Conference on Sustainable Pharmacy. Osnabrück, Germany.

Cyris M, Bens T, Hoffmann G, Rübel A, Schwesig D, Schmidt T C (2011): Adsorption Gadolinium-basierter Diagnostika an Pulveraktivkohle. Wasser 2011. Norderney, Germany.

Cyris M, Rübel A, Schwesig D, Schmidt T C (2011): Sorption of Gadolinium-based diagnostics on activated carbon. Metallomics 2011. Münster, Germany.

Cyris M, Tuerk J, Bester K, Dopp E, Schmidt T C (2009): Investigations for assesment and prevention of toxic oxidation by-products in waste water treatment. Conference and Exhibition on Water in the Environment - enviroWater. Stellenbosch, South Africa.

Tuerk J, Cyris M, Sayder B, Kiffmeyer T K, Kabasci S, Kuss H-M (2009): Development of an AOP pilot plant for the degradation of pharmaceuticals in hospital waste waters. Conference and Exhibition on Water in the Environment - enviroWater. Stellenbosch, South Africa.

Oral presentations

Cyris M, González Lagunilla M, Ulloa Almendras P, Schmidt T C (2012): Gadolinium-based diagnostics in water treatment. Wasser 2012. Neu-Ulm.

Cyris M (2012): Gadolinium-basierte Diagnostika in der weitergehenden Abwasserbehandlung. 111. Stipendiatenseminar der Deutschen Bundesstiftung Umwelt auf Burg Lenzen. Lenzen, Germany.

Cyris M, Hoffmann G, Rübel A, Schwesig D, Schmidt T C (2011): Removal of Gadolinium-based diagnostics by activated carbon. 13th EuCheMS International Conference on Chemistry and the Environment, ICCE 2011. Zürich.

Cyris M (2011): Verhalten und Bewertung Gadolinium-basierter Diagnostika in der weitergehenden Abwasserbehandlung. 106. Stipendiatenseminar der Deutschen Bundesstiftung Umwelt auf Burg Lenzen. Lenzen, Germany.

Cyris M (2010): Verhalten und Bewertung Gadolinium-basierter Diagnostik in der weitergehenden Abwasserbeahndlung. 102. Stipendiatenseminar der Deutschen Bundesstiftung Umwelt im Internationalen Begegnungszentrum St. Marienthal, Ostritz. Ostritz, Germany.

7.4 Erklärung

Hiermit versichere ich, dass ich die vorliegende Arbeit mit dem Titel

„Behavior of Gadolinium based Diagnostics in Water Treatment"

selbst verfasst und keine außer den angegebenen Hilfsmitteln und Quellen benutzt habe, und dass die Arbeit in dieser oder ähnlicher Form noch bei keiner anderen Universität eingereicht wurde.

Essen, im Februar 2013

Maike Cyris

7.5 Acknowledgment

I thank the German Federal Environmental Foundation (Deutsche Bundesstiftung Umwelt, DBU) for financial and ideational support.

Financial support from the Center for Water and Environmental Research (Zentrum für Wasser und Umweltforschung, ZWU) is also gratefully acknowledged.

Also, I thank:

Prof. T.C. Schmidt for encouragement and advice,

Prof. C. von Sonntag for sharing his knowledge and professional discussions, that changed my view,

Dr. A. Rübel and Dr. D. Schwesig as this work would not have been possible without their support.

All my colleagues and friends at the Institute of Instrumental Analytical Chemistry at the University of Duisburg-Essen and the department for Anorganic Chemistry Analytics at the IWW-Water Center for their support, help and assistance.

Special thanks go to Patricia Ulloa Almendras, Dominic Brecht, Marta González Lagunilla, Grit Hoffmann, Ralph Hobby, Marina Horstkott, Uli Klümper, Wolfgang Knolle, Lukas Landwehkamp, Holger Lutze, Robert Lobe, Andreas Nahrstedt, Christoph Nolte, Jessica Richard and Renate Schulz.

Last, but not least, I thank my parents for their support and encouragement all along.